Intensification of polyester synthesis by continuous reactive distillation

Citation for published version (APA):
Shah, M. R. (2011). *Intensification of polyester synthesis by continuous reactive distillation*. [Phd Thesis 1 (Research TU/e / Graduation TU/e), Chemical Engineering and Chemistry]. Technische Universiteit Eindhoven. https://doi.org/10.6100/IR718721

DOI:
10.6100/IR718721

Document status and date:
Published: 01/01/2011

Document Version:
Publisher's PDF, also known as Version of Record (includes final page, issue and volume numbers)

Please check the document version of this publication:

• A submitted manuscript is the version of the article upon submission and before peer-review. There can be important differences between the submitted version and the official published version of record. People interested in the research are advised to contact the author for the final version of the publication, or visit the DOI to the publisher's website.
• The final author version and the galley proof are versions of the publication after peer review.
• The final published version features the final layout of the paper including the volume, issue and page numbers.

Link to publication

General rights
Copyright and moral rights for the publications made accessible in the public portal are retained by the authors and/or other copyright owners and it is a condition of accessing publications that users recognise and abide by the legal requirements associated with these rights.

- Users may download and print one copy of any publication from the public portal for the purpose of private study or research.
- You may not further distribute the material or use it for any profit-making activity or commercial gain
- You may freely distribute the URL identifying the publication in the public portal.

If the publication is distributed under the terms of Article 25fa of the Dutch Copyright Act, indicated by the "Taverne" license above, please follow below link for the End User Agreement:

www.tue.nl/taverne

Take down policy
If you believe that this document breaches copyright please contact us at:

openaccess@tue.nl

providing details and we will investigate your claim.

Download date: 04. Oct. 2023

Intensification of Polyester Synthesis by Continuous Reactive Distillation

Mayankkumar Rameshchandra Shah

Graduation committee:

Chairman:	prof.dr. G. de With	Eindhoven University of Technology
Promoter:	prof.dr.ir. A.B. de Haan	Eindhoven University of Technology
Copromotor:	dr.ir. E. Zondervan	Eindhoven University of Technology
Committee members:	prof.dr.ing. A. Gorak	Dortmund University of Technology
	prof.dr.ir. A.I. Stankiewicz	Delft University of Technology
	prof.dr. J. Meuldijk	Eindhoven University of Technology
	prof.dr. T. Salmi	Åbo Akademi University
	dr. A.A. Kiss	Akzo Nobel Chemicals B.V.

The research described in this thesis was carried out at the Process Systems Engineering Group, the Department of Chemistry and Chemical Engineering, the Eindhoven University of Technology. This research was funded by the Institute for Sustainable Process Technology (ISPT), project SC-00-05, and supported by AkzoNobel and DSM.

Intensification of Polyester Synthesis by Continuous Reactive Distillation

M. R. Shah

A catalogue record is available from the Eindhoven University of Technology Library

ISBN: 978-90-386-2840-0

Cover design by M. R. Shah

Copyright © 2011, M. R. Shah

All rights reserved.

Printed by Gilderprint Drukkerijen B.V. Enschede

Intensification of Polyester Synthesis by Continuous Reactive Distillation

PROEFSCHRIFT

ter verkrijging van de graad van doctor aan de
Technische Universiteit Eindhoven, op gezag van de
rector magnificus, prof.dr.ir. C.J. van Duijn, voor een
commissie aangewezen door het College voor
Promoties in het openbaar te verdedigen
op woensdag 9 november 2011 om 16.00 uur

door

Mayankkumar Rameshchandra Shah

geboren te Vadodara, India

Dit proefschrift is goedgekeurd door de promotor:

prof.dr.ir. A.B. de Haan

Copromotor:
dr.ir. E. Zondervan

Acknowledgements

This dissertation would not have been possible without the guidance and the help of several individuals who in one way or another contributed and extended their valuable assistance in the preparation and completion of this study. Foremost, I would like to express my sincere gratitude to Prof.dr.ir. A.B. de Haan for the continuous support, his patience, motivation, enthusiasm and immense knowledge. His guidance helped me all the time of research, solving the practical issues and writing this thesis and several publications. The knowledge I have gained from him will surely boost my further career. He also gave me chance to visit several universities, industries, conferences and courses nationally and internationally which have broadened my views towards the research, life and culture. I can never imagine a better promoter than him for my PhD study.

I would like to express my heartily thanks to my daily supervisor Dr.ir. E. Zondervan for all discussion regarding project, journal and conference papers, PhD thesis, MATLAB and models. Moreover, I could not forget his humorous nature, having friendly environment during the last four years of work and discovering the Zondervan dimensionless number. I am indebted to Dr. A.A. Kiss for his valuable guidance during the PhD study and inspiring me for writing publications. I am grateful to him as few sections of this thesis are resulted from his active participation and our co-operations. I also would like to thank the members of the doctorate committee Prof.dr. G. de With, Prof.dr.ing. A. Gorak, Prof.dr.ir. A.I. Stankiewicz, Prof.dr. J. Meuldijk, Prof.dr. T. Salmi and Dr.ir. A.A. Kiss. I am honored that you are willing to participate in my promotion.

I would like to thank the Institute for Sustainable Process Technology (ISPT) for the financial support and the industrial partners AkzoNobel and DSM for their co-operation in the project.

I would like to thank all my master students for their help during the PhD project. My appreciation also goes to Dolf Liempt, Wouter Gerritsen and Wilko Weggemans who helped me to build the pilot plant setups, their efforts and technical help to get running the pilot plant setups so the data contained in this thesis could be measured.

I am greatly indebted to my colleagues during my time at Eindhoven University of technology. I would like to say special thanks to my officemate Juan Pablo and Esteban for all discussions, lively and friendly environment and for their inspirations. I also would like to thank Lesly, Caecilia, Ana, Agnieszka, Antje, Marjette, Tanja, Mark, Miran, Jeroen, Martijn, Ferdy, Alex, Miguel and Esayas for their support, help, interesting coffee break discussions and for being good companion during conferences, excursions and courses.

I would also like to thanks all my friends in Europe for their moral support and encouragement during the last 6 years. I wish to express my deepest gratitude to my late mother Sulochana Shah, my father Rameschandra Shah, my mother-in-law Mrudula Shah, my father-in-law Kiran Shah and my sister-in-law Kejal Shah for constantly encouraging me to put all my efforts and concentration into the work. Last but not the least; I especially thank my beloved wife Bhakti Shah for her love, support and encouragement during the critical stages of my PhD period. Without her fullest support and encouragement, I could not have completed my PhD within four years.

Finally, I would like to thank all the people who were not mentioned above but have helped me in some or other way to complete my work successfully.

Summary

The thesis starts with a brief overview of unsaturated polyesters. In particular, the usage of raw materials, the application of unsaturated polyester resins, and, the worldwide supply and demand of the unsaturated polyester resins are discussed. Unsaturated polyester is traditionally produced in a batch-wise-operating reaction vessel connected to a distillation unit. The total production time is around 12 hours and often leads to batch-to-batch inconsistency. Process intensification is required for the unsaturated polyester process to reduce the production time and to achieve a better quality of the product. An attractive alternative to batch-wise polyester production is reactive distillation. In chapter 1, the attractiveness of reactive distillation for the synthesis of unsaturated polyester is discussed. The goal of the thesis is to develop and evaluate a reactive distillation process for the production of unsaturated polyester from anhydrides and glycols.

To accurately predict the behavior of reactive distillation process, reliable kinetic and thermodynamic models are required. Therefore, in chapter 2 a dynamic model for a batch-wise operating reaction vessel connected to a flash separation unit is developed in order to validate the kinetic and thermodynamic models and their parameters. This model includes kinetics, description of the change of rate order during the reaction, the polymer NRTL non-ideal thermodynamic model based on non-random theory of liquid (NRTL) and mass balances. The reaction between maleic anhydride and propylene glycol has been taken as a case study. The reaction scheme is complex and the proposed model takes four types of reactions into account; ring opening, polyesterfication, isomerization and saturation reactions. The acid value of the polyester, number-average molecular weight, distilled mass and glycol concentration in the distillate have been subsequently used to validate the model and the model predicts these important variables reliably. The process description is improved by using the vapor liquid equilibrium data predicted from the polymer NRTL model.

After successful validation of the kinetic and thermodynamic models, the feasibility of the reactive distillation process for the unsaturated polyester is presented in chapter 3. Moreover, the simulation results of reactive distillation model are compared with the batch reactor model simulation results to determine advantages gained by the reactive distillation over the traditional batch process. The simulation study shows that the total production time of polyester in a continuous reactive distillation system is reduced to 1.8-2 hours compared to the12 hours of the industrial batch reactor process. The model demonstrated that reactive distillation has the potential to intensify the process by factor of 6 to 8 in comparison to the batch reactor process. After finding that reactive distillation is an attractive alternative for the polyesters synthesis, a more in depth analysis is performed. Particularly, the influence of the liquid back mixing on the description of the reactive distillation process, product transition time, the amount of undesired product formation during the product changeover is investigated. Since the current state of the art modelling approach does not account for

liquid back mixing, the rate-based model is extended to account for liquid back mixing. The simulation results of extended rate-based model demonstrated that axial dispersion significantly influences the reactive distillation process and cannot be neglected.

On the basis of current research work and literature review, a novel design methodology for the economical and technical evaluation of reactive distillation is proposed in chapter 4. Moreover, the applicability of various design methods for reactive distillation is discussed. The proposed framework for the economical evaluation determines the boundary conditions (e.g. relative volatilities, target purities, equilibrium conversion and equipment restriction), checks the integrated process constrains, evaluates economical feasibility, and provides guidelines to any potential reactive distillation process application. Providing that a reactive distillation process is economically attractive, a technical evaluation is performed afterward in order to determine the technical feasibility, the process limitations, working regime and requirements for internals as well as the models needed for reactive distillation. This approach is based on dimensionless numbers such as Damkohler and Hatta numbers, as well as the kinetic, thermodynamic and mass transfer limits. The proposed framework for economical and technical evaluation of reactive distillation allows a quick and easy feasibility analysis for a wide range of chemical processes. Several industrial relevant case studies (synthesis of di-methyl carbonate (DMC), methyl acetate hydrolysis, toluene hydro-dealkylation (HDA) process, fatty acid methyl esters (FAME) process and unsaturated polyesters synthesis) are used to illustrate the validity of the proposed framework.

In chapter 4, it is found that the bubble column is the potential device for producing unsaturated polyesters by the reactive distillation. Moreover, the introduction of packing or partition trays in the bubble column significantly improves the unsaturated polyester process because packing or partition trays provide a better mass transfer and the multi-stage effect in the column. But considering the lack of information about the behavior of counter-currently operated bubble columns in the presence of structured packing or partition trays and in a viscous system, a systematic investigation on the gas holdup, axial dispersion and mass transfer in the packed bubble column and the trayed bubble column is undertaken in chapter 5. Four different types of structured packings (Super-Pak, Flexipac, Mellapak and Gauze) and two types of perforated partition trays (with 25% and 40% tray open area) are used to characterize the packed and trayed bubble column, respectively. It is observed that the packed and trayed bubble columns improve the gas holdup and mass transfer compared to the empty bubble column and reduces the axial dispersion significantly. Particularly, the Gauze packing improves the gas holdup and mass transfer and, sufficiently reduces the axial dispersion. In contrast, Super-Pak offers only a modest improvement because of its open structure. Comparison of the experimental data of the packed and trayed bubble column indicates that the partition trays improve the bubble column in the same order as packing. The gas holdup, axial dispersion and mass transfer depend more strongly on the gas velocity compared to the liquid velocity. The liquid viscosity also significantly influences these parameters and therefore the empirical correlations obtained from the air-water system cannot be applied for the viscous system. Moreover, experimental data of the packed, trayed and empty bubble column are correlated by dimensionless numbers. Empirical correlations for the gas holdup, Bodenstein number (for the axial dispersion coefficient) and Stanton number (for the volumetric mass transfer coefficient) as a function of the Froude and Gallilei dimensionless numbers are proposed.

In chapter 6, an experimental pilot plant validation of the reactive distillation process for the polyester synthesis is presented. Two different configurations are investigated: 1) a reactive distillation column and 2) a reactive distillation column coupled with a pre-reactor. Due to a relatively short residence time of 0.32 hours and an operating temperature of 190°C in case of the first configuration, a maximum conversion of 37% was achieved; which indicates monoester formation in the reactive distillation column. In the case of the second configuration, a 90% conversion is achieved within 0.55 hours at a temperature of 250°C in the reactive distillation column coupled with a pre-reactor; which confirms the polyester formation in the reactive distillation column. The extended rate-based model developed in chapter 3 is used to simulate the pilot reactive distillation column. The model predicted the experimental data (acid value, conversion, isomerization and saturation fraction, number-average molecular weight, the degree of polymerization and water fraction in the distillate) adequately (5-22%). Moreover, the product specifications of the polyester produced at 250°C in the reactive distillation column is in the range of polyesters produced in the traditional industrial batch reactor setup. Furthermore, discoloration of the polyester was hardly noticed even though the column was operated at 250°C.

Finally in chapter 7, the validated model is used to find the best suitable internal and feed configurations of the reactive distillation process for unsaturated polyester synthesis. Moreover, multi-product simulations are performed to find the operational parameters for producing two different grades of polyester in the same equipment. Finally, the product transition time during product changeover is determined. The criteria to select the best configuration are minimum volume and energy requirement to produce 100 ktonnes/year polyester. First the best suitable internal for the column is identified and then the best suitable feed configuration is identified. From simulations, we concluded that the configuration which contains the reactive stripping section as a packed bubble column and the reactive rectifying section as a packed column requires minimum volume and energy to produce 100 ktonnes/year polyester. With respect to the feed configuration, we concluded that the feeding of monoesters to the reactive distillation column significantly intensifies the polyester process compared to an anhydrous reactant fed to the column. Moreover, the product transition time in this configuration is also significantly lower compared to the other configurations.

In conclusion, a reactive distillation column coupled with a pre-reactor is the most promising alternative to continuously produce unsaturated polyesters. It requires a factor 10 (90%) lower volume, a factor 15 (93%) lower production time and a factor 3 (66%) lower energy as compared to the traditional batch reactor process to produce 100 ktonnes/year of polyester. Hence, the reactive distillation process improves the unsaturated polyester synthesis in all domains of structure, energy and time compared to the traditional batch reactor process coupled with a distillation column.

Contents

Acknowledgments……………………………………………………………………...............i

Summary…………………………………………………………………...........................iii

Chapter 1 – Introduction………………………………………………………………….1

Chapter 2 – Process modeling for unsaturated polyesters synthesis……….......................11

Chapter 3 – Conceptual design of the reactive distillation process………………………..29

Chapter 4 – A systematic framework for the economical and technical evaluation of reactive distillation processes………………………………………………………………51

Chapter 5 – Gas holdup, mass transfer and axial dispersion in the bubble column with and without internals…………………………………..69

Chapter 6 – Validation of the reactive distillation concept and model by pilot plant testing……………………………………………………...91

Chapter 7 – Evaluation of configuration alternatives for the multi-product polyester synthesis by reactive distillation………………………………………………………………….105

Chapter 8 – Conclusion and outlook…………………………………………………..119

Appendix………………………………………………………………………………….123

List of publications…………………………………………………………………….129

Curriculum vitae…………………………………………………….…………….131

Chapter 1

Introduction

In this chapter we briefly review unsaturated polyesters; the usage of raw materials, the application of unsaturated polyester resins and, worldwide supply and demand of the unsaturated polyester resins are discussed. Moreover, the current industrial polyester batch process and why a reactive distillation can be an attractive alternative for the synthesis of unsaturated polyester are discussed. Finally, the motivation behind the research work, objectives and outline of the thesis are presented.

1.1 Unsaturated polyesters

Unsaturated polyester resins are step-growth polymers formed by the interaction of stoichiometric mixtures of unsaturated and saturated dibasic acids or anhydrides with dihydric alcohols or oxides [1-3]. The unsaturated acid component is essential for the reactivity of the low molecular weight polymers formed and is derived primarily from 1,2-olefinic dibasic acids such as maleic acid or anhydride [3]. The solutions of unsaturated polyesters are further blended with unsaturated co-reactant liquid monomers such as styrene to enhance the reactivity and processibility [1, 3]. Free radical catalysts are used to initiate the cross-linking reactions between the unsaturated polyester and the unsaturated co-reactant monomer. This blend is rapidly transformed into a low viscosity resin and a rigid thermoset plastic state, comprising a three-dimensional polymer network.

The degree of unsaturation in both the polyester polymer and liquid monomer determines the complexity and physical characteristics of the cross-linked network, although properties such as hardness, flexibility, heat resistance, fire retardance, and others can be modified by substitution with glycols and saturated dibasic acids into the polyester polymer backbone [2]. Although other unsaturated monomers can be more effective in enhancing specific properties of the cross-linked plastic, styrene, in accordance with general cost-performance criteria, is the principal co-reactant monomer in commercial formulations [3].

The evolution in petro-chemistry since 1945 has provided an extensive range of raw materials for polyester resin synthesis, resulting in the development of a family of resins whose composition and performance versatility are unmatched by most other polymeric materials. In early research, polyester resins formed by condensing tartaric acid, glycerol, succinnic acid, and salicylic acid supplied the basis for many scientific studies. Reactions between glycerol and phthalic anhydride were also investigated and when these compositions were modified with the fatty acids of unsaturated vegetable drying oils for use as protective coatings, their commercial potential was recognized [1]. Later, propylene glycol, ethylene glycol, maleic anhydride and phthalic anhydride were identified as the potential raw materials to produce unsaturated polyesters [3]. This is due to enhanced and better reactivity with styrene monomer and easily adaptable to simple fabricating process under ambient conditions. This classical formulation has remained essentially unchanged and is typically used in most of the industrial processes. This family of unsaturated polyester resins is known as (ortho) phthalic resins or general-purpose resins in view of their commercial derivation and wide adaptability and performance characteristics. Even though the applications of this formulation is successfully commercially acknowledged, the phthalic resins exhibit certain limitations with regard to heat resistance, fire retardancy, resistance to chemical attack and processibility [1, 4, 5]. Therefore, new families of polyester resins have evolved with improved and specialized properties and, characteristics of certain organic constituents [4, 5]. These organic constituents are aromatic derivatives such as isophthalic and terephthalic acid or diols derived from bisphenol, and aliphatic constituents such as adipic acid, 1, 4 butandiol and diethylene glycol [1, 4]. In view of the wide choice of functional components, unsaturated polyester resins can be tailor-made with specific and exclusive properties. Most unsaturated polyester resins in commercial applications include different types of glycols, dibasic acids and monomers as listed in table 1.1.

Table 1.1: raw materials of polyester resin in descending order of commercial use [1]

Glycol	Dibasic acid Or anhydride	Unsaturated acid Or anhydride	Unsaturated monomer for blending
propylene glycol	phthalic anhydride	maleic anhydride	styrene
propylene glycol and ethylene glycol/ diethylene -glycol	phthalic anhydride	maleic anhydride	styrene
ethylene glycol	isophthalic acid	fumaric acid	sinyl toluene
diethylene glycol	adipic acid	methacrylic acid	methyl methacrylate
neopentyl glycol	chlorendic anhydride	acrylic acid	diallyl phthalate
dipropylene glycol	tetrabromophthalic anhydride	itaconinc acid	$\tilde{\alpha}$ methylstyrene
dibromoneopentyl -glycol	tetrahydophthalic anhydride		trially cyanurate
bisphenol -dipropoxy ether	terephthalic acid		divinylbenzene

The cross-linked unsaturated polyester resins have limited structural integrity therefore they are often combined with fiberglass or mineral fillers before cross-linking to enhance their mechanical strength. Although the resin is combined with fiberglass, they are lightweight and durable. They are referred to as fiberglass-reinforced plastic (FRP). FRP composites are consumed primarily in the construction, marine and land transportation industries, although they also find use in a variety of other applications [1, 3]. Moreover, non-reinforced cross-linked unsaturated polyester resin is used to make cultured marble and solid surface counter tops, gel coats, automotive repair putty and filler, and other items such as bowling balls and buttons [1, 3].

The consumption of unsaturated polyester resin in the primary end markets - construction, automotive and marine depends on the performance of the general economy and tends to swing dramatically with any change in gross domestic product (GDP). The world supply and demand for unsaturated polyester resins in 2004-2009 according to SRI consulting is shown in figure 1.1 [6]. The world's five largest unsaturated polyester resin producers are Ashland, Reichhold, AOC, Total and DSM; representing almost 40% of world capacity. The economic recession of 2008-2009 has affected all the industries in the world including unsaturated polyester resin market. The unsaturated polyester resin market is declined in 2009 and therefore, sales of these major players have also declined by 20-30% approximately. Over the next 5 years from 2010, the total unsaturated polyester consumption across the globe is expected to continue with strong growth at 9.7% CAGR (compound annual growth rate) [7]. The unsaturated polyester market is expected to reach US $ 7.5 billion by 2015 [7].

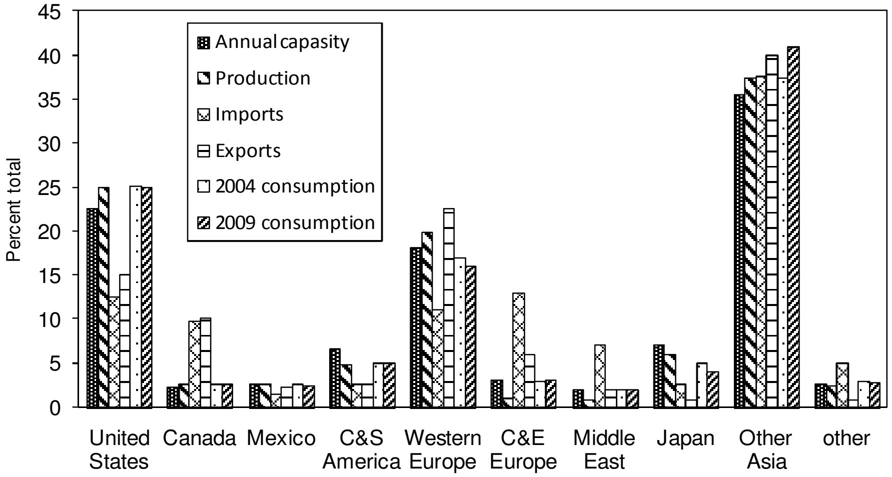

Figure 1.1 World supply and demand for unsaturated polyester resins- 2004-2009 [6]

1.2 Industrial production process

Unsaturated polyesters are produced by polycondensation of saturated and unsaturated carboxylic acids with glycols. Water is formed as by product during the polycondensations reaction [8]. The glycols and dibasic acids are fed in an equimolar ratio to the reactor vessels where they are being heated, reacted and cooled. In order to prevent the discoloration due to the oxidation reaction, the reactor is continuously purged with nitrogen. Xylene or toluene is added as stripping agent to the reaction mixture to assist the fast removal of water. However, the stripping agent causes impurity in the polyester resins and is therefore not preferred [9]. The process is carried out at atmospheric pressure and as replacement to the stripping agent for the fast removal of water from the reaction mixture; vacuum is applied at the end of process [9, 10]. The reactor is gradually heated from ambient temperature up to 210°C by supplying heat from hot oil circulated in the jacket [3, 9]. Agitation is maintained throughout the reaction to dissipate heat and promote the evaporation of water. The water starts to evaporate at 150°C. During the reaction some glycol is vaporized and lost. This loss of glycols by evaporation from the reaction mixture can be largely avoided by coupling the reactor vessel with an overhead fractionation column. An industrial unsaturated polyester process unit consists of a reactor, a flash separation unit and a distillate accumulator which are shown in figure 1.2. A 5 to 10% excess glycol is used to compensate for any glycol losses that may occur during the course of reaction [2, 11, 12]. Cis-trans isomerization generally occurs during polyesterification of unsaturated dibasic acids and anhydrides [13]. This is due to the use of maleic anhydride, which becomes incorporated into the polymer chains mostly as fumarate groups. The polymerization of maleic anhydride with propylene glycol gives almost 70 to 90% fumarate groups and 10 to 30% maleic groups [13]. The total production time (dosing + heating + reaction + cooling) is around 12 hours [9]. The polyesterification reaction is continued until the acid value of the polyester melt reaches around 25 mg/g and the required number-average molecular weight (M_n) is between 1000 and 2000 [11, 12]. The reactor is then cooled to 90°C and pumped into the blending tank containing vinyl monomer (styrene) to which an inhibitor (hydroquinone) is added which avoids the premature gelation and to extend shelf life to at least 6 months [1, 3].

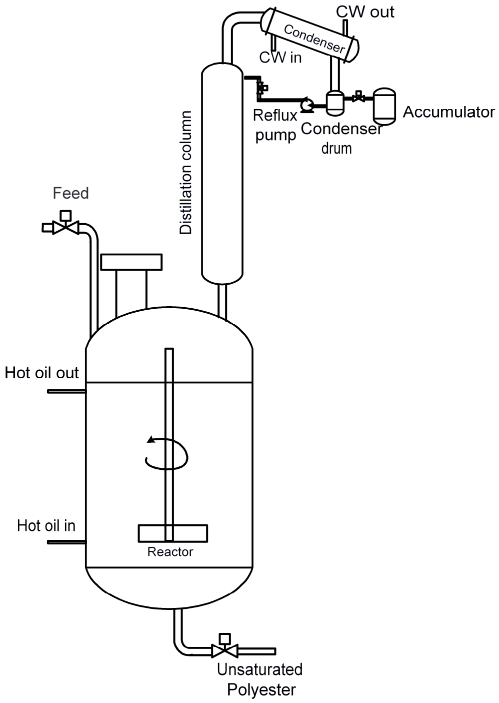

Figure 1.2: Industrial unsaturated polyester process unit

1.3 Reactive distillation

A Polyesterification reaction is equilibrium-controlled, and continuous removal of water is necessary to obtain high conversions [10, 14, 15]. A promising alternative for the intensification of this process is reactive distillation, which provides an alternative to the traditional processing scheme by combining the reaction and separation in a single unit as shown in figure 1.3. Since the processing units are reduced and the heat is directly integrated between reaction and separation, the capital investments as well as the utility costs can be reduced [16-22]. The overall conversion can also be increased by the continuous removal of the by products from the reaction zone through distillation and drives the equilibrium-limited reactions to completion [16-22].

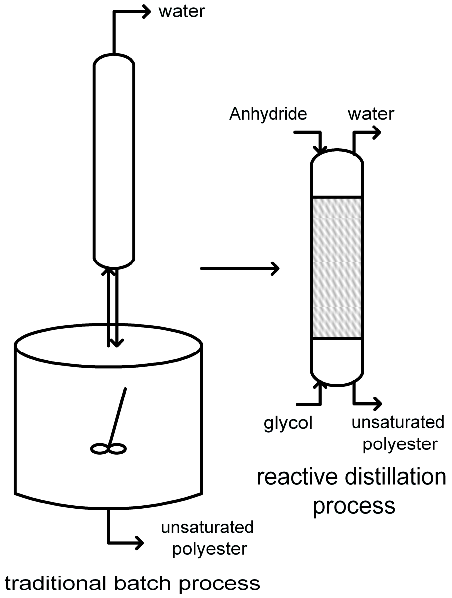

Figure 1.3: Unsaturated polyester process intensification by reactive distillation

Reactive distillation has been used extensively to produce esters from alcohols and carboxylic acids [23]. The production of esters from carboxylic acid and alcohol occurs by a reversible chemical reaction which also results in water as by-product. The maximum amount of ester formed is limited by the chemical equilibrium between forward and reverse reactions. Without simultaneous distillation, the conversion of carboxylic acid into ester would be limited by the accumulation of ester and water within the reactor. Alternatively, in a continuous process, the conversion could be increased by loading the reactor with an excess of alcohol, but this would only complicate the subsequent separation problem. Reactive distillation provides an economic and efficient method for bringing the reaction to near completion [19-24]. Along with esterification, reactive distillation is also potential candidate for trans-esterification, etherification, nitration, condensation and alkylation reactions [21, 22].

The concept of combining the reaction and separation for the enhancement of overall performance is not new to the chemical engineering world. The recovery of ammonia in the classic Solvay process for soda ash in the 1860s may be the first commercial application of reactive distillation [22]. The commercial success of reactive distillation for the production of methyl tert-butyl ether (MTBE) and methyl acetate demonstrated the ability of reactive distillation to render the cost effectiveness and compactness to the chemical plants [21, 22]. Approximately, more than 150 industrial scale reactive distillation columns are operated worldwide at the capacity of 100-300 ktonnes/year [16, 17]. CDTECH and Sulzer Chemtech are the major commercial technology providers for reactive distillation. Scientific literature and patents on reactive distillation are abundantly reported since 1920s [16, 17, 21, 22]. Extensive overviews of industrial application, feasibility analysis, design and synthesis methods, modeling strategy and internal design of reactive distillation is reported in several papers [18, 19, 21-23, 25-35].

1.4 Problem statement

Unsaturated polyester resins are produced from a wide range of raw materials. Raw material selection depends on the desired physical and chemical properties of the end product. In a continuous process, many product changeovers are required for relatively short-time of production runs. Therefore, the multi-product plants for unsaturated polyester production are equipped with batch reactors of various sizes and thereby these plants provide flexibility towards the multi-product production environment, the usage of various type and number of raw materials, and the way and timing of dosing of these materials. Hence, batch technology in the first place does not suffer from differences in kinetics and/or thermodynamics of the various production processes. Moreover, batch technology can easily adapt to these changes just by changing the batch parameters such as pressure, temperature and residence time. However, batch technology also has clear disadvantages, which are difficult to overcome, like the limited volumetric efficiency, the rather long dosing, heating and cooling times and most important, the inevitable batch to batch variations with respect to quality. This clearly highlights that a need could exist for a new technology which can overcome the disadvantages of current unsaturated polyester process and make the unsaturated polyester process smart and efficient.

For the continuous production of esters or other poly-condensates, the potential candidates are reactive distillation, water removal through pervaporation membranes and spinning disc reactors [36]. Although pervaporation membrane and spinning disc reactor technologies hold the specific advantage that the internal volume of the equipment is small which allows for fast and smooth product changeovers, both technologies do not qualify as reasonable alternatives for the traditional polyester process [37]. The membrane technologies suffer from fouling and the difficulty to produce reliable membranes which can operate at the required reaction temperatures [37]. The spinning disc reactors are indeed capable of speeding-up the reaction rate due to fast water removal, but they are difficult to operate if more residence time is required [37]. Moreover, the potential of an optimized reactive distillation column makes both technologies no reasonable candidates for the polyester production.

Multi-product production of relatively small capacities in a reactive distillation column is not yet addressed in the scientific literature and the current scientific and industrial research in the area of reactive distillation reported in the literature is limited to a single product produced at relatively large capacities. Therefore application of these studies is not useful to evaluate the multi-product production in a reactive distillation column. Hence, in order to be able to apply reactive distillation technology in the polyester industry, novel concepts need to be developed which allow the combination of a significant increase in volumetric productivity with sharp product transitions while switching from one grade to another.

1.5 Objectives and outline

In this research work, the goal is to develop a reactive distillation process for the production of unsaturated polyester from anhydrides and glycols. The main objectives of this research work are:

1. develop reliable dynamic and steady state models for the reactive distillation process
2. provide the proof of the concept that the polyester can be produced in the reactive distillation column by conducting experiments at the reactive distillation pilot plant
3. validate the developed model with experimental results of the reactive distillation pilot plant
4. obtain the model parameters such as gas holdup, mass transfer coefficient and liquid back mixing by conducting experiments
5. identify the best internal and feed configurations of the reactive distillation process, which require a minimum volume and energy requirement to produce unsaturated polyester combined with a minimum product transition time during the product changeover.

In chapter 2 a dynamic model for the industrial batch process is developed to validate the kinetic and thermodynamic models and their parameters. A kinetic model and its parameters are obtained from literature and the interaction parameters for the polymer NRTL (nonrandom theory of liquid) non ideal thermodynamic model are estimated. Moreover, the influence of ideal and non ideal thermodynamic models on the description of the polyester process is compared.

In chapter 3 a conceptual design of the reactive distillation process for the synthesis of unsaturated polyester is performed and, the design and operational parameters are obtained. Moreover, the simulation results of the reactive distillation process were compared with the traditional polyester process to obtain the improvement gained by reactive distillation application. After finding that reactive distillation is an attractive alternative for the polyester synthesis, a more in depth analysis is performed. Particularly, the influence of the liquid back mixing on the description of the reactive distillation process, product transition time, the amount of undesired product formation during the product changeover is investigated.

In chapter 4 a systematic framework is developed for the economical and technical evaluation of the reactive distillation process based on dimensionless numbers, kinetic, thermodynamic and mass transfer limits. Moreover, a technical framework is developed which provides a guideline for the reactive distillation process limitations, working regime and requirements for internals as well as the models needed for reactive distillation. To demonstrate the applicability of the proposed framework, various industrial relevant case studies are examined.

In chapter 5 the gas holdup, axial dispersion and mass transfer correlations are obtained for the empty bubble column, packed bubble column and trayed bubble column by conducting experiments. Four different types of structured packings are used to obtain the correlations for the packed bubble column and two different types of sieve trays are used to obtain the correlations for the trayed bubble column.

In chapter 6 the experimental results obtained from the reactive distillation pilot plant are discussed and the polyester produced in the pilot plant is compared with the polyester produced in industry. Moreover, the experimental results are compared with the simulation results in order to check the validity of the developed model.

In chapter 7 the different internal and feed configurations for the reactive distillation process are examined and the best suitable configuration is identified on the basis of minimum requirement of volume and energy to produce 100 ktonnes/year polyester. Moreover, the multi-product simulations are performed to find the operational parameter for producing two different grades of polyester and to find the product transition time during the product changeover.

In chapter 8 conclusions and recommendations for the future work are presented.

References

[1] H.F. Mark, Encyclopedia of Polymer Science and engineering, 2 ed., Wiley-Interscience, 1988.
[2] E.E. Parker, Unsaturated polyesters, Industrial & Engineering Chemistry, 58 (1966) 53.
[3] P. Penczek, P. Czub, J. Pielichowski, Unsaturated Polyester Resins: Chemistry and Technology, in: Crosslinking in Materials Science, Springer Berlin / Heidelberg, 2005, pp. 405.
[4] B. Cherian, E.T. Thachil, Synthesis of unsaturated polyester: Effect of choice of reactants and their relative proportions, International Journal of Polymeric Materials, 53 (2004) 829 - 845.
[5] B. Cherian, E.T. Thachil, Synthesis of Unsaturated Polyester Resin: Effect of Sequence of Addition of Reactants, Polymer-Plastics Technology and Engineering, 44 (2005) 931 - 938.
[6] H. Chinn, Y. Ishikawa, U. Loechner, Unsaturated polyester resins, in, SRI consulting, 2004.
[7] Lucintel, The Global Unsaturated Polyester Resin Market 2010-2015: Trends, Forecast and Opportunity Analysis, in, Lucintel - Global market research firm, 2010.

[8] W.H. Carothers, Studies on polymerization and ring formation. I An introduction to the general theory of condensation polymers, Journal of the American Chemical Society, 51 (1929) 2548.
[9] M.P. Stevens, J.D. Gardner, Reduction in Processing Time of Unsaturated Polyesters, Industrial & Engineering Chemistry Process Design and Development, 4 (1965) 67.
[10] M. Shah, E. Zondervan, A.B. de Haan, Modelling and simulation of an unsaturated polyester process, Journal of applied sciences, 10 (2010) 2551-2557.
[11] R. Jedlovčnik, A. Šebenik, J. Golob, J. Korbar, Step-growth polymerization of maleic anhydride and 1,2-propylene glycol, Polymer Engineering & Science, 35 (1995) 1413.
[12] J. Korbar, J. Golob, A. Šebenik, Process of unsaturated polyester resin synthesis on a laboratory and industrial scale, Polymer Engineering & Science, 33 (1993) 1212.
[13] S.S. Feuer, T.E. Bockstahler, C.A. Brown, I. Rosenthal, Maleic-Fumaric Isomerization in Unsaturated Polyesters, Industrial & Engineering Chemistry, 46 (1954) 1643.
[14] P.J. Flory, Kinetics of Polyesterification: A Study of the Effects of Molecular Weight and Viscosity on Reaction Rate, Journal of the American Chemical Society, 61 (1939) 3334.
[15] T. Salmi, E. Paatero, P. Nyholm, M. Still, K. Narhi, Kinetics of melt polymerization of maleic acid phthalic acids with propylene glycol, Chemical Engineering Science, 49 (1994) 5053.
[16] J. Harmsen, Reactive distillation: The front-runner of industrial process intensification: A full review of commercial applications, research, scale-up, design and operation, Chemical Engineering and Processing, 46 (2007) 774.
[17] J. Harmsen, Process intensification in the petrochemicals industry: Drivers and hurdles for commercial implementation, Chemical Engineering and Processing: Process Intensification, 49 (2010) 70.
[18] K. Huang, Q. Lin, H. Shao, C. Wang, S. Wang, A fundamental principle and systematic procedures for process intensification in reactive distillation columns, Chemical Engineering and Processing: Process Intensification, 49 (2010) 294.
[19] R. Krishna, Reactive separations: more ways to skin a cat, Chemical Engineering Science, 57 (2002) 1491.
[20] A. Stankiewicz, Reactive separations for process intensification: an industrial perspective, Chemical Engineering and Processing, 42 (2003) 137.
[21] R. Taylor, R. Krishna, Modelling reactive distillation, Chemical Engineering Science, 55 (2000) 5183.
[22] K. Sundmacher, A. Kienle, Reactive distillation- status and future directions, Willey-VCH, 2003.
[23] H. Sawistowski, P.A. Pilavakis, Performance of esterification in a reaction-distillation column, Chemical Engineering Science, 43 (1988) 355.
[24] C. Noeres, E.Y. Kenig, A. Górak, Modelling of reactive separation processes: reactive absorption and reactive distillation, Chemical Engineering and Processing, 42 (2003) 157.
[25] A.M. Katariya, R.S. Kamath, K.M. Moudgalya, S.M. Mahajani, Non-equilibrium stage modeling and non-linear dynamic effects in the synthesis of TAME by reactive distillation, Computers & Chemical Engineering, 32 (2008) 2243.

[26] G. Buzad, M.F. Doherty, Design of three-component kinetically controlled reactive distillation columns using fixed-points methods, Chemical Engineering Science, 49 (1994) 1947.

[27] A.C. Dimian, C.S. Bildea, F. Omota, A.A. Kiss, Innovative process for fatty acid esters by dual reactive distillation, Computers & Chemical Engineering, 33 (2009) 743.

[28] A. Higler, R. Krishna, R. Taylor, Nonequilibrium cell model for multicomponent (reactive) separation processes, AIChE Journal, 45 (1999) 2357.

[29] J.R. Jackson, I.E. Grossmann, A disjunctive programming approach for the optimal design of reactive distillation columns, Computers & Chemical Engineering, 25 (2001) 1661.

[30] D.B. Kaymak, W.L. Luyben, Quantitative comparison of dynamic controllability between a reactive distillation column and a conventional multi-unit process, Computers & Chemical Engineering, 32 (2008) 1456.

[31] E. Kenig, K. Jakobsson, P. Banik, J. Aittamaa, A. Górak, M. Koskinen, P. Wettmann, An integrated tool for synthesis and design of reactive distillation, Chemical Engineering Science, 54 (1999) 1347.

[32] A.A. Kiss, Separative reactors for integrated production of bioethanol and biodiesel, Computers & Chemical Engineering, 34 (2010) 812.

[33] A. Kolodziej, M. Jaroszynski, H. Schoenmakers, K. Althaus, E. Geißler, C. Übler, M. Kloeker, Dynamic tracer study of column packings for catalytic distillation, Chemical Engineering and Processing, 44 (2005) 661.

[34] Y.-D. Lin, J.-H. Chen, J.-K. Cheng, H.-P. Huang, C.-C. Yu, Process alternatives for methyl acetate conversion using reactive distillation. 1. Hydrolysis, Chemical Engineering Science, 63 (2008) 1668.

[35] M.J. Okasinski, M.F. Doherty, Design Method for Kinetically Controlled, Staged Reactive Distillation Columns, Industrial & Engineering Chemistry Research, 37 (1998) 2821.

[36] K.V.K. Boodhoo, R.J. Jachuck, Process intensification: spinning disc reactor for condensation polymerisation, Green Chemistry, 2 (2000) 235.

[37] J. Kluytmans, Reactive distillation for multi-product continuous plants, in, Dutch separation technology insititute, 2006.

Chapter 2

Process modeling for unsaturated polyesters synthesis

In this chapter a dynamic model for a batch-wise operated reaction vessel connected to a flash separation unit is developed in order to validate the kinetic and thermodynamic models and their parameters. This model includes kinetics, description of the change of rate order during the reaction, the polymer NRTL non-ideal thermodynamic model based on non-random theory of liquid (NRTL) and mass balances. The reaction between maleic anhydride and propylene glycol has been taken as a case study. The reaction scheme is complex and the proposed model takes four types of reactions into account; ring opening, polyesterfication, isomerization and saturation reactions. The acid value of the polyester, number-average molecular weight, distilled mass and glycol concentration in the distillate have been subsequently used to validate the model and the model predicts these important variables reliably. The process description is improved by using the vapor liquid equilibrium data predicted from the polymer NRTL model. Particularly, the prediction of distilled mass (regression coefficient (R^2) = 0.995) and the prediction of propylene glycol concentration (R^2 = 0.97) in the distillate are significantly improved.

2.1 Introduction

The American chemist Wallace Carothers has discovered in the late 1920's that reactions between dibasic acids and diols produce molecules with a high molecular weight [1]. These molecules contain multiple ester linkage and are therefore named polyester. The polyesterification of dicarboxylic acids with diols is a commonly applied process in the polymer industry. Polyesterification reactions are usually equilibrium-controlled, and continuous removal of water is necessary to obtain high conversions. Thus the polyesters are produced in semi-batch reactors and usually a distillation column is directly coupled to the reactor vessel in order to avoid excessive loss of the reactants during a batch, and separate nearly pure water from the polymer mixture in the reactor to increase conversion.

The kinetics of the polyesterification reaction between dicarboxylic acids and diols was studied for the first time by Flory in 1939 [2]. Since then a large number of kinetic models have been reported for the polyesterification reaction [2-10]. Flory [2] has investigated that the reaction order of self-catalyzed polyesterification changes during the reaction. The reaction follows first order with respect to the acid at the beginning and second order at the end of the reaction. This increase in reaction order is due to the fact that the dielectric constant of the mixture decreases with the conversion, which in turn affects the equilibrium ionization constant of the acid [3, 7]. Fang et al. [7] developed a rate equation for the polyesterification reaction, which takes into account these phenomena. However, this implies an introduction of a large number of adjustable parameters in the rate equation. Beigzadeh et al. [4] has studied the polyesterification of adipic and fumaric acid with ethylene glycol, both in the absence and presence of a foreign acid, and subsequently attempted to fit the data to a number of models. They conclude that only the model proposed by Chen and Wu [5] gives a satisfactory fit to experimental observations. However, this model does not include the changing rate order phenomena. The models proposed by Flory [2], Tang and Yao [6], Fang et al. [7] and Lin and Hsieh [8] are found to be incapable of reproducing the experimental data. Paatero et al. [3] and Salmi et al. [10] have proposed simple rate equation for polyesterification reaction which could describe the polyesterification over the entire range of conversions. The proposed rate equation by Paatero et al. [3] and Salmi et al. [10] consists of only two adjustable parameters.

The synthesis of polyester is carried out with a combination of different reagents for varying physical and chemical properties [11]. One of the reagents in the synthesis of polyester is always unsaturated carboxylic acid [11]. The presence of unsaturated carboxylic acids essentially leads to a complex reaction mechanism. The double-bond of the acid undergoes *cis-trans* (maleate-fumarate) isomerization [12] and the double-bond saturation takes place through the Ordelt reaction [13]. The kinetics of the maleate-fumarate isomerization with different glycols has been studied and confirmed that the isomerization reaction is acid catalyzed and of second order with respect to the carboxylic acid [12]. The kinetics of the electrophilic addition of alcohol to the double bond of the carboxylic acids is studied by Fradet and Marechal [13], who used unsaturated dicarboxylic acids and propylene glycol as model compounds and showed that the reaction is acid catalyzed and of first order with respect to the carboxylic acid and the alcohol. Although the reactions appearing in this kind of polyesterification are well known, detailed kinetics studies of the esterification reaction and side reactions of different carboxylic acids and diols mixtures are limited [14]. Only Paatero et al. [3] and Salmi et al. [10] have reported a detailed kinetic model for the reactions between maleic anhydride and propylene glycol. They have used empirical functions to fit distillate composition profiles with experimental data. Fitting is required to correct the liquid phase mass balance. However, the fitted empirical parameters are limited to isothermal and isobaric operating conditions which is not a case in the industrial application. Hence, although the kinetic model is complete, it cannot describe the complete process due to incapability of predicting vapor phase composition, which is an important factor to describe the combined reactive separation system.

The complete process model for the synthesis of unsaturated polyester process should be composed of 1) a detailed kinetic model consisting of changing order rate equations for polyesterification, isomerization and double bond saturation reactions 2) a thermodynamic model to obtain components compositions at inter phase of vapor and liquid 3) a mass transfer model to predict mass transfer from liquid to vapor phase. To the best of our knowledge, such a complete process model for the non-linear polyesterification process is not yet addressed in the scientific literature. In earlier work [14], we reported a dynamic model for a batch reactor that includes detailed kinetics describing the change of rate order during the reaction and the ideal behaviour thermodynamic model. However, the ideal behaviour assumption prohibits a reliable prediction of the vapor liquid equilibrium and thus the concentration of components in the vapor and liquid phase. Therefore, in the present work we have extended the previously developed reaction model with non-ideal behaviour thermodynamics to improve the description of the vapor liquid equilibrium. Non-ideal behaviour of the unsaturated polyester mixture and the effect of an unsaturated polyester mixture on the activity of the components have to our knowledge not been addressed yet in the scientific literature.

The aim of this chapter is to develop the process model for the synthesis of unsaturated polyester and to show how the incorporation of vapor liquid equilibrium data improves the description of polyester kinetics. In addition to that, the vapor phase compositions predicted by ideal behaviour thermodynamics and non-ideal behaviour thermodynamics are compared and an improvement in the vapor phase composition prediction is noticed. The process model is developed in Aspen Custom Modeler and the polyesterification of maleic anhydride with propylene glycol is used as model reaction in this study. This model is validated with the experimental data obtained from Salmi et al. [10], Larry et al. [15] and Korbar et al. [16].

2.2 kinetic modeling

2.2.1 Theory

The synthesis of unsaturated polyester from maleic anhydride and propylene glycol involves four types of reactions. First the reactants, anhydride (A) and glycol (G) are mixed and heated to temperatures higher than 60-80 ^{O}C. A very fast exothermic reaction ($\triangle H$ = -40 KJ/mol) occurs and produces an acid end group (COOH) and an alcohol end group (OH) with an ester (E) bridge as shown in eq. (2.1).

$$A + G \rightarrow COOH + E + OH \qquad (2.1)$$

Esterification proceeds by the reaction between acid and alcohol end groups to form new ester bridges (POLY) and water, or by reaction of a glycol hydroxyl group with an acid end group to form an ester bridge (POLY) and water as shown in eq. (2.2).

$$COOH + OH \leftrightarrows POLY + WATER \qquad (2.2)$$

Half of the water is consumed in the ring opening reaction as the ring of anhydride opens by reacting with water. The double-bond of the acid undergoes *cis-trans* isomerization [12] and the double-bond saturation takes place through the Ordelt reaction [13]. The double bond in maleic acid (MA) is isomerized at the higher reaction temperatures and produces fumaric acid (FA) according to eq. (2.3).

$$\text{Cis (MA)} \leftrightarrows \text{Trans (FA)} \qquad (2.3)$$

When the reaction temperature exceeds 180^{o}C maleic acid effectively relieves the strain by transforming to the more planar trans-fumarate isomer, which reduces the steric congestion [17, 18]. The corresponding fumarate polymers are subject to less steric interference as the trans form and are able to assume a planar configuration, displaying reactivity almost 20 times of the maleate reaction products in subsequent copolymerization reaction with styrene [19]. The isomerization of maleate esters and oligomers to the corresponding fumarate derivatives during the polyesterfication process is of fundamental importance in the development of optimum physical characteristics [11]. The fumarate derivative gives stability to the polyester [11]. Hence, the byproducts resulting from the side reactions are not regarded as a loss. The double bond in maleic acid (MA) is saturated by reaction with glycol and produces saturated acid (SACID) according to eq. (2.4).

$$\text{Dbb (MA)} + \text{OH} \leftrightarrows \text{SatDbb (SACID)} \qquad (2.4)$$

The saturation of the double bond causes cross-linking in the polymer, and approximately 10-20 % of the double bonds are saturated in the preparation of the polyester [11, 13]. This side reaction occurs in the first reaction stage and the destruction of unsaturation is favored by higher initial temperatures. The thermal polymerization of maleic anhydride double bonds can also occur at elevated temperature, which resulting an optimum temperature for polyester production. The optimal temperature of the polyester process to avoid destruction of unsaturation and found optimal temperature is between 210°C and 220°C [11].

Table 2.1: The functional groups in the polyesterification of maleic anhydride and 1, 2-propylene glycol

Functional group	**Abbreviation**	**Structure**
Propylene glycol (PG) end group	R'OH	R'—OH
Maleic acid (MA) end group	RCOOH$_{1D}$	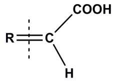
Fumaric acid (FA) end group	RCOOH$_{2D}$	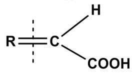
Saturated acid (SACID) end group	RCOOH$_{S}$	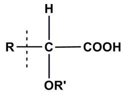
Maleate polyester (POLY$_{1D}$) monomer	RCOOR'$_{1D}$	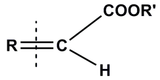
Fumarate polyester (POLY$_{2D}$) monomer	RCOOR'$_{2D}$	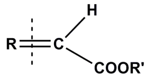
Saturated polyester (POLY$_{S}$) monomer	RCOOR'$_{S}$	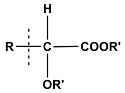
R refers to 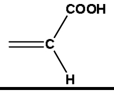	R' refers to	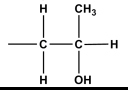

2.2.2 Rate equation

The three types of carboxylic acid (MA, FA and SACID) functional groups are involved in the esterification reaction. These three carboxylic acid functional groups produce three ester functional groups via an esterification reaction. The isomerized fumaric acid (FA) and saturated acid (SACID) functional groups esterify and produce isomerized polyester (POLY$_{2D}$) and saturated polyester (POLY$_{s}$) functional groups, respectively. Polyester

($POLY_{1D}$) functional group produces from maleic anhydride which also isomerizes and saturates to produce isomerized polyester ($POLY_{2D}$) and saturated polyester ($POLY_s$) functional groups, respectively. The isomerized acid (FA) and isomerized polyester ($POLY_{2D}$) functional groups also saturates and produces saturated acid (SACID) and saturated polyester ($POLY_s$) functional groups, respectively. The overall six basic functional groups of the carboxylic acids and esters, and hydroxyl group with their abbreviations are depicted in table 2.1. The three reactions, esterification, isomerization and saturation form a network of nine reactions. These reactions and their rate equations are summarized in table 2.2.

Table 2.2: Reactions and rate equations

Reactions	**Rate equations**
Esterification reactions:	
$RCOOH_{1D} + R'OH \leftrightarrows RCOOR'_{1D} + H_2O$	$r_1 = C^{n-1}_{RCOOH_{1D}}(k_1 C_{RCOOH_{1D}} C_{R'OH} - k'_1 C_{RCOOR'_{1D}} C_{H_2O})$
$RCOOH_{2D} + R'OH \leftrightarrows RCOOR'_{2D} + H_2O$	$r_2 = C^{n-1}_{RCOOH_{1D}}(k_2 C_{RCOOH_{2D}} C_{R'OH} - k'_2 C_{RCOOR'_{2D}} C_{H_2O})$
$RCOOH_S + R'OH \leftrightarrows RCOOR'_S + H_2O$	$r_3 = C^{n-1}_{RCOOH_{1D}}(k_3 C_{RCOOH_S} C_{R'OH} - k'_3 C_{RCOOR'_S} C_{H_2O})$
Isomerization reactions:	
$RCOOH_{1D} \leftrightarrows RCOOH_{2D}$	$r_4 = C^{n-1}_{RCOOH_{1D}}(k_4 C_{RCOOH_{1D}} - k'_4 C_{RCOOH_{2D}})$
$RCOOR'_{1D} \leftrightarrows RCOOR'_{2D}$	$r_5 = C^{n-1}_{RCOOH_{1D}}(k_5 C_{RCOOR'_{1D}} - k'_5 C_{RCOOR'_{2D}})$
Saturation reactions:	
$RCOOH_{1D} + 0.5\ R'OH \leftrightarrows RCOOH_S$	$r_6 = C^{n-1}_{RCOOH_{1D}}(k_6 C_{RCOOH_{1D}} C_{R'OH} - k'_6 C_{RCOOH_S})$
$RCOOH_{2D} + 0.5R'OH \leftrightarrows RCOOH_S$	$r_7 = C^{n-1}_{RCOOH_{1D}}(k_7 C_{RCOOH_{2D}} C_{R'OH} - k'_7 C_{RCOOH_S})$
$RCOOR'_{1D} + 0.5R'OH \leftrightarrows RCOOR'_S$	$r_8 = C^{n-1}_{RCOOH_{1D}}(k_8 C_{RCOOR'_{1D}} C_{R'OH} - k'_8 C_{RCOOR'_S})$
$RCOOR'_{2D} + 0.5R'OH \leftrightarrows RCOOR'_S$	$r_9 = C^{n-1}_{RCOOH_{1D}}(k_9 C_{RCOOR'_{2D}} C_{R'OH} - k'_9 C_{RCOOR'_S})$

The esterification, isomerization and saturation reactions have been thoroughly discussed by Paatero et al. [3], Chen et al. [5], Salmi et al. [9, 10], Jedlovcnik et al. [20] and Zetterlund et al. [21]. In this modeling, the rate expressions have been adopted from the literature [3, 10]. The variable rate order expression from Salmi et al. [10] has been changed by setting a different definition of the chemical equilibrium concentration and based on that a new rate expression is derived. Salmi et al. [10] has obtained the rate order (n) expression according to eq. (2.5) and (2.6) from the semi-empirical differential equation $dn = -pn^q dc_{RCOOH}$.

$$n = \left[1-(1-2^{1-q})\frac{C_0 - C_{COOH}}{C_0 - C_{eq}}\right]^{1/(1-q)} \tag{2.5}$$

$$= \left[1-(1-2^{1-q})X\right]^{1/(1-q)} \tag{2.6}$$

where, q is an adjustable exponent. This parameter is fitted in this work for the maleic anhydride and propylene glycol system. In this system the parameter q value is 7. The value for proportionality factor p is determined by integration of the differential equation using the limits $n = 1$, $C_{RCOOH} = C_0$ and $n = 2$, $C_{RCOOH} = C_{eq}$. C_0 is the initial concentration of maleic anhydride and C_{eq} is the equilibrium concentration. Salmi et al. [10] has considered the water and glycol vaporization effect to define the equilibrium concentration of carboxylic acid. In this paper, the equilibrium concentration of carboxylic acid is defined by eq. (2.7) and the water and glycol vaporization effect is incorporated in the dynamic batch reactor model by introducing the polymer NRTL thermodynamic model. The conversion of carboxylic acid is given by eq. (2.8).

$$C_{eq} = \frac{k'_E \, C_{COOR} C_{H_2O}}{k_E C_{OH}} \tag{2.7}$$

$$X = \frac{C_0 - C_{COOH}}{C_0 - C_{eq}} \tag{2.8}$$

The esterification, isomerization and saturation reactions are acid catalyzed and the strongest carboxylic acid gives the dominant catalytic effect. The maleic acid is the strongest acid with respect to all acids in the system. Hence, the main contribution to the catalytic effect is from maleic acid. The kinetic model presented in this paper accounts for the autocatalytic effect of the strongest carboxylic acid. Since only total carboxylic acid ($C_{COOH} = C_{COOH_{1D}} + C_{COOH_{2D}} + C_{COOH_S}$), total isomerization ($C_I = C_{COOH_{2D}} + C_{COOR'_{2D}}$) and total saturation ($C_S = C_{COOH_S} + C_{COOR'_S}$) concentrations can be measured experimentally, it is presumed that all esterification rate constants are equal, all isomerization rate constants are equal and all saturation rate constants are equal. These rate constants are derived from experimental data of Salmi et al. [10] and depicted in table 2.3.

Table 2.3: Experimental data from Salmi et al. [10]

T (^oC)	k_E (kg mol^{-1} hr^{-1})	$\frac{k_E}{k'_E}$ (-)	k_I (kg mol^{-1} hr^{-1})	$\frac{k_I}{k'_I}$ (-)	k_S (kg mol^{-1} hr^{-1})	$\frac{k_S}{k'_S}$ (-)
160	0.060	25	1.020	12.5	0.032	0.87
180	0.130	19	3.000	9.10	0.046	2.30
200	0.372	40	4.680	45.0	0.090	2.60
220	0.720	36	7.200	12.4	0.150	---
	$k_E = k_1 = k_2 = k_3$, $k'_E = k'_1 = k'_2 = k'_3$,		$k_I = k_4 = k_5$, $k'_I = k'_4 = k'_5$,		$k_S = k_6 = k_7 = k_8 = k_9$, $k'_S = k'_6 = k'_7 = k'_8 = k'_9$	

Table 2.4: Arrhenius parameters for the polyesterification reaction between maleic anhydride and propylene glycol

Reaction	**forward reaction**		**backward reaction**	
	k_o (kg mol^{-1} hr^{-1})	E_a (J/mol)	k_o' (kg mol^{-1} hr^{-1})	E_a (J/mol)
Esterification	72000000	75000	37200	59000
Isomerization	7620000	56000	10680	41700
Saturation	16380	47000	10560	49600

It is noted that experimental data of Salmi et al. [10] are intrinsic. The standard deviation of the experimental data is reported between 3% and 8% in Salmi et al. [10]. In this paper, the pre-exponential constant (k_o) and the activation energy (E_a) for forward and backward reactions are predicted from linear regression of the Arrhenius law ($k = k_o e^{-E_a/RT}$) and depicted in table 2.4.

2.3 Thermodynamic Modeling

2.3.1 Model selection

The current unsaturated polyester process is operated at low pressure (1 bar), and at the end of the process vacuum is applied to completely remove water from the polymer mixture. As the system is operating at 1 bar, the activity coefficient approach is sufficient to predict the vapor-liquid equilibrium. The vapor phase is ideal and the partial pressure of species *i* in the vapor phase, p_i equals to

$$p_i = x_i \gamma_i (x_i, T) p_i^{sat}(T) = y_i P \tag{2.9}$$

where, x_i is the liquid mole fraction of species *i*, $\gamma_i(x_i, T)$ is the activity coefficient of species *i* as function of liquid composition x_i, temperature T and P_i^{sat} is the vapor pressure of pure species *i*. The selection of the activity coefficient model is crucial to reliably predict the activity coefficients. None of the present models – Van Laar, Wilson, NRTL, UNIQUAC, Flory-Huggins and others are really mathematically correct, but each may be useful and superior for specific conditions [22, 23]. For strongly non-ideal systems, such as those where strong chemical interactions like hydrogen bonding occurs, the difference in the results from each model may be large. For completely miscible systems, the Wilson equation can give adequate results [24, 25]. If the system is highly polar, NRTL and UNIQUAC models usually generate the best results [26, 27].

As the unsaturated polyester system is highly polar and non-ideal, the only suitable models are the NRTL and UNIQUAC. From these possible models, the NRTL model is selected because the extension of NRTL model - the polymer NRTL model - includes the effect of polymer properties on the activity coefficients of the components. The main difference between the polymer NRTL model and Flory-Huggins model is that in the polymer NRTL activity coefficients model, the binary interaction parameters are independent of the polymer concentration and the polymer molecular weight [25, 26]. Furthermore, in the case of copolymers, the polymer NRTL binary parameters are independent of the relative compositions of the repeating units of the polymer chain. The polymer NRTL model [25] is summarized in table 2.5 and the binary interaction parameters of this model for the segment-segment interactions, segment-solvent interactions, and for the solvent-solvent interactions are used to predict the activity coefficients of the components including the polymer.

Table 2.5: The polymer NRTL model [25]

$$\ln \gamma_i = \ln \gamma_i^{NRTL} + \ln \gamma_i^{FH}$$

$$\ln \gamma_i^{FH} = \ln\left(\frac{\phi_i}{x_i}\right) + 1 - m_i \sum_j \left(\frac{\phi_j}{m_j}\right), \quad m_j = s_j P_j^{\varepsilon_j}, \quad \phi_i = \frac{n_i m_i}{\sum_k n_k m_k}$$

$$\ln \gamma_{i=s}^{NRTL} = \frac{\sum_j x_j G_{js} \tau_{js}}{\sum_k x_k G_{ks}} + \sum_j \frac{x_j G_{sj}}{x_k G_{kj}} \left(\tau_{sj} - \frac{\sum_k x_k G_{kj} \tau_{kj}}{\sum_k x_k G_{kj}} \right)$$

$$\ln \gamma_{i=p}^{NRTL} = \sum_i r_{i,p} \left[\frac{\sum_j x_j G_{ji} \tau_{ji}}{\sum_k x_k G_{ki}} + \sum_j \frac{x_j G_{ij}}{x_k G_{kj}} \left(\tau_{sj} - \frac{\sum_k x_k G_{kj} \tau_{kj}}{\sum_k x_k G_{kj}} \right) \right]$$

$$- \sum_i r_{i,p} \left[\frac{\sum_j x_{j,p} G_{ji} \tau_{ji}}{\sum_k x_{k,p} G_{ki}} + \sum_j \frac{x_{j,p} G_{ij}}{x_{k,p} G_{kj}} \left(\tau_{sj} - \frac{\sum_k x_{k,p} G_{kj} \tau_{kj}}{\sum_k x_{k,p} G_{kj}} \right) \right]$$

$$x_{i,p} = \frac{r_{i,p}}{\sum_j r_{j,p}} \quad \tau_{ji} = \frac{(g_{ji} - g_{ij})}{RT} \quad G_{ji} = \exp\left(-\alpha_{ji} \tau_{ji}\right)$$

2.3.2 Binary interaction parameters estimation procedure

The unsaturated polyester process is multicomponent reactive system. The vapor liquid equilibrium data could be determined experimentally for such reactive system by obtaining the measurements at the temperature where the reaction rates are very slow. However, such measurements may not be representative for the actual conditions of the combined reaction and separation unit and would be of limited use. Measurements could also be made in the absence of the catalyst if the reaction is catalytic driven. Unfortunately, the reactions involved in this process are auto catalyzed [2]. Thus, it is impossible to avoid reactions to carry out the vapor liquid equilibrium experiments.

In the absence of the experimental vapor liquid equilibrium data, the activity coefficients at infinite dilution are predicted from the group contribution methods of the modified UNIFAC model proposed by Weldich et al [27]. These activity coefficients at the infinite dilution for each binary system are used to calculate the binary interaction parameters for the polymer NRTL model. Since the polyester process is highly polar, the parameter α_{ji} of the polymer NRTL model for the polar system is equal to 0.3 [27]. There are 28 binary pairs required to represent the 8 component mixture. The activity coefficients at infinite dilution are only known experimentally for a binary system of propylene glycol and water. The activity coefficient of propylene glycol in water at infinite dilution and at $25^{\circ}C$ is reported to be 1 ± 0.2 [28]. The predicted activity coefficient of propylene glycol in water at infinite dilution and at $25^{\circ}C$ is 1.24 which shows good agreement with the experimental data of Sulieman et al. [28]. The predicted interaction parameters of the polymer NRTL model are tabulated in table 2.6. These interaction parameters are used to describe the vapor liquid equilibrium of the unsaturated polyester process.

Table 2.6: The polymer NRTL activity coefficients model interaction parameters

Component i =1	Component j =2	$b_{12} = \frac{(g_{12} - g_{11})}{R}$	$b_{21} = \frac{(g_{21} - g_{22})}{R}$
PG	WATER	-248.25	790.27
PG	FA	303.67	-229.11
PG	SACID	398.41	-217.16
PG	$POLY_S$	431.80	-221.43
PG	$POLY_{1D}$	540.32	-129.89
PG	$POLY_{2D}$	201.60	93.53
WATER	FA	761.89	-354.33
WATER	SACID	1421.77	-567.46
WATER	$POLY_S$	2109.51	-509.44
WATER	$POLY_{1D}$	1374.88	-266.50
WATER	$POLY_{2D}$	1565.88	272.87
FA	SACID	-597.18	965.66
FA	$POLY_S$	-1113.58	3084.73
FA	$POLY_{1D}$	-631.65	1126.21
FA	$POLY_{2D}$	520.63	-229.98
SACID	$POLY_S$	-108.42	109.36
SACID	$POLY_{1D}$	-56.25	290.92
SACID	$POLY_{2D}$	-56.25	290.92
$POLY_S$	$POLY_{1D}$	581.21	-416.24
$POLY_S$	$POLY_{2D}$	581.21	-416.24
$POLY_{1D}$	$POLY_{2D}$	128.83	-114.78
MAD	$POLY_{1D}$	-631.65	1126.21
MAD	$POLY_{2D}$	520.63	-229.98
MAD	FA	128.83	-114.78
MAD	SACID	-597.18	965.66
PG	MAD	303.67	-229.11
WATER	MAD	761.89	-354.33
MAD	$POLY_S$	-1113.58	3084.73
For all binary pairs $\alpha_{ji} = 0.3$			

2.4 Reactor Model

The dynamic model presented here accounts for a reactor-separation system which consist of a reactor, a flash separation unit and a distillate accumulator as shown in figure 1.2 of chapter 1. Focus is on the reactor and the prediction of the polymerization and properties such as acid value, water content, isomerization fraction, saturation fraction and molecular weight. The distillation column is modeled as a flash separator [14]. The reaction takes place in the liquid phase. The liquid phase mass balance for component *i* in the reaction vessel can be written according to,

$$\frac{dc_i}{dt} = r_i - \frac{v_i}{M_0} \tag{2.10}$$

Where, c is the concentration of component i, r is the reaction rate, v_i is the vapor phase flow rate and M_0 is the initial total mass of the reactant. The vapor-liquid interface can be considered as a double film without reaction, where the mass transfer is mainly limited by the highly viscous liquid phase. Thus, the following equation with the overall mass transfer coefficient $K_l a$ and the vapor-liquid equilibrium ratio K_i can be written as eq. (2.11).

$$v_i = K_l a\left(x_i - \frac{y_i}{K_i}\right) \tag{2.11}$$

The vapor phase mass balance according to eq. (2.12) includes the mass transfer from liquid phase and the flow out from the vapor phase of the reactor.

$$\frac{dy_i}{dt} = \frac{-F_{out} y_i + v_i}{v_{vap}} \tag{2.12}$$

Where, y_i is the vapor mole fraction, F_{out} is the out flow from vapor phase and v_{vap} is the vapor hold up in the reactor. The flow out from the vapor phase is separated to an outgoing vapor flow, V and a liquid flow, L from the flash condenser. The liquid flow is collected in the accumulator. The mole fraction of vapor is calculated by an isothermal flash calculation [29] as,

$$Z_i F_{out} = L x_i + V y_i \tag{2.13}$$

$$y_i = K_i x_i \qquad K_i = \gamma_i \frac{p_i}{P} \tag{2.14}$$

Where, K_i is the vapor-liquid equilibrium ratio for component i which is a function of temperature, pressure, liquid mole fraction and vapor mole fraction. In this work, K_i is calculated from the activity coefficients predicted by the polymer NRTL model. p_i is the vapor pressure of the pure component i and P is the total pressure of the system. The properties of the liquid melt polymerized polyester: the degree of polymerization (DP), the number-average molecular weight (M_n) and the weight-average molecular weight (M_W) are calculated as respectively,

$$DP = \frac{1}{(1-X)} \tag{2.15}$$

$$M_n = \frac{158}{(1-X)} \tag{2.16}$$

$$M_W = 158\frac{(1+X)}{(1-X)} \tag{2.17}$$

Where, X is the conversion and 158 is the molecular weight of the repeating unit in the polymer chain.

2.5 Results and discussion

The dynamic model for a batch reactor equipped with a distillation column can be used for the unsaturated polyester production from different reagents. The simulation results presented in this paper are for the reaction of maleic anhydride with propylene glycol. In order to validate the model, the model is simulated with the operating conditions of experiments. The simulation is performed at the temperatures 160°C, 180°C and 200°C, and at atmospheric pressure. The molar ratio of the anhydride and glycol is 1:1.1. The initial amounts of maleic anhydride and propylene glycol are 5.0 mol and 5.5 mol, respectively. The simulation is carried out in Aspen Custom Modeler. The dynamic model is validated with experimental results for the acid value, isomerization concentration, unsaturation concentration, distilled mass and glycol content in the distillate with data from Salmi et al.[10]. The acid value presented here is in terms of total carboxylic acid concentration (C_{COOH}) in mol/kg as shown in figure 2.1 (a). The profiles of isomerization concentration (C_I) and unsaturation concentration (C_D) at 180°C are shown in figure 2.1 (b). From figure 2.1 (a)-(b) it is clear that the model reliably describes these concentration profiles. Due to the autocatalytic effect of acid and high concentration of maleic acid in the liquid phase at the beginning of the reaction, the carboxylic acid reaction rate is very steep at the beginning of the reaction.

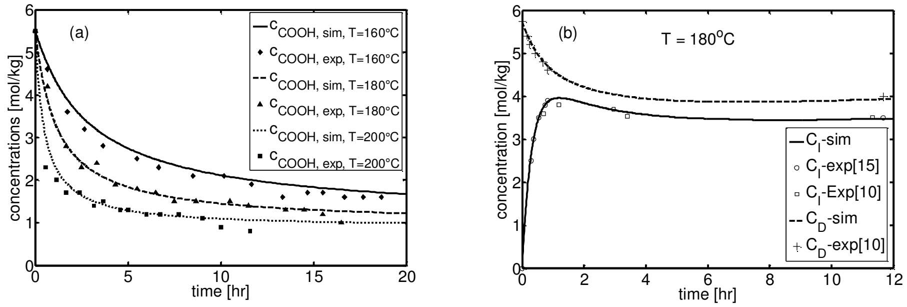

Figure 2.1: (a) Comparison of simulated concentration profile of carboxylic acid with experimental data reported in [10], (b) Comparison of isomerization and double bond saturation concentration with experimental data reported in [10] and [15]

The order of the reaction with respect to carboxylic acid at the beginning of the reaction (0% conversion) is 1 and 2 at the end of the reaction (100% conversion), respectively. The polyesterification reaction is an equilibrium reaction and thus maximum 88-90 % conversion can be obtained. The order of reaction at the end of the process is 1.4 at 200°C, 1.33 at 180°C and 1.25 at 160°C as illustrated in figure 2.2. The order of reaction increases with the temperature because the order of reaction (eq. (2.6)) is a function of conversion and the conversion increases with increasing temperature.

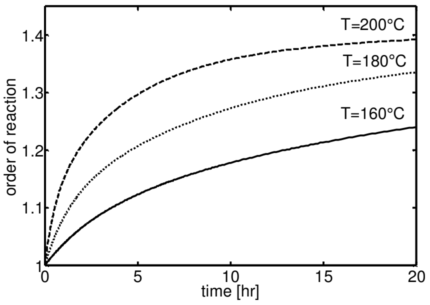

Figure 2.2: Order of reaction at different temperature

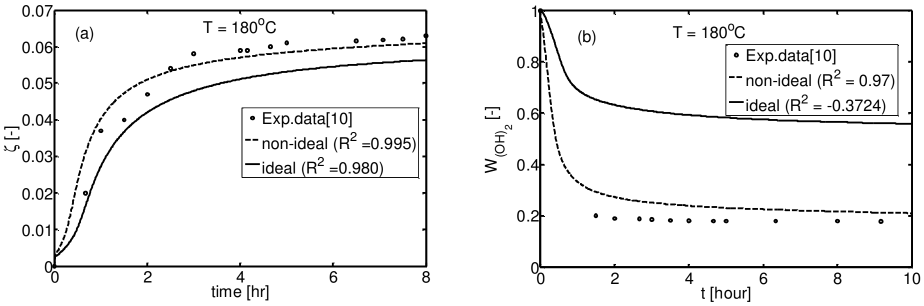

Figure 2.3: (a) Comparison of distilled mass profile with experimental data reported in [10], (b) Simulated profile of weight fraction of propylene glycol in the distillate and comparison with experimental data [10]

In the dynamic model to represent the vapor liquid equilibrium two thermodynamic models are compared. One is the ideal solution thermodynamic model which obeys Raoult's law and the second is the polymer NRTL non-ideal thermodynamic model. The experimental data for the distilled mass and for the propylene glycol fraction in the distillate are obtained from Salmi et al. [10]. An accumulation of the distilled mass ($\varsigma = M_D/M_O$, where M_D is distilled mass and M_O is the initial total mass of the reactants) in the accumulator during the synthesis of unsaturated polyester is plotted in figure 2.3 (a). It can be seen that the distilled mass predicted by the polymer NRTL non-ideal thermodynamic model is in good agreement with the experimental data while the distilled mass is under predicted in the case of the ideal behaviour modeling compared to the experimental results. The reasons are as follows, (1) in the ideal behaviour modeling, the assumption has been made that only glycol and water are present in the vapor phase which is not the case for the non-ideal polymer mixture. In principle, any component which is volatile can be present in the vapor phase. It is predicted from the polymer NRTL model that not only the glycol and water are present in the vapor phase but also the maleic and fumaric acid. Polyester ($POLY_{1D}$ + $POLY_{2D}$ + $POLY_S$) and saturated acid (SACID) are not present in the vapor phase. This is due to the non volatile nature and high molecular weight of the polyester and the saturated acid. (2) In the ideal behaviour modeling, the activity coefficients for the components are kept constant value of 1 and obey Raoult's law. However, in the non-ideal polymer mixture, there is always a positive or negative deviation from Raoult's law and the activity coefficient differ from the value of 1. The regression coefficient (R^2) for the dimensionless distilled mass is 0.980 in the ideal behaviour modeling and 0.995 in the non-ideal behaviour modeling, which confirms the improvement in predictive capabilities of the vapor phase compositions by the polymer NRTL model.

The weight fraction of the propylene glycol in the distillate is plotted in figure 2.3 (b). The propylene glycol weight fraction in the distillate is significantly over-predicted using the ideal behaviour thermodynamic model compared to the experimental data. The regression coefficient (R^2) for the weight fraction of propylene glycol is 0.97 for the non-ideal behaviour modeling, which confirms that the polymer NRTL model reliably predicted the weight fraction of propylene glycol. Because the effect of the polymer properties such as i) chain length, ii) molecular size and iii) molecule structure are not accounted on the activity coefficients in the ideal behaviour modeling. However, it is accounted with the help of polymer NRTL model in the non-ideal behaviour modeling.

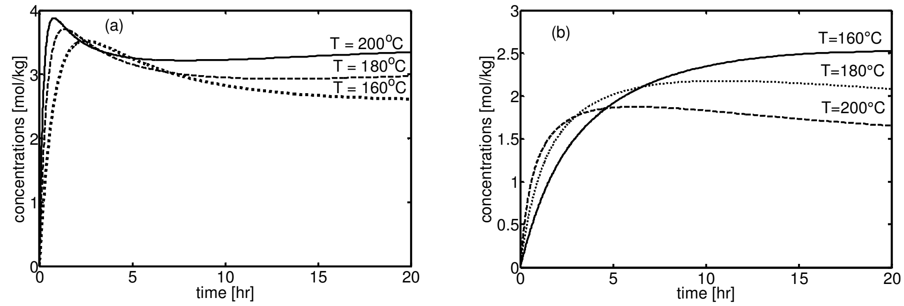

Figure 2.4: (a) Isomerization fraction at different temperatures, (b) Saturation concentration at different temperatures

The isomerization concentration ($C_{COOH_{2D}}$ + $C_{COOR'_{2D}}$) and the saturation concentration (C_{COOH_S} + $C_{COOR'_S}$) increases at higher temperature as shown in figure 2.4 (a) and 2.4 (b), respectively. The isomerization concentration increases steeply at the beginning of the reaction and reaches a peak value. Then the isomerization concentration decreases and at the end of the process isomerization reaction reaches equilibrium. The rate of the isomerization reaction is higher than the rate of the polyesterification reaction at the beginning of the reaction. Therefore maleate-formed acid and ester effectively relieve the strain by transforming to the more planar trans-fumarate isomer and produces fumarate-formed acid and esters. The maleate formed acid and ester, and isomerized formed acid and esters saturate by breaking the double bond with glycol. Thus, the saturation concentration increases throughout the reaction and reaches equilibrium as shown in figure 2.4 (b). Due to a high temperature adaption at the beginning of the reaction, the double bond saturation increases steeply. The saturation effect of the double bond of an unsaturated acid can be lowered by setting the process at a low initial temperature.

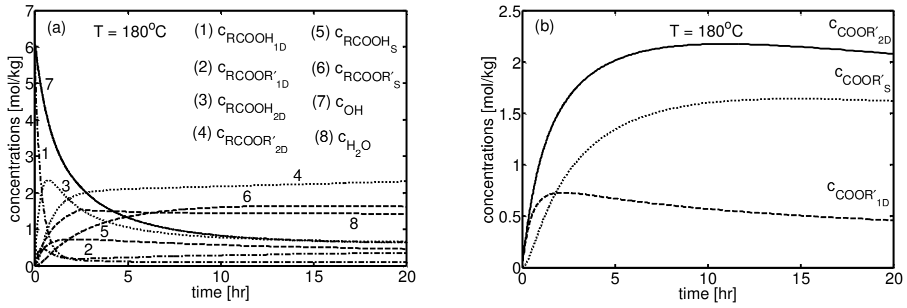

Figure 2.5: (a) Simulated liquid-phase concentration profile of functional group and H_2O, (b) Simulated product distribution profile of melt polymerized polyester

The concentration of each functional group and the H_2O concentration are shown in figure 2.5 (a). The total carboxylic acid concentration, total isomerization concentration and total saturation concentration are calculated from the functional groups illustrated in figure 2.5 (a). The total concentration of carboxylic acid is a summation of the functional groups $COOH_{1D}$, $COOH_{2D}$, $COOH_s$, and the total isomerization concentration is a summation of the functional groups $COOH_{2D}$, $COOR'_{2D}$ and the total saturation concentration is summation of the functional groups $COOH_S$ and $COOR'_S$. The maleate to fumarate percentage is calculated from the concentration of these functional groups and found to be 92% which corresponds to the results reported by Parker et al. [11] and Larry et al. [15]. Frandet et al. [13] have reported 15-20% loss of double bond due to saturation of maleic anhydride with propylene glycol. The model predicts 19% of double bond loss during the synthesis which shows good agreement with the saturation composition reported by Frandet et al. [13]. The product distribution in maleate-formed esters, fumarate-formed ester and saturated ester of melt polymerized polyester is shown in figure 2.5 (b).

The degree of polymerization, number-average molecular weight and weight–average molecular weight derived from conversion and molecular weight of repeating unit are calculated according to eq. (2.15)-(2.17), respectively. The degree of polymerization is between 8 and 10. To validate the number-average molecular weight profile with the industrial data reported in Korbar et al. [16], the model is simulated with the temperature profile shown in figure 2.6. It can be seen from figure 2.6 that the number-average molecular weight throughout the process is in good agreement with the industrial data reported in Korbar et al. [16].

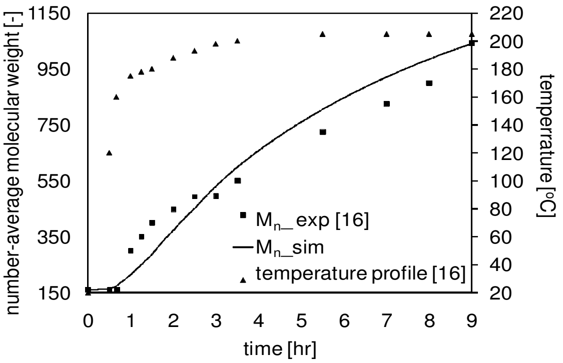

Figure 2.6: Comparison of number-average molecular weight (M_n) profile with experimental data reported in [16]. To compare M_n profile, the process is simulated with the temperature profile reported in [16].

2.6 Conclusions

The aim in this work was to develop a process model for the synthesis of unsaturated polyester. We find that the polymer NRTL model significantly improved the prediction capability of the process model compared to the ideal-behaviour modeling. The behaviour of the model system, the polyesterification of the unsaturated carboxylic acid and two side reactions, isomerization and double bond saturation are reliably predicted. We conclude that the process model which consists of kinetics with changing rate order connected with the polymer NRTL thermodynamic model give a better representation of the industrial unsaturated polyester process. The validated process model can also be used for the unsaturated polyester synthesis from reagents other than maleic anhydride and propylene glycol with appropriate kinetic and thermodynamic parameters, respectively.

List of symbols

a	vapor-liquid mass transfer area (m^2)
b	interaction parameter in the polymer NRTL model
C	concentration (mol kg^{-1})
E_a	activation energy (J mol^{-1})
F_{out}	flow to the distillation column from reactor (mol hr^{-1})
G	parameter in the polymer NRTL model
k	rate constant (kg mol^{-1} hr^{-1})
k_l	mass transfer coefficient (mol m^{-2} hr^{-1})
k_i	vapor liquid equilibrium ratio
L	liquid flow from flash condenser (mol hr^{-1})
M_0	total mass in reactor (kg)
m	characteristic size of component
n_i	number of moles of component

n	order of reaction
p	partial pressure (bar)
P	total pressure (bar)
q	fitting parameter in eq. (2.5)
r	reaction rate (mol kg^{-1} hr^{-1})
R	gas constant
T	temperature (^{o}C)
t	time (hr)
v	vapor flow (mol hr^{-1})
V	vapor flow from the flash condenser (mol hr^{-1})
v_{vap}	vapor holdup in the reactor (mol)
X	conversion
x	liquid phase mole fraction
y	vapor phase mole fraction
z	mole fraction in eq. (2.13)

Greek letters

ς	dimensionless distilled mass
α	non randomness factor in the polymer NRTL model
γ_i	activity coefficient
ϕ_i	volume fraction in the polymer NRTL model
τ	parameter in the polymer NRTL model

Subscripts and superscripts

1D	cis formed component
2D	trans formed component
D	double bond
E	esterification
i, j	component indexes
I	isomerization
S	saturated component

Abbreviations

Cis	cis formed component
COOH	acid end group
Dbb	unsaturated double bond in maleic acid
DP	degree of polymerization
E	ester
FA	fumaric acid
MA	maleic acid end group
MAD	maleic anhydride
OH	hydroxyl group
POLY$_{1D}$	maleate formed polyester
POLY$_{2D}$	fumarate formed polyester
POLY$_{s}$	saturated polyester

PG	propylene glycol
M_n	number-average molecular weight
M_W	weight-average molecular weight
R	regression coefficient
SatDbb	saturated double bond in maleic acid
Sat acid	saturated acid
Trans	trans formed component

References

[1] W.H. Carothers, Studies on polymerization and ring formation: An introduction to the general theory of condensation polymers, Journal of the American Chemical Society, 51 (1929) 2548.

[2] P.J. Flory, Kinetics of Polyesterification: A Study of the Effects of Molecular Weight and Viscosity on Reaction Rate, Journal of the American Chemical Society, 61 (1939) 3334.

[3] E. Paatero, K. Närhi, T. Salmi, M. Still, P. Nyholm, K. Immonen, Kinetic model for main and side reactions in the polyesterification of dicarboxylic acids with diols, Chemical Engineering Science, 49 (1994) 3601.

[4] D. Beigzadeh, S. Sajjadi, F.A. Taromi, Kinetic study of polyesterification: Unsaturated polyesters, Journal of Polymer Science Part A: Polymer Chemistry, 33 (1995) 1505.

[5] S.-a. Chen, K.C. Wu, Kinetics of polyesterification. II. Foreign acid-catalyzed dibasic acid and glycol systems, Journal of Polymer Science: Polymer Chemistry Edition, 20 (1982) 1819.

[6] T. Au-Chin, Y. Kuo-Sui, Mechanism of hydrogen ion catalysis in esterification. II. Studies on the kinetics of polyesterification reactions between dibasic acids and glycols, Journal of Polymer Science, 35 (1959) 219.

[7] Y.-R. Fang, C.-G. Lai, J.-L. Lu, M.-K. Chen, Kinetics and mechanism of polyesterification of binary acids and binary alcohols, Scientia Sinica, 18 (1975) 72-87.

[8] C.C. Lin, K.H. Hsieh, The kinetics of polyesterification. I. Adipic acid and ethylene glycol, Journal of Applied Polymer Science, 21 (1977) 2711.

[9] T. Salmi, E. Paatero, J. Lehtonen, P. Nyholm, T. Harju, K. Immonen, H. Haario, Polyesterification kinetics of complex mixtures in semibatch reactors, Chemical Engineering Science, 56 (2001) 1293.

[10] T. Salmi, E. Paatero, P. Nyholm, M. Still, K. Narhi, Kinetics of melt polymerization of maleic acid phthalic acids with propylene glycol, Chemical Engineering Science, 49 (1994) 5053.

[11] E.E. Parker, Unsaturated polyesters, Industrial & Engineering Chemistry, 58 (1966) 53.

[12] I.V. Szmercsányi, L.K. Maros, A.A. Zahran, Investigations of the kinetics of maleate–fumarate isomerization during the polyesterification of maleic anhydride with different glycols, Journal of Applied Polymer Science, 10 (1966) 513.

[13] A. Fradet, E. Marechal, Study on models of double bond saturation during the synthesis of unsaturated polyesters, Die Makromolekulare Chemie, 183 (1982) 319.

[14] M. Shah, E. Zondervan, A.B. de Haan, Modelling and simulation of an unsaturated polyester process, Journal of applied sciences, 10 (2010) 2551-2557.
[15] L.G. Curtis, D.L. Edwards, R.M. Simons, P.J. Trent, P.T. Von Bramer, Investigation of Maleate-Fumarate Isomerization in Unsaturated Polyesters by Nuclear Magnetic Resonance, I&EC Product Research and Development, 3 (1964) 218.
[16] J. Korbar, J. Golob, A. Šebenik, Process of unsaturated polyester resin synthesis on a laboratory and industrial scale, Polymer Engineering & Science, 33 (1993) 1212.
[17] H.F. Mark, Encyclopedia of Polymer Science and engineering, 2 ed., Wiley-Interscience, 1988.
[18] S.S. Feuer, T.E. Bockstahler, C.A. Brown, I. Rosenthal, Maleic-Fumaric Isomerization in Unsaturated Polyesters, Industrial & Engineering Chemistry, 46 (1954) 1643.
[19] H.W. Melville, G.M. Burnett, Rate constants for polymerization reactions, Journal of Polymer Science, 13 (1954) 417.
[20] R. Jedlovčnik, A. Šebenik, J. Golob, J. Korbar, Step-growth polymerization of maleic anhydride and 1,2-propylene glycol, Polymer Engineering & Science, 35 (1995) 1413.
[21] P.B. Zetterlund, W. Weaver, A.F. Johnson, Kinetics of polyesterification: Modelling of the condensation of maleic anhydride, phthalic anhydride, and 1,2 propylene glycol, Polymer Reaction Engineering, 10 (2002) 41 - 57.
[22] D.S. Lafyatis, L.S. Scott, D.M. Trampe, C.A. Eckert, A test of the functional dependence of gE(x) in liquid-liquid equilibria using limiting activity coefficients, Industrial & Engineering Chemistry Research, 28 (1989) 585.
[23] B.E. Poling, J.M. Prausnitz, J.P. O'connell, The properties of gas and liquids, 5 ed., McGrawHill, Singapore, 2007.
[24] M.A. Gess, R.P. Danner, M. Nagvekar, Thermodynamic analysis of vapor-liquid equilibiria: recommended models and as standard data base, in, Design institute for physical property data (DIPPR), Pensylvania, 1991.
[25] C.-C. Chen, A segment-based local composition model for the gibbs energy of polymer solutions, Fluid Phase Equilibria, 83 (1993) 301.
[26] H. Renon, J.M. Prausnitz, Local compositions in thermodynamic excess functions for liquid mixtures, AIChE Journal, 14 (1968) 135.
[27] U. Weidlich, J. Gmehling, A modified UNIFAC model. 1. Prediction of VLE, hE, and.gamma.infin, Industrial & Engineering Chemistry Research, 26 (1987) 1372.
[28] D. Suleiman, C.A. Eckert, Limiting Activity Coefficients of Diols in Water by a Dew Point Technique, Journal of Chemical & Engineering Data, 39 (1994) 692.
[29] J.D. Seader, E.J. Henley, Separation process principles, 2 ed., Willey, New York, 2006.

Chapter 3

Conceptual design of the reactive distillation process

The aim of this chapter is to study the feasibility of the reactive distillation process and to find out whether reactive distillation is potentially interesting compared to the traditional batch reactor process. The simulation study shows that the total production time of polyester in a continuous reactive distillation system is reduced from 12 hours to 1.8-2 hours compared to the industrial batch reactor process. The model demonstrated that reactive distillation has the potential to intensify the process by factor of 6 to 8 in comparison to the batch reactor process. After finding that reactive distillation is an attractive alternative for the polyesters synthesis, a more in depth analysis is performed. Particularly, the influence of the liquid back mixing on the description of the reactive distillation process, product transition time, the amount of undesired product formation during the product changeover is investigated. However, the current state of the art modelling approach does not account for liquid back mixing. Therefore, the rate-based model is extended to account for liquid back mixing. The simulation results demonstrated that axial dispersion significantly influences the reactive distillation process and cannot be neglected.

3.1 Introduction

As discussed in chapter 1 and 2, a polyesterification reaction is an equilibrium limited process and continuous removal of water is necessary to obtain high conversion. Traditionally, the unsaturated polyesters are produced in a batch reactor and usually a distillation column is directly coupled to the reactor vessel in order to avoid excessive loss of reactants during a batch, and nearly pure water is separated from the polymer mixture in the reactor [1, 2]. The total production time in such a batch process is around 12 hours and often leads to batch-to-batch inconsistency [1, 2]. Therefore, it is worthwhile to investigate intensification possibilities of the current state of the art unsaturated polyester process in order to reduce the production time and to achieve better product quality. A promising alternative for this process is reactive distillation.

Reactive distillation is a well-known technology for reactive-separation systems close to equilibrium [3]. The integration of reaction and separation holds clear advantages for many systems in comparison with subsequent reaction and separation [3-5]. Recently, it has drawn more and more attention because of its advantages over traditional processes such as:

- economical: capital and operating costs reduction, energy requirement reduction

- environmental: emissions reduced by 20% or more compared to the classic set-up of a rector followed by distillation
- social: improvement on safety, health and society by low reactive content, low chances of runaway sensitivity and lower space occupation [3, 6-9].

Reactive distillation process design is carried out either by simulation or by synthesis design. Simulations are currently based on either equilibrium (EQ) modeling or rate-based modeling. Both modeling approaches are extensively reported in the literature [3, 4, 10-15]. In the equilibrium modeling approach, the vapor and liquid are assumed to be in equilibrium. This approach is very useful to simulate the kinetically controlled process where mass transfer is significantly faster than a reaction. However, this approach is not reliable for a mass transfer limited process because equilibrium is rarely achieved. Compared to equilibrium modeling, the rate-based approach offers accuracy in the design of a column as it accounts for:

- vapor-liquid equilibrium only at the interface between the bulk liquid and vapor phases,
- a transport-based approach to predict the flux of mass and energy across the interface,
- the real hydrodynamic situation of either a tray or a packed column.

Due to these reasons, over-design and under-design are avoided, there is no need for efficiencies and HETPs and the column is designed more realistic as compared to EQ modeling, thereby reducing the capital and operating costs.

Although the state of the art rate-based model provides better prediction than the EQ model, the rate-based model is limited to reliably predict mass transfer limited processes. The rate-based model is not sufficient to represent a slow reaction process that is kinetically controlled due to neglecting the liquid back mixing. To enhance the rate of reaction for the kinetically controlled processes, a high liquid holdup is required. The requirement of a high liquid holdup leads to high residence time of the species inside the column which remarkably increases the liquid back mixing. Liquid back mixing strongly influences the end product compositions and thus the physical and chemical properties of the product are significantly altered. Since the rate-based model does not account for axial dispersion, the effect of the liquid back mixing is neglected on the whole reactive distillation process. Therefore, the rate-based model is not sufficient to predict the kinetically controlled process and must be extended to account for the effect of axial dispersion on the reactive distillation process. Currently, reactive distillation processes are designed using rate-based or EQ models while the non-ideal flow behavior (mixing effect) of RD column is separately investigated by the axial dispersion model (ADM) as described in the literature [16, 17].

In this chapter, the feasibility of the reactive distillation process is investigated for the synthesis of unsaturated polyester. The equilibrium modelling approach is used to obtain the design and operational parameters for the reactive distillation process and proved that reactive distillation is a feasible option. Moreover, the simulation results of the reactive distillation process were compared with the traditional polyester process to obtain the improvement gained by reactive distillation application. Since the polyester process governs slow reaction kinetics, liquid back mixing may influence the description of the whole reactive distillation process. Moreover, to apply reactive distillation technology in the polyester industry, the reactive distillation column must be designed in such a way that several products can be produced in the same column, while during switching from one product to other the undesired product formation is avoided or minimized. This undesired product formation is strongly influenced by the liquid back mixing and can be reduced by reducing the liquid back mixing in the system. This clearly suggests the necessity to incorporate the liquid back mixing in the model in order to accurately design a multi-product reactive distillation process. Therefore, a new modeling approach is proposed to extend the rate-based model to account for the effect of liquid back mixing (LBM) on the reactive distillation process. The extended model is simulated for the polyester synthesis in steady state mode to predict the influence of liquid back mixing on the whole reactive distillation process. Moreover, the predicted product composition profiles by the EQ, the rate-based and the extended rate-based models are compared to determine the difference in the predicted values. The influence of the back mixing on the product changeover and the undesired product formation is also demonstrated by dynamic simulations of the extended rate-based model.

3.2 Results and discussion

3.2.1 Equilibrium modeling

In this section, an equilibrium model is developed for the synthesis of unsaturated polyester. Since the product transition is an important parameter for grade switching, a dynamic material balance is considered in this model. However, a dynamic model for the energy balance is not used as the temperature transition is not an important parameter. The polyester process encounters a multicomponent system. However, these components are miscible with each other and therefore the liquid phase split is not observed. Since, the polyester is produced at high temperature (over 230^{o}C), the viscosity (around 0.05 Pas) of the polyester is significantly lower at the operating conditions compared to that at the atmospheric conditions. Therefore, the large molecules of polyester do not influence the mass transfer and the distribution of species between vapor and liquid phases. Moreover, the polyester process governs slow kinetics. Hence as a starting point for the conceptual design of a reactive distillation process, the vapor and liquid are assumed to be in equilibrium (VLE) on all stages. Both liquid and vapor phase are assumed to be perfectly mixed on each stage. The pressure drop is neglected. There is negligible vapor holdup on each stage. The polyester process involves autocatalytic reactions therefore reactions take place on each stage. The kinetic and thermodynamic models and their parameters from chapter 2 are used.

A schematic view of the reactive distillation column is given in Figure 3.1. The column is operated as a counter current vapor-liquid contactor. The maleic anhydride is fed as a liquid at the top of the column and propylene glycol is fed as a vapor at the bottom of the column. The polyester product leaves at the bottom of the column and water, glycol and acids leave at the top of the column. The reactive distillation model consists of J $(j = 1,..., J)$ stages. A schematic view of the equilibrium stage balance is shown in figure 3.1. The first stage $(j=1)$

is the top stage, where the anhydride is fed with flow rate L_F (kmol/hr) to the column and the vapor comes out from the top stage with flow rate V_{out} (kmol/hr). The last stage *(j=20)* is the bottom stage, where the glycol is fed with flow rate V_F (kmol/hr) to the column and the bottom product flows out with flow rate L_{out} (kmol/hr). The composition of component *i* in the liquid phase is $x_{i,j}$ and in the vapor phase is $y_{i,j}$. The total molar holdup per stage is denoted by M_j (kmol) and $\nu_{i,m}$ represents the stoichiometric coefficient of component *i* in reaction *m* and ε_j represents the reaction volume.

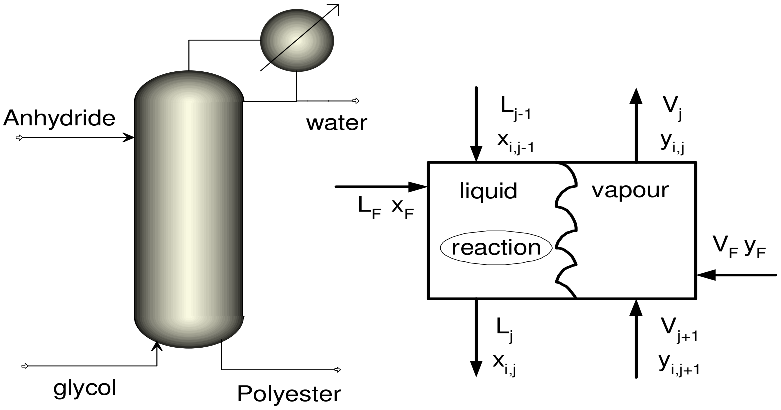

Figure 3.1: Schematic view of RD column and the corresponding stage balance

The vapor flows between the stages are expressed as V_j (kmol/hr) and liquid flows between the stages are expressed as L_j (kmol/hr).The component material balance for each of the stages *J (j = 1,..., J)* is:

$$M_j \frac{dx_{i,j}}{dt} = L_{j-1}x_{i,j-1} - L_j x_{i,j} + V_{j+1}y_{j+1} - V_j y_{i,j} + \sum_{m=1}^{r} \nu_{i,m} r_{m,j} \varepsilon_j \tag{3.1}$$

For the top stage *(j=1)*, $L_{j-1} = L_F$, $x_{i,j} = x_F$, $V_j = V_{out}$, $y_j = y_{out}$ and for the bottom stage *(j)*, $V_{j+1} = V_F$, $y_{j+1} = y_F$, $L_j = L_{out}$, $x_{i,j} = x_{out}$ The total material balance for stages *J (j = 1,..., J)* is:

$$\frac{dM_j}{dt} = L_{j-1} - L_j + V_{j+1} - V_j + \sum_{m=1}^{r} \sum_{i=1}^{C} \nu_{i,m} r_{m,j} \varepsilon_j \tag{3.2}$$

The vapor-liquid equilibrium at the interface is represented by:

$$y_{i,j} P_j = x_{i,j} \gamma_{i,j}(x_{i,j}, T_j) p_{i,j}^{sat} \tag{3.3}$$

The steady state energy balance for stages *J (j = 1,..., J)* is:

$$L_{j-1} CP_L (T_{j-1} - T_j) + V_{j+1} CP_V (T_{j+1} - T_j) = \sum_{i=1}^{C} V_{j+1} y_{i,j+1} H_{i,j+1}^{V} \tag{3.4}$$

where, T_j (°C) is the temperature at stage *j*, CP_L is the liquid mixture heat capacity and CP_V is the vapor mixture heat capacity, $H^{v}_{i,j+1}$ is the heat of vaporization of component *i* on stage *j+1*. For the top stage *(j=1)*, $T_{j-1} = T_{lf}$ (°C) is the liquid feed temperature, $T_j = T_{tout}$ (°C) is the temperature of the vapor outlet stream at the top of the column and for the bottom stage *(j=20)*, $T_{j+1} = T_{vf}$ (°C) is the vapor feed temperature, $T_j = T_{bout}$ (°C) is the temperature of the liquid outlet stream at the bottom of the column, $H^{v}_{i,j+1} = H^{v}_{F}$ is the heat of vaporization of the vapor feed. Since the enthalpies are referred to their elemental state in the energy balance, the heat of reaction is automatically accounted in the energy balance and no separate term is required [3]. The required residence time in order to obtain desired conversion in the reactive distillation column is estimated by,

$$\tau = \sum_{j=1}^{j} \frac{M_j}{L_j} \tag{3.5}$$

3.2.1.1 *Process parameter estimation*

The simulation results presented in this section are for the reaction of maleic anhydride with propylene glycol. The model is developed in Aspen custom modeler (ACM). The components, properties, thermodynamics are defined by the problem definition file of Aspen plus/property plus. The non-conventional component properties are estimated by Aspen property plus. Steady state simulation is performed to obtain the operating conditions of the reactive distillation column. We have used sensitivity analysis to evaluate

- the equilibrium stages required to produce pure top and bottom product,
- the required residence time to obtain higher equilibrium conversion by reactive distillation,
- the best range of the parameters such as feed ratio (propylene glycol/ maleic anhydride), reflux ratio and temperature of feed streams.

The anhydride is fed as liquid at the top of the column and propylene glycol is fed at the bottom of the column as vapor, as shown in figure 3.1. The polyester product leaves at the bottom of the column and water, glycol and acids leave at the top of the column as shown in figure 3.1. Since the reactive distillation process is not yet studied for the synthesis of the unsaturated polyester, the operating conditions such as temperature of the feed streams, feed ratio and pressure for this process are not yet known. Therefore the reactive distillation model is first simulated with similar operating conditions as the traditional batch reactor process. The feed ratio of maleic anhydride (liquid feed) and propylene glycol (vapor feed) is 1.0:1.1, the liquid feed temperature 185°C (which is below boiling temperature (T_b = 200°C) of maleic anhydride), the vapor feed temperature 250°C (which is more than boiling temperature (T_b = 189°C) of propylene glycol) and the column pressure is 1 bar. From figure 3.2, it is clear that at least 20 equilibrium stages are required to achieve pure polyester at the bottom and pure water at the top of the column. The equilibrium stages below 20 lead impurities in the top and bottom products and the equilibrium stages above 20 do not contribute to enhance the purity of the top and bottom products.

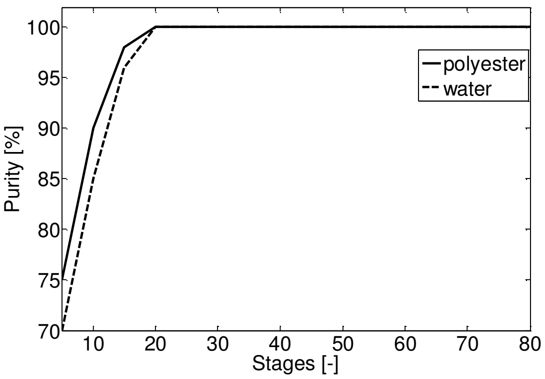

Figure 3.2: Influence of the number of stages on product purity

Since 20 equilibrium stages are the required number of stages to produce pure polyester and water by reactive distillation, the further sensitivity analysis is performed with 20 equilibrium stages. The predicted equilibrium conversion at different residence times of the liquid in the reactive distillation column and different feed ratios is shown in figure 3.3. In order to obtain highly concentrated polyester at the bottom of the column, at least 95% equilibrium conversion of carboxylic acid is required at the bottom stage. This desired equilibrium conversion is achieved by allowing a residence time longer than 1.5 hours in the reactive distillation. From figure 3.3, it is clear that the equilibrium conversion of 50% is achieved in quarter of an hour which is due to a very high reaction rate of the monoesters formations and very high evaporation of water from the reaction phase. However, the polyesterification reaction rate is much slower than the monoester formation rate and thus it requires at least another 1.25 hours to reach the desired equilibrium conversion.

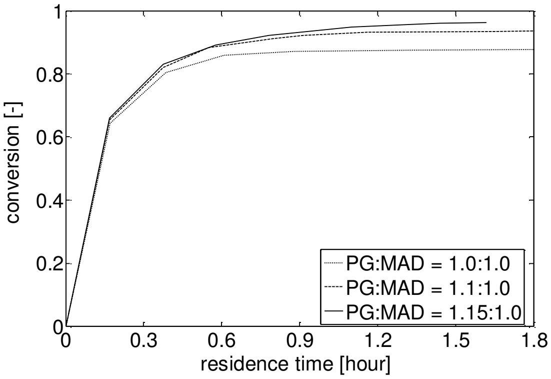

Figure 3.3: Influence of residence time on conversion

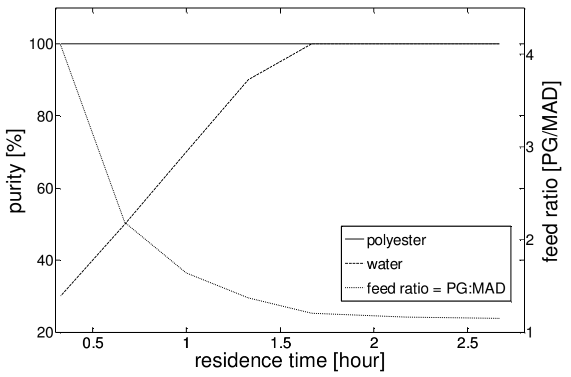

Figure 3.4: Effect of residence time and feed ratio on purity of the top product (water) and bottom product (polyester)

The model is simulated for different feed ratios with different residence times to obtain the desired equilibrium conversion. It is found that there is trade-off between the residence time and the feed ratio to obtain the same amount of equilibrium conversion and the same polyester purity as shown in figure 3.4. We concluded from figure 3.3 that at least 1.5 hours of residence time is required in the reactive distillation column to produce polyester with target purity. However, it can be noticed from figure 3.4 that the polyester with target purity can also be produced by allowing lower residence times in the reactive distillation column but it requires an excess amount of glycol. This excess amount of glycol leads to a significant impurity in the top stream coming out from the column which leads to the requirement of an additional column and energy to separate them. Moreover, an equimolar ratio of the reactants (glycol/anhydride) is not sufficient to achieve the desired equilibrium conversion because 10% glycol is lost during the double bond saturation reaction. Thus the excess glycol of 10% is required to achieve desired equilibrium conversion. On the other hand, a lower molar ratio between glycol and anhydride leads to an incomplete conversion of the acids that contaminates the bottom (polyester) product. Since the separation of acids from polyesters is difficult, this situation must be avoided. From figure 3.4, it can be seen that top product (water) and bottom product (polyester) obtained nearly pure when the residence time of 1.8 hours is allowed in the reactive distillation column and the feed ratio of 1.15:1.0 is applied.

The polyester is the bottom product which is highly non volatile and therefore a reboiler is not connected to the column to vaporize the bottom product but one of the reactants – glycol is fed to the column as vapor. Thus, the glycol vapor feed temperature have significant influence on the conversion and the product purity. The model which consists of 20 equilibrium stages is simulated for 1.8 hours of residence time with a molar ratio of reactant - 1.15:1.0 to analyze the effect of the glycol vapor feed temperature on the conversion of the acids. It is noticeable from figure 3.5 that to obtain highly concentrated polyester (min. 95%) at the bottom of the column and a high purity of the top product, the best temperature range of glycol vapor stream is 250-300^{o}C.

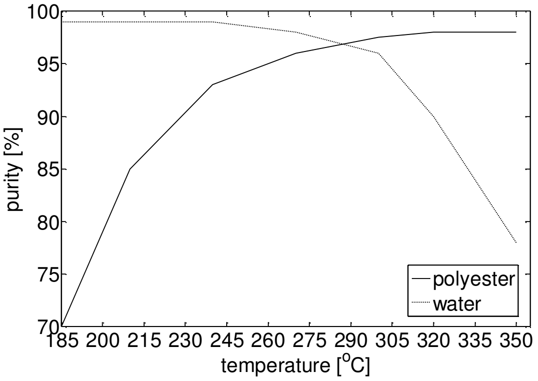

Figure 3.5: Effect of glycol vapor feed temperature on the conversion

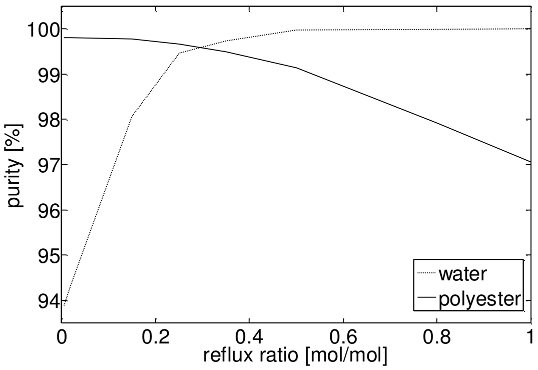

Figure 3.6: Influence of reflux ratio on purity of the top and bottom product

The purity of the top product (water) and the bottom product (polyester) as function of the reflux ratio is shown in figure 3.6. The reflux has no significant influence on the purity of the top and bottom product. However, to obtain a highly purified top product from the column, a minimum 0.2 mol/mol reflux ratio is required. It is also noticeable from figure 3.6 that high reflux ratio to the column gives a low purity of the bottom product which is due to feeding back the by-product water to the column which shifts chemical equilibrium to the reactant side.

Table 3.1: Summary of parameter settings found from sensitivity analysis

Parameters	**values**
Required equilibrium stages [-]	20
Required residence time [hours]	1.8
Feed ratio [PG:MAD]	1.15:1.0
Liquid feed temperature [^oC]	185
Vapor feed temperature [^oC]	270
Reflux ratio [mol/mol]	0.3

3.2.1.2 Steady-state analysis

The reactive distillation process is further evaluated with the best parameters found from the sensitivity analysis. These optimal parameters are tabulated in table 3.1. Polyester (POLY = $POLY_{1D}$ + $POLY_{2D}$ + $POLY_s$) and saturated acid (SACID) are not present in the vapor phase which can be seen in figure 3.7 (a). This is due to the non volatile nature and high molecular weight of the polyester and the saturated acid. The glycol concentration in the vapor phase decreases slowly in the bottom stages and decreases steeply in the top stages as depicted in figure 3.7 (a). This is because of the effect of the temperature change in the column, and the glycol reacts much faster with the free anhydride and acid to form monoesters at the top stages than with diesters or long chain esters to form polyesters at the bottom stages. Thus the glycol concentration decreases steeply in the top stages. Water is stripped out throughout the column with propylene glycol which acts as stripping agent for the water. Since the vapor of propylene glycol is fed at the bottom of the column, the vapor compositions of propylene glycol at the bottom stages is much higher than the water. Because of this the stripping rate of water is much higher in the bottom stages. The vapor composition of water is significantly high at the top stages, which is due to high water formation rate governed by the reaction between glycol and free acid at the top stages. Water compositions in the vapor and liquid phase have been depicted in figure 3.7 (a) and (b), respectively.

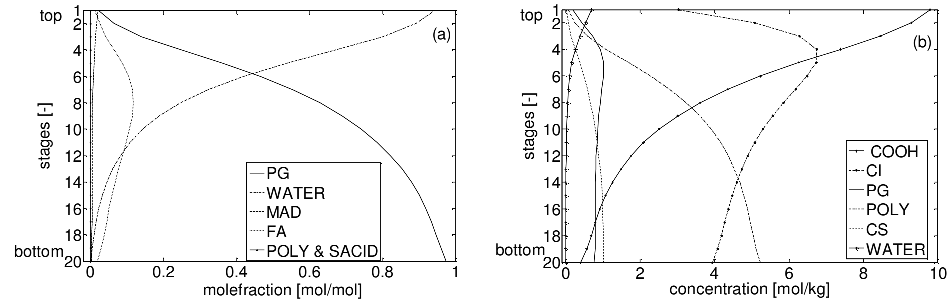

Figure 3.7: Vapor phase concentrations (a), Liquid phase concentrations (b)

The degree of isomerization (CI = FA + $POLY_{2D}$) in the vapor and liquid phase has been shown in figure 3.7 (a) and (b), respectively. The isomerization concentration increases steeply in the top stages and after that reaches a peak and then the isomerization concentration decreases throughout the column towards the bottom stages. Because there is free maleic anhydride and maleic acid available at the top stages, they effectively relieve the strain by transforming to the more planar trans-fumarate isomer when the reaction temperature exceeds 180°C. The polyesterification reaction rate also increases with temperature and when the temperature exceeds 210°C, isomerized acids also esterify with the glycol and produce isomerized ester ($POLY_{2D}$). However, certain isomerized ($POLY_{2D}$) and maleate ester ($POLY_{1D}$) saturate by breaking the double bond with glycol. Thus, the saturation concentration (CS = SACID + $POLY_s$) increases throughout the column and reaches equilibrium as shown in figure 3.7 (b).

The temperature profile and the number-average molecular weight profile are plotted in figure 3.8. It can be seen from figure 3.8 that the number-average molecular weight is 166 at the top stage and 2800 at the bottom stage which is due to monoester formation at the top stage and high concentrated polyester at the bottom stage, respectively. An equilibrium conversion of 95% is achieved at the bottom stage which justifies the number-average molecular weight of 2800 and the degree of polymerization of 17 at the bottom stage according to eq. (2.16) and eq. (2.15), respectively.

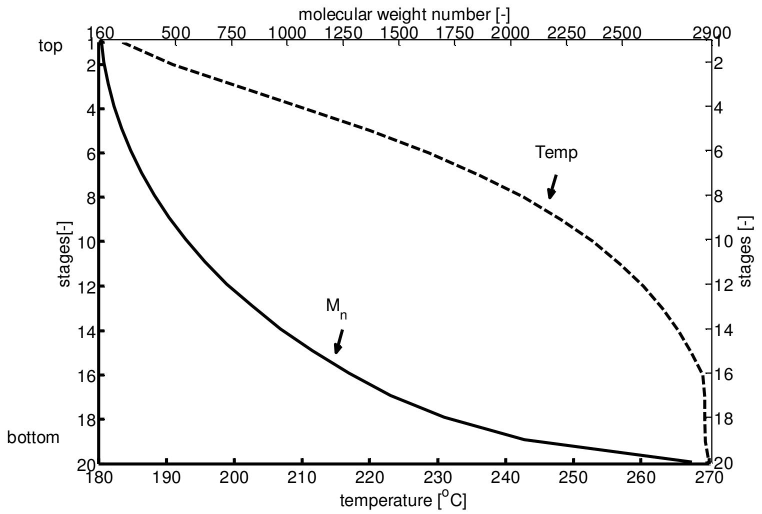

Figure 3.8: Temperature and the number-average molecular weight profiles

3.2.1.3 RD process versus traditional batch process

The reactive distillation model simulation results are compared with the batch reactor model simulation results to check the quality of the product and to notice any advantages of the reactive distillation process over the traditional batch process. The simulation results of the traditional batch process are taken from chapter 2. The operating conditions of the reactive distillation process and batch process are listed in table 3.2.

Table 3.2: Operating conditions for RD process and the batch process

Operating conditions	RD process	Industrial batch process
Temperature range (^{o}C)	185-270	40-210
Pressure (bar)	1	1
Process	Continuous	Batch

The optimum reaction temperature of the polyester process in batch production is between 210^{o}C and 220^{o}C to avoid destruction of the unsaturated acid. Although the reaction temperature is kept between 185^{o}C and 270^{o}C, it is presumed that there is no possibility of destruction of unsaturated acid in the reactive distillation process due to the short residence time requirement and the free acid (or anhydride) is present only in the 3 top stages of the reactive distillation column where the reaction temperature is between 185°C and 210°C as shown in figure 3.8. However, it is necessary to prove experimentally that there is no destruction of double bonds at high temperature for a short residence time. The product specifications that are achieved in the reactive distillation process are compared with the batch reactor process in table 3.3. The reactive distillation process model predicts acid value, hydroxyl value, maleate, fumarate, saturation compositions and polymer attributes of the polymer in the range of industrial unsaturated polyester production in batch reactor.

Table 3.3: Comparison of the product specifications

Product specifications	RD process	Batch reactor process
Acid value	20-25	20-25
Hydroxyl value	70-90	80-100
Maleate ester (%)	20-40	20-40
Fumarate ester (%)	50-65	50-65
Saturated ester (%)	10-15	10-15
Number-average molecular weight (M_n)	1000-4000	800-1600
Degree of polymerization	8-27	8-15

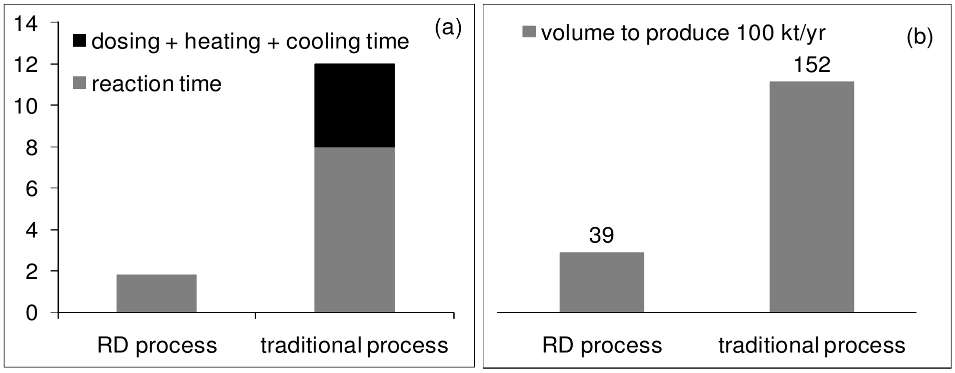

Figure 3.9: Advantages of the Reactive distillation (RD) process over the industrial batch reactor process

The benefits of the reactive distillation process over the conventional batch reactor process are shown in figure 3.9. The industrial unsaturated polyester production time is around 12 hours. However, the reactive distillation process simulation study shows that the total production time of unsaturated polyester in a continuous reactive distillation system is 1.8 hours when the temperature of vapor feed stream is 270°c and, 2 hours when the temperature of the vapor feed stream is 250°C for the same product quality as during 12 hours of batch production. Because in industrial batch process the total production time consists of dosing, heating, reaction and cooling time and in the continuous reactive distillation process total production time consists of only reaction time. The reaction is significantly faster in the reactive distillation process compared to the industrial batch reactor process due to fast removal of water (by product) from reaction phase. The required total volume to produce 100 ktonnes/year polyester is reduced from 152 m^3 to 39 m^3. The production time is reduced by 85% and the required volume to produce 100 ktonnes/year is reduced by 74% which shows significant improvement by reactive distillation over the traditional process. Based on these comparisons, it is concluded that reactive distillation intensifies the process by at least factor of 6 to 8 in comparison to the batch reactor process.

Moreover, the maximum equilibrium conversion in a batch reactor process that can be achieved is up to 88-90% for the given operating conditions in table 3.2. However, in the reactive distillation process the equilibrium conversion that can be achieved is significantly high as compared to the batch reactor and can be up to 97% for given operating conditions in table 3.2. The limiting factor for the equilibrium conversion is water evaporation from the liquid phase and shifting the equilibrium to the product side. In the batch reactor process, vacuum is applied to remove the remaining water from the polyester mixture and thereby a higher conversion up to 97% obtained. In the reactive distillation process, glycol acts as a stripping agent to remove water from the liquid phase and, due to the high temperature (250-270^{o}C) and the high concentration of glycol in the vapor phase at the bottom stages, water evaporation is much more efficient in the reactive distillation process compared to the batch reactor process. Therefore, there is no need to operate the reactive distillation column under vacuum to remove water.

3.2.2 Extension of the rate-based model

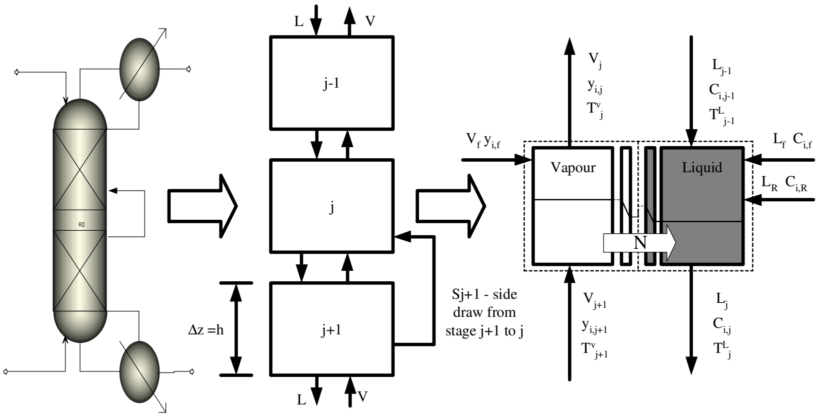

Figure 3.10: Schematic view of a reactive distillation column and the corresponding stage balance

Since reactive distillation is proven to be as potential candidate for intensifying the polyester process in the previous section, a more in depth analysis is made in this section. Particularly the influence of the liquid back mixing on the whole process is investigated by using the extended rate-based model. The dynamic rate-based model is extended to account for liquid back mixing, by considering each stage as a stirred tank reactor. The extended model accounts for convection, mass transfer, reaction and axial dispersion. The liquid phase balance is discussed in detail in order to show explicitly how the axial dispersion is introduced into the reactive distillation model. The description of the vapor phase, the mass transfer between phases and the reactions in liquid phase remains the same as in the rate-based modeling. The model consists of *n* number of stages in series and each stage is considered as stirred tank reactor as shown in figure 3.10.

Note that *n* number of stirred tank reactors in series represents plug flow behavior hence the liquid phase balance can be represented by a plug flow reactor (PFR) model that is composed of partial differential equation (PDE):

$$\frac{\partial C_i}{\partial t} = -v\frac{\partial C_i}{\partial z} + D_{ax}\frac{\partial C_i^2}{\partial z^2} + R_i + \dot{N}_i \qquad (3.6)$$

where, C_i is the concentration of component i, t is the time, v is the linear flow velocity, z is the position coordinate down the length of the column, D_{ax} is the axial dispersion coefficient, R_i is the reaction rate of component i and $\dot{N}_i$ is the liquid mass transfer flux. By discretization of spatial derivatives of eq. (3.6), the liquid phase balance is represented as ordinary differential equation (ODE):

$$\frac{dC_{i,j}}{dt} = -v\frac{C_{i,j} - C_{i,j-1}}{\Delta z} + D_{ax}\frac{C_{i,j-1} - 2C_{i,j} + C_{i,j+1}}{\Delta z^2} + R_{i,j} + \dot{N}_{i,j} \qquad (3.7)$$

where, $C_{i,j}$ is the concentration of component i at a stage j and Δz is the height of stage. Eq. (3.7) is reformulated by substitution of $C_{i,j} = n^L_{i,j}/M_j$ and $\Delta z = h$ on the left and right sides, respectively:

$$\frac{dn^L_{i,j}}{dt} = -vM_j\frac{C_{i,j} - C_{i,j-1}}{h} + D_{ax}M_j\frac{C_{i,j-1} - 2C_{i,j} + C_{i,j+1}}{h^2} + M_jR_{i,j} + M_j\dot{N}_{i,j} \qquad (3.8)$$

where, $n^L_{i,j}$ is the number of moles of component i on a stage j, M_j is the hold up on a stage j. In order to compare eq. (3.8) to the traditional liquid phase balance of the rate-based model, vM_j/h is substituted by L_j and $M_j\dot{N}_{i,j}$ is substituted by $N^L_{i,j}$:

$$\frac{dn^L_{i,j}}{dt} = L_{j-1}C_{i,j-1} - L_jC_{i,j} + D_{ax}M_j\frac{C_{i,j-1} - 2C_{i,j} + C_{i,j+1}}{h^2} + M_jR_{i,j} + N^L_{i,j} + L_fC_{i,f} + L_RC_{i,R} \qquad (3.9)$$

where, L_j is the liquid flow rate on a stage j, $N^L_{i,j}$ is the liquid mass transfer rate. L_f and L_R are the liquid flow rate and, $C_{i,f}$ *and* $C_{i,R}$ are the concentration of component i for the feed and reflux, respectively. The Dirichlet and Neumann boundary conditions [18] are applied to solve eq. (3.9) for the top stage ($j=1$) and for the bottom stage ($j=J$), respectively. A side draw is introduced from each stage in the rate-based model for the coupled RD and side reactor process by [3]. We have used this concept to introduce the concentration of component i, $C_{i,\,j+1}$ from stage $j+1$ to a stage j by using the side draw (S_{j+1}) from a bottom stage ($j+1$) to a subsequent top stage (j). Since eq. (3.9) accounts for convection, dispersion, reaction and mass transfer, eq. (3.9) represents the complete liquid phase component material balance for the kinetically controlled processes. The total material balance for liquid phase is given by:

$$\frac{dn_j^L}{dt} = L_{j-1} - L_j + S_{j+1} + M_j \sum_{i=1}^{i=k} R_{i,j} + \sum_{i=1}^{i=k} N_{i,j}^L + L_f + L_R \qquad (3.10)$$

The component and total material balances for vapor phase are described by eq. (3.11) and (3.12), respectively:

$$\frac{dn_{i,j}^V}{dt} = V_{j+1} y_{i,j+1} - V_j y_{i,j} - N_{i,j}^V + V_f y_{i,f} \qquad (3.11)$$

$$\frac{dn_j^V}{dt} = V_{j+1} - V_j - \sum_{i=1}^{i=k} N_{i,j}^V + V_f \qquad (3.12)$$

where, V_j, V_{j+1} are respectively the vapor flow rate on a stage j and $j+1$, $y_{i,j}$, $y_{i,j+1}$ are respectively the mole fraction of component i of the vapor phase on a stage j and $j+1$, $N^V{}_{i,j}$ is the vapor mass transfer rate, V_f is the vapor feed flow rate and $y_{i,f}$ is the vapor feed mole fraction. The energy balances for liquid phase, vapor phase and at vapor-liquid interface are described by eq. (3.13), (3.14) and (3.15), respectively:

$$\frac{dE_j^L}{dt} = L_{j-1} H_{j-1}^L - L_j H_j^L + S_{j+1} H_{j+1}^L + a\left(h_j^L (T_j^* - T_j^L) + \sum_{i=1}^{i=n} N_{i,j}^L \overline{H}_{i,j}^L \right) + L_f H_F^L + L_R H_R^L \qquad (3.13)$$

$$\frac{dE_j^V}{dt} = V_{j+1} H_{j+1}^V - V_j H_j^V - a\left(h_j^V (T_j^V - T_j^*) + \sum_{i=1}^{i=n} N_{i,j}^V \overline{H}_{i,j}^V \right) + V_f H_F^V \qquad (3.14)$$

$$h_j^L (T_j^* - T_j^L) + \sum_{i=1}^{i=n} N_{i,j}^L \overline{H}_{i,j}^L = h_j^V (T_j^V - T_j^*) + \sum_{i=1}^{i=n} N_{i,j}^V \overline{H}_{i,j}^V \qquad (3.15)$$

where, $E^L{}_j$, $E^V{}_j$ are respectively the liquid and vapor energy hold up on stage j, $H^L{}_j$, $H^V{}_j$, are respectively the liquid and vapor enthalpy on stage j, $H^L{}_F$, $H^V{}_F$ are respectively the liquid and vapor feed enthalpy, $h^L{}_j$, $h^V{}_j$ are the heat transfer coefficients, $T^L{}_j$, $T^V{}_j$ are respectively the liquid and vapor temperature on stage j, $T^*{}_j$ and a are respectively the temperature and area at the vapor-liquid interface. The vapor-liquid equilibrium at the interface is represented by:

$$y_{i,j} P_j = x_{i,j} \gamma_{i,j} (x_{i,j}, T_j) p_{i,j}^{sat} \qquad (3.16)$$

where, P_j is the total pressure, $\gamma_{i,j}$ is the activity coefficient of component i as function of $x_{i,j}$ and T_j and $p^{sat}{}_{i,j}$ is the vapor pressure of pure component i. The mass transfer rates at the interface are represented by eq. (3.17), (3.18) and (3.19):

$$N_{i,j}^V = N_{i,j}^L \qquad (3.17)$$

$$N_{i,j}^L = k_l a (x_{i,j}^* - x_{i,j}) \qquad (3.18)$$

$$N_{i,j}^V = k_g a (y_{i,j} - y_{i,j}^*) \qquad (3.19)$$

where, k_l, k_g are respectively liquid and vapor side mass transfer coefficients, a is the interfacial area and $C^*{}_{i,j}$, $y^*{}_{i,j}$ are the liquid and vapor side equilibrium concentration of component i, respectively.

Aspen Custom Modeler (ACM) is used as CAPE tool to formulate the EQ, rate-based and extended rate-based models for the synthesis of unsaturated polyester by reactive distillation. Note that, the EQ model accounts only for phase equilibrium and reaction kinetics. The rate-based model accounts for phase equilibrium, reaction kinetics and mass transfer between the phases and, the extended-rate based model accounts for axial dispersion in addition to the traditional rate-based model.

3.2.2.1 Influence of the liquid back mixing

The column is operated as a counter current vapor-liquid contactor. The anhydride is fed as liquid at the top of the column and glycol is fed at the bottom of the column as a vapor. The polyester product leaves at the bottom of the column and water leaves at the top of the column. To investigate the influence of the liquid back mixing on the reactive distillation process, first the extended rate-based model is simulated with hypothetical values of an axial dispersion coefficient as illustrated in figure 3.11 (a). The simulations of the reactive distillation process show that there is a significant influence of the axial dispersion on the conversion. When the axial dispersion is neglected, a conversion of 96% is predicted. However, the conversion significantly reduces to 90% with increase of the axial dispersion coefficient. This clearly shows that – due to the low conversion of the reactant in this highly back mixing system – the end product composition is also significantly altered. To achieve the same conversion in the dispersed system as in the ideal system ($D_{ax} = 0\ m^2/s$), more stages are required. Figure 3.11 (b) shows the required number of stages to achieve 96% conversion for various axial dispersion coefficients. The required stages increase linearly with respect to the axial dispersion coefficient for the polyester process.

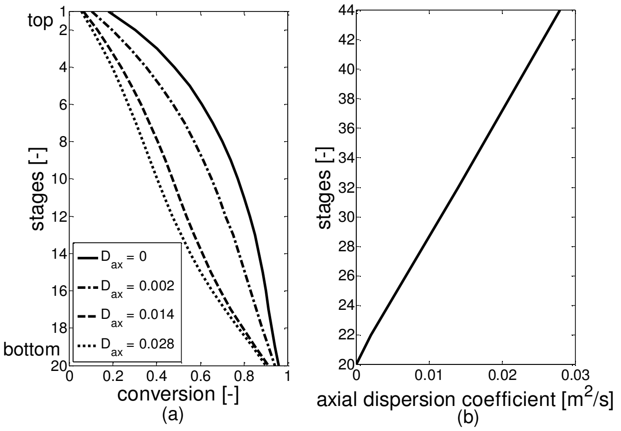

Figure 3.11: (a) Influence of axial dispersion on conversion (b) required number of stages to obtain a conversion of 96% for various dispersed systems

In practice, the column internals influence the axial dispersion and therefore it is necessary to investigate internals that provide low axial dispersion. Because the reactive distillation process for the synthesis of unsaturated polyester is kinetically controlled and a high liquid holdup is required to enhance the rate of reaction, three internal configurations - bubble column, packed bubble column and tray bubble column are selected. The selected internal configurations provide significantly higher liquid holdup as compared to traditional internal configurations of reactive distillation columns such as packings and trays. This is because the liquid is in the continuous phase and vapor is in dispersed phase in the selected configurations and vice versa in the traditional internal configurations.

The rate-based and extended rate-based models are adopted for the hydrodynamics, mass transfer and back mixing correlations of the respective internals. These correlations are taken from [19-22]. The conversion profiles predicted from the EQ, rate-based and extended rate-based for three different internal configurations are compared in figure 3.12. It can be seen that the models predict different conversion profiles. However, it is clear from figure 3.12 that the bubble column with packing or partition trays has lower axial dispersion compared to the empty bubble column and thus the conversion profiles for the packed bubble or tray bubble configurations are closer to the conversion profile of the rate-based model. Since the experimental data is not yet known for the synthesis of the polyester by reactive distillation, it cannot be generalized yet which model predicts best.

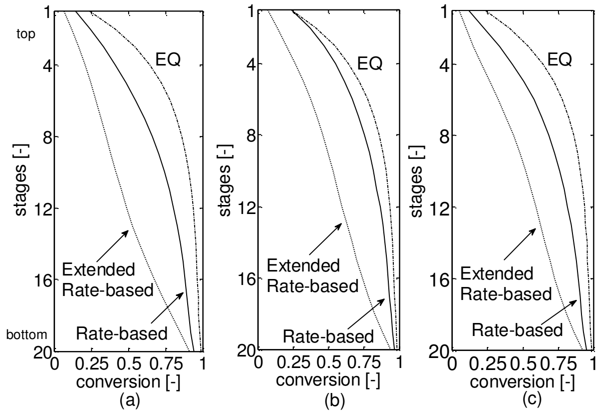

Figure 3.12: The conversion profile over the reactive stripping column for the empty bubble column (a) sieve trayed bubble column (b) packed bubble section with metal pall rings (c)

3.2.2.2 Multi-product simulation

The extended rate-based model is used to simulate a multi-product reactive distillation column. As discussed earlier, undesired products are often formed during the product changeover in a multi-product continuous reactive distillation column. The formation of undesired product is reduced by altering the product transition time. Therefore, the influence of liquid back mixing on the product transition time is the most important parameter to investigate. The influence of liquid back mixing on the product changeover is demonstrated by producing two different grades of polyester in a single reactive distillation column. To produce the polyester of grade P_1, the maleic anhydride is only fed as the liquid feed. To produce the polyester of grade P_2, the maleic anhydride and fumaric acid are fed equimolar as liquid feed to the column. In both grades of polyester, another reactant, propylene glycol, is fed as a vapor at the bottom of the column. The dynamic simulation of product changeover from grade P_1 to grade P_2 in a reactive distillation column is shown in figure 3.13, for various axial dispersion coefficients.

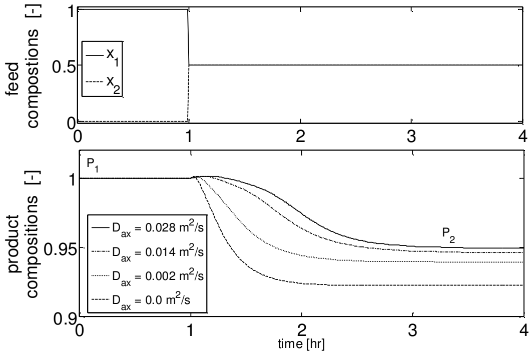

Figure 3.13: Dynamic profile of product changeover

Due to the fact that different conversions are achieved with varying axial dispersion coefficients (as illustrated in figure 3.11 (a)), the steady state composition of product P_2 is different. It is noticeable that during product changeover, the product transition time from a steady state composition of product P_1 to a steady state composition of product P_2 is significantly higher in the highly dispersed system as compared to a less dispersed system. This results in more undesired product formation in the highly dispersed system.

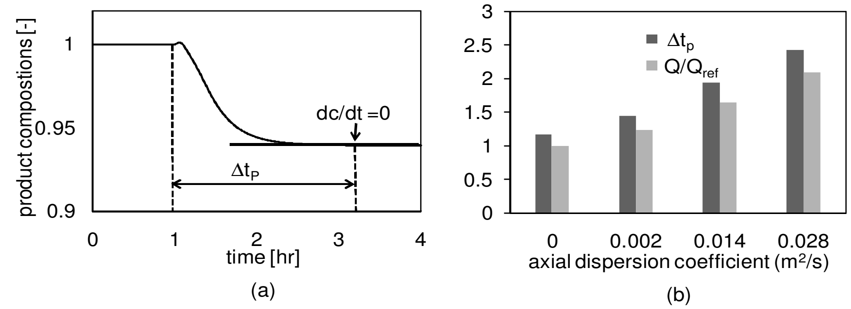

(a)

(b)

Figure 3.14: (a) The product transition period determination, (b) ratio of the amount of undesired product formed in the dispersed system with respect to the ideal system (D_{ax} = 0 m^2/s)

The product transition period ends at the first point after the product changeover started, where the slope (dc/dt) of the curve is zero as illustrated in figure 3.14 (a). The amount of undesired product formed during the product changeover is calculated from production rate, undesired product compositions and product transition time such as:

$$Q = F\int_{t1}^{t2} C_i dt \qquad (3.20)$$

The product transition time and the amount of undesired product produced in the dispersed system with reference to the ideal system ($D_{ax} = 0\ m^2/s$) are shown in figure 3.14 (b). It can be seen from figure 3.14 (b) that the product transition time increases with the increase in the axial dispersion coefficient. Therefore, the amount of undesired product formed during the product changeover also increases with the increase in the axial dispersion coefficient. The formation of such undesired product during the product changeover in the more highly dispersed system, is at least 1.5 times higher as compared to a low dispersed system. This means that the reactive distillation model without the axial dispersion is not sufficient to represent the multi-product continuous reactive distillation process realistically. The extended rate-based model improves the predictive capability of the slow reaction process (kinetically controlled process) compared to conventional reactive distillation models and provides a better platform to analyze the multi-product reactive distillation process.

3.3 Conclusions

In this chapter a reactive distillation model for the unsaturated polyester process is formulated. The model predicts the polymer attribute, isomerization and saturation composition of the polymer in the range of industrial polyester production data. From sensitivity analysis of the reactive distillation process, it is concluded that 20 equilibrium stages are required to obtain pure top (water) and bottom (polyester) products. The best feed ratio (propylene glycol/ maleic anhydride) is 1.15:1.0, the best range of vapor feed stream temperature is between 250-270^{o}C and the reflux ratio is 0.2 mol/mol for unsaturated polyester synthesis by reactive distillation. Afterwards, the reactive distillation process with these operating and design parameters is compared with the batch reactor process. It is found that the reactive distillation process has distinct advantages over the traditional batch reactor process. The unsaturated polyester synthesis by reactive distillation is intensified in all domains of structure, energy, synergy and time. A 7% higher equilibrium conversion is achieved in the reactive distillation process compared to the batch reactor process. The required residence time is only 1.8-2 hours compared to 12 hours of batch time in the conventional process.

In the second part of this chapter, the traditional rate-based model is extended to account for the axial dispersion. The predictions of the extended model were efficiently compared with the traditional rate-based and equilibrium models. The simulation results demonstrated that the axial dispersion significantly influences the reactive distillation process and cannot be neglected. The extended model predicts lower conversion in a highly dispersed system, as compared to a low dispersed one. The application of packing or partition trays in the bubble column reduces the axial dispersion and thus the conversion is higher for packed/tray bubble configurations as compared to an empty bubble column. The extended model can also be used to describe realistically a multi-product reactive distillation column. It predicts that the product transition time is significantly increased at high liquid back mixing. Undesired product is formed at >1.5 times larger amounts in higher dispersed systems as compared to a less dispersed one.

List of symbols

a	interfacial area (m^2)
C	concentration of component (mol/kg)
CP_L	Heat capacity of liquid mixture (kJ/kg/C)
CP_V	Heat capacity of vapor mixture (KJ/kmol/C)
D_{ax}	axial dispersion coefficient (m^2/s)
E^L, E^V	liquid and vapor energy holdup (KJ)
F	bottom product flow rate (kg/hr)
h	height of a stage (m)
H_i^V	Heat of vaporization of component i (KJ/kmol)
H^L	liquid enthalpy (KJ/kg)
H^V	vapor enthalpy (KJ/mol)
h^L,h^V	the heat transfer coefficients (w/m^2-k)
k_l, k_g	the mass transfer coefficients (mol/m^2-s)
L	liquid flow rate (kg/s)
M	liquid holdup (in kg for eq. (3.1) and in kmol for eq. (3.8))
n	number of moles of component (mole)
N^L	liquid side mass transfer rate (mol/s)
N^V	vapor side mass transfer rate (mol/s)
P	pressure (bar)
Q	amount of undesired product (mol)
R	reaction rate (mol/kg-s)
T_j	temperature on stage j (K)
v	liquid velocity (m/s)
V	vapor flow rate (mol/s)
X	equilibrium conversion (-)
x	liquid mole fraction (mol/mol)
y	vapor mole fraction of (mol/mol)

Greek letters

ε_j	reaction volume on stage j (kmol)
$\gamma_{I,j}$	activity coefficient of component i on stage j (-)
$\nu_{I,m}$	stoichiometry coefficient of component i in reaction m (-)
τ	residence time of the liquid in the column (hr)

Subscripts

F	feed stage
i	component indices
j	stage indices
R	reflux

Superscripts

L	liquid phase
V	vapor phase

sat	saturated

Abbreviations

Cis	cis formed component
COOH	acid end group
FA	fumaric acid
MA	maleic acid
MAD	maleic anhydride
OH	hydroxyl group
POLY	polyester
$POLY_{1D}$	maleate formed polyester
$POLY_{2D}$	fumarate formed polyester
$POLY_s$	saturated polyester
PG	propylene glycol
SACID	saturated acid
Trans	trans form component

References

[1] J. Korbar, J. Golob, A. Šebenik, Process of unsaturated polyester resin synthesis on a laboratory and industrial scale, Polymer Engineering & Science, 33 (1993) 1212.

[2] M. Shah, E. Zondervan, A.B.D. Haan, Modelling and simulation of an unsaturated polyester process, Journal of applied sciences, 10 (2010) 2551-2557.

[3] R. Taylor, R. Krishna, Modelling reactive distillation, Chemical Engineering Science, 55 (2000) 5183.

[4] K. Sundmacher, A. Kienle, Reactive distillation- status and future directions, Willey-VCH, 2003.

[5] R. Krishna, Reactive separations: more ways to skin a cat, Chemical Engineering Science, 57 (2002) 1491.

[6] C. Noeres, E.Y. Kenig, A. Górak, Modelling of reactive separation processes: reactive absorption and reactive distillation, Chemical Engineering and Processing, 42 (2003) 157.

[7] A. Stankiewicz, Reactive separations for process intensification: an industrial perspective, Chemical Engineering and Processing, 42 (2003) 137.

[8] J. Harmsen, Reactive distillation: The front-runner of industrial process intensification: A full review of commercial applications, research, scale-up, design and operation, Chemical Engineering and Processing, 46 (2007) 774.

[9] J. Harmsen, Process intensification in the petrochemicals industry: Drivers and hurdles for commercial implementation, Chemical Engineering and Processing: Process Intensification, 49 (2010) 70.

[10] A. Higler, R. Krishna, R. Taylor, Nonequilibrium cell model for multicomponent (reactive) separation processes, AIChE Journal, 45 (1999) 2357.

[11] R. Baur, A.P. Higler, R. Taylor, R. Krishna, Comparison of equilibrium stage and nonequilibrium stage models for reactive distillation, Chemical Engineering Journal, 76 (2000) 33.

[12] J. Peng, T. F. Edgar, R. Bruce Eldridge, Dynamic rate-based and equilibrium models for a packed reactive distillation column, Chemical Engineering Science, 58 (2003) 2671.
[13] A.M. Katariya, R.S. Kamath, K.M. Moudgalya, S.M. Mahajani, Non-equilibrium stage modeling and non-linear dynamic effects in the synthesis of TAME by reactive distillation, Computers & Chemical Engineering, 32 (2008) 2243.
[14] M. Shah, E. Zondervan, A.B. de Haan, Development of a model for the synthesis of unsaturated polyester by reactive distillation, in: Distillation Absorption 2010, Eindhoven, The Netherlands, 2010, pp. 247-252.
[15] A.A. Kiss, Separative reactors for integrated production of bioethanol and biodiesel, Computers & Chemical Engineering, 34 (2010) 812.
[16] C. Noeres, A. Hoffmann, A. Górak, Reactive distillation: Non-ideal flow behaviour of the liquid phase in structured catalytic packings, Chemical Engineering Science, 57 (2002) 1545.
[17] A. Kolodziej, M. Jaroszynski, H. Schoenmakers, K. Althaus, E. Geißler, C. Übler, M. Kloeker, Dynamic tracer study of column packings for catalytic distillation, Chemical Engineering and Processing, 44 (2005) 661.
[18] H. Fogler, Elements of Chemical Reaction Engineering, 2 ed., Prentice hall, 1992.
[19] J. Alvaré, M.H. Al-Dahhan, Liquid phase mixing in trayed bubble column reactors, Chemical Engineering Science, 61 (2006) 1819.
[20] F. Rendtorff Birrer, U. Böhm, Gas-liquid dispersions in structured packing with high-viscosity liquids, Chemical Engineering Science, 59 (2004) 4385.
[21] P. Therning, A. Rasmuson, Liquid dispersion and gas holdup in packed bubble columns at atmospheric pressure, Chemical Engineering Journal, 81 (2001) 69.
[22] K. Thaker, D.P. Rao, Effects of Gas Redispersion and Liquid Height on Gas-Liquid Hydrodynamics in a Multistage Bubble Column, Chemical Engineering Research and Design, 85 (2007) 1362.

Chapter 4

A systematic framework for the economical and technical evaluation of reactive distillation processes

This chapter presents a novel design methodology for the economical and technical evaluation of reactive distillation (RD) and, discusses the applicability of various design methods of RD. A proposed framework for economical evaluation determines the boundary conditions (e.g. relative volatilities, target purities, equilibrium conversion and equipment restriction), checks the integrated process constrains, evaluates economical feasibility, and provides guidelines to any potential RD process application. A proposed framework for technical evaluation determines the technical feasibility of RD, the process limitations, working regime and requirements for internals as well as the models needed for RD. This approach is based on dimensionless numbers such as Damkohler and Hatta numbers, and the kinetic, thermodynamic and mass transfer limits. A proposed framework for economical and technical evaluation of RD allows a quick and easy RD feasibility analysis for a wide range of chemical processes. In this study several industrial relevant case studies (e.g. synthesis of di-methyl carbonate (DMC), methyl acetate hydrolysis, toluene hydro-dealkylation (HDA) process, fatty acid methyl esters (FAME) process and unsaturated polyesters synthesis) illustrate the validity of the proposed framework.

4.1 Introduction

Reactive distillation (RD) combines reaction and separation into a single operating unit, and represents one of the most important industrial applications of the multifunctional reactor concept. Recently, RD has drawn increased attention due to its key advantages over conventional processes, such as: 1) economical profit: significant reduction of capital and operating costs, major energy savings, 2) environmental gains: emissions reduced by 20% or more compared to a classic set-up (e.g. reactor followed by distillation column) and 3) social benefits: improvement on safety, health and society by little reactive content, low chances of runaway sensitivity and lower space occupation [1-5].

Scientific literature and patents on RD are abundantly published since the early 20th century. Extensive overviews of industrial application, feasibility analysis, design and synthesis methods, modeling strategy and internal design of RD was reported in several papers [1, 2, 5, 6]. RD process design is carried out either by simulation or by synthesis design. Simulation involves specifying the inputs, operating variables and equipment sizes and solving for the resulting outputs. In contrast, synthesis design involves specifying the inputs and selected outputs, operating variables and also design variables, and determine whether a feasible set exits for the given product specifications. Although simulation and synthesis design are two different approaches, they are complementary to determine the design parameters. Remarkably, using first synthesis design methods to determine the design parameters enables the chemical engineers to perform more effective simulations [7].

Mixed-integer nonlinear programming (MINLP) and fixed-point methods are two approaches used for the synthesis design methods. Ciric and Gu [8], Jackson and Grossmann [9] and Gangadwala et al. [10] used a MINLP model for synthesizing a reactive distillation column by minimizing the total annual cost. Buzad and Doherty [7] have proposed a fixed-point based design method for equilibrium reactive distillation processes which is further extended to non-reactive and reactive residue curve maps (RCM). Venimadhavan et al. [11] have studied the effects of kinetics on reactive distillation residue curve maps. They have identified singular points of the fixed-point method as a function of Damkohler number (*Da*) which is used in combination with the chemical equilibrium constant to describe the feasibility of RD applications. From the synthesis design method, the feasibility of applying RD and the process limitations can be easily identified and the suitable model for the simulation studies selected.

Simulations are currently based on either equilibrium (EQ) modeling or rate-based modeling. Equilibrium modeling and rate-based modeling were extensively studied by Taylor and Krishna [5], Sundmacher and Kienle [6], Baur et al. [12], Higler et al. [13], Katariya et al.[14], Kiss [15], Peng et al.[16] and Shah et al. [17]. In equilibrium modeling, the vapor and liquid are assumed to be in equilibrium. In practice, the theoretical number of stages obtained from equilibrium model calculations is converted to the required real number of stages, either through the overall efficiency of a tray or by the height equivalent of a theoretical plate (HETP) for packed columns. This is a useful approach to simulate a binary system or an existing column. However, this approach is not reliable to simulate a multi-component system or an existing column with different operating conditions [12, 14, 16]. Compared to equilibrium modeling, rate-based modeling offers accuracy in design of a column as it accounts for: 1) vapor-liquid equilibrium only at the interface between the bulk liquid and vapor phases 2) a transport-based approach to predict the flux of mass and energy across the interface, and 3) the real hydrodynamic situation of either a tray or a packed column. For these reasons, over-design and under-design are avoided, there is no need for efficiencies and HETPs and the column is designed more realistic as compared to EQ modeling, thereby reducing the capital and operating costs. However, the establishment of a detailed rate-based model is complex since it requires a significant amount of input data, which can be reduced by adopting the model according to the process limitations of RD.

4.2 Problem statement

Currently, the typical design of RD is still based on extensive simulation studies followed by expensive and time-consuming sequences of laboratory and pilot plant experiments – the main reason being the absence of an established RD design procedure that is suitable for a straightforward economical and technical evaluation. Hence, the problem is how to determine quickly but reliably when RD is an economically and technically feasible alternative for an existing or a new chemical process. To solve this problem a systematic framework is developed in this work through which the economical and technical feasibility, the process limitations, the working regime, internal and model requirements for RD process can be quickly and reliably evaluated. A major advantage of this approach is its applicability to a wide range of all-scale processes and multiproduct environments. The systematic approach proposed in this work determines the boundary conditions for RD (relative volatilities, target purities, equilibrium conversion, equipment restrictions), checks the integrated process constraints, evaluates the technical and economic feasibility and provides guidelines applicable to almost any potential RD process application. In order to illustrate the applicability of the proposed methodology, several industrial relevant case studies are examined.

4.3 Framework for economical evaluation

The proposed approach for the economical evaluation of RD is based on industrial applications of RD reported in the scientific literature [5, 6, 15, 17-28] as shown in figure 4.1. To perform the economical evaluation, some basic information on the chemical process is required such as: vapor liquid equilibrium, stoichiometry of reaction, kinetics, enthalpy of reaction. The first step is to check the number of products and reaction type. If there is only one product present, the last step of the main reaction is irreversible and when there are no side reactions present there is no advantage of using RD over a simple reactor [21]. One must not forget that the main advantages of RD rely on overcoming the equilibrium limitations and enhancing the selectivity towards the desired product [1, 5]. As both operations occur simultaneously in the same unit, there must be a proper match between the temperatures required for reaction and separation [5, 20]. If there is no significant overlapping of the operating conditions of reaction and separation, then the combination of reaction and distillation is not possible (e.g. a high pressure reaction can not be combined with a vacuum distillation). Moreover, one must also consider that working in the limited overlapping window of operating conditions is not always the optimal solution, but merely a trade-off. For example, in the conventional hydro-dealkylation (HDA) process the temperature difference between the reaction and the separation process is 120°C. In this case, RD was found to be technically applicable, yet it was not economically attractive [28]. Therefore, for a feasible RD process the temperature difference between separation and main reaction should be lower than about 50°C – this figure not being so strictly limiting.

Moreover, the operating pressure and temperature should not be close to the critical region of the key components, since that would potentially lead to one supercritical phase [19]. If the column operates at the critical pressure of key components, these will be present in the vapor – while in the vast majority of the RD processes the reaction takes place in liquid phase [19]. For example, the synthesis of di-methyl carbonate (DMC) by catalytic esterification of carbon dioxide and methanol occurs in the near critical region of carbon dioxide at 73 bar and 80-100°C [29]. Hence, the RD alternative is not applicable in this process as the main reaction takes place in gas phase.

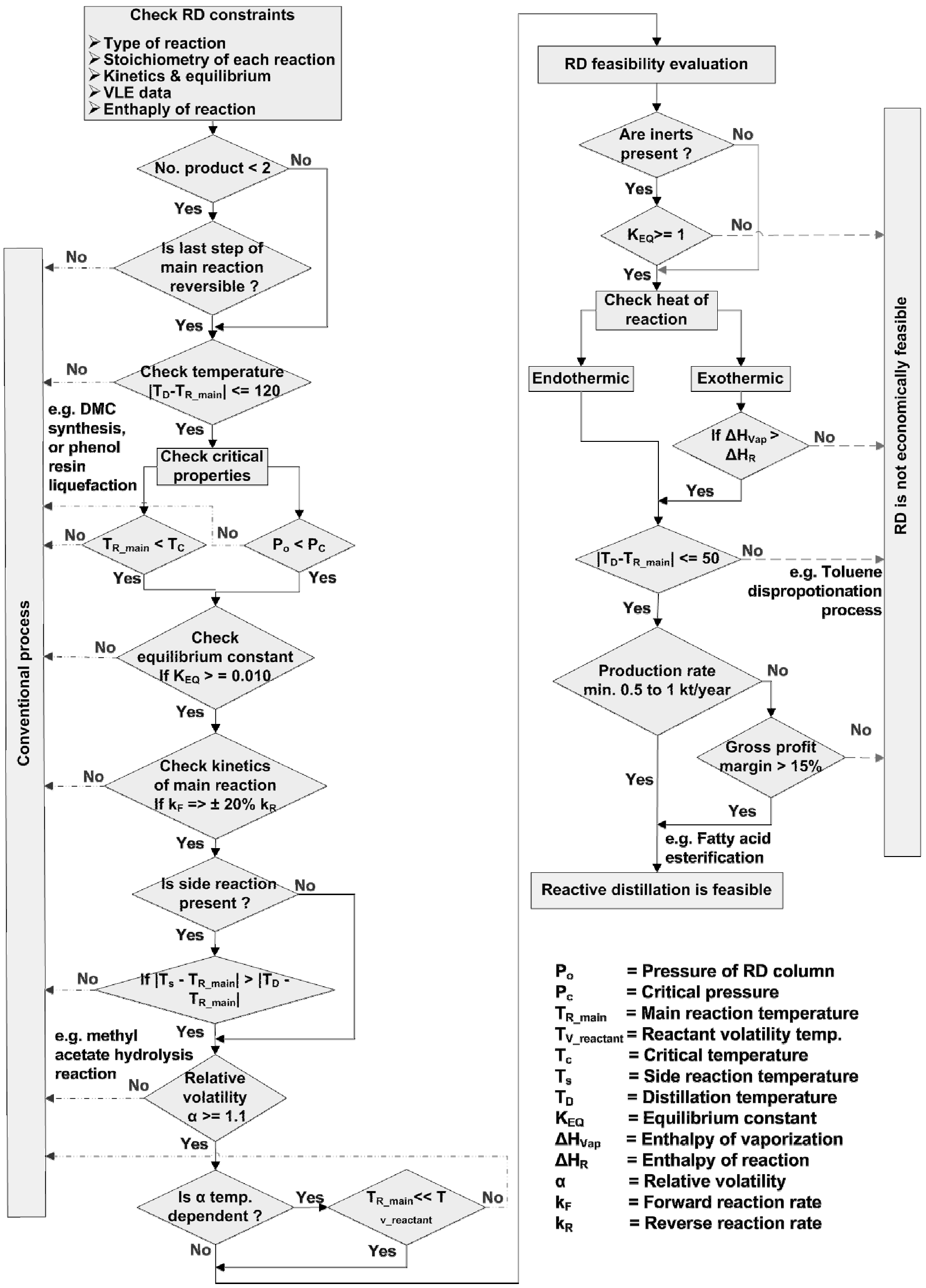
Check RD constraints
Type of reaction
Stoichiometry of each reaction
Kinetics & equilibrium
VLE data
Enthaply of reaction
No. product < 2
No
Yes
Is last step of main reaction reversible ?
No
Yes
Check temperature $|T_D-T_{R\_main}| <= 120$
No
e.g. DMC synthesis, or phenol resin liquefaction
Yes
Check critical properties
$T_{R\_main} < T_C$
No
No
$P_o < P_C$
Yes
Yes
Check equilibrium constant If $K_{EQ} > = 0.010$
No
Yes
Check kinetics of main reaction If $k_F => \pm 20\%\ k_R$
No
Yes
Is side reaction present ?
No
Yes
If $|T_s - T_{R\_main}| > |T_D - T_{R\_main}|$
No
e.g. methyl acetate hydrolysis reaction
Yes
Relative volatility $\alpha >= 1.1$
No
Yes
Is α temp. dependent ?
Yes
$T_{R\_main} << T_{v\_reactant}$
No
No
Yes
Conventional process
RD feasibility evaluation
Are inerts present ?
No
Yes
$K_{EQ} >= 1$
No
Yes
Check heat of reaction
Endothermic
Exothermic
If $\Delta H_{Vap} > \Delta H_R$
No
Yes
$|T_D-T_{R\_main}| <= 50$
No
e.g. Toluene dispropotionation process
Yes
Production rate min. 0.5 to 1 kt/year
No
Gross profit margin > 15%
No
Yes
Yes
e.g. Fatty acid esterification
Reactive distillation is feasible
RD is not economically feasible
P_o = Pressure of RD column
P_c = Critical pressure
T_{R_main} = Main reaction temperature
$T_{V\_reactant}$ = Reactant volatility temp.
T_c = Critical temperature
T_s = Side reaction temperature
T_D = Distillation temperature
K_{EQ} = Equilibrium constant
ΔH_{Vap} = Enthalpy of vaporization
ΔH_R = Enthalpy of reaction
α = Relative volatility
k_F = Forward reaction rate
k_R = Reverse reaction rate

Figure 4.1: Systematic framework for economical evaluation of reactive distillation

Relative volatility of key chemical components is also a crucial parameter for the economical analysis of RD. Temperature dependence of vapor pressure of individual components can results in decreased relative volatility as temperature increases in multicomponent systems. This can create a mismatch of favorable temperature for kinetics and relative volatilities which can make the RD process unattractive [24]. For instance, in the hydrolysis reaction of methyl-acetate, the reactant (MeAc) is the lightest component and it is difficult to keep it in the reactive zone. Therefore, a conventional RD process is not applicable in this case. A relative volatility of minimum 1.1 was chosen for this RD feasibility analysis, as this is the typical minimum value for distillation process [6, 24].

The chemical equilibrium constant influences the reactant flow and residence time in a RD column. A low equilibrium constant will require an excess of reactants and a higher number of reactive trays for RD column [19]. However, this will result in an increased total annual cost (TAC) of RD process. In the case of methyl-acetate hydrolysis, the equilibrium constant is small ($K_{EQ} \sim 0.0013$ at 50°C) [23]. Still, non-conventional RD processes such as a reactive dividing-wall column could be an attractive alternative for this process [26]. Nevertheless, for conventional RD processes a $K_{EQ} > 0.01$ is recommended, in order to be economically attractive.

Inerts are present in many processes and in some RD commercial systems the lighter reactants are fed together with an inert. The presence of inerts reduces the concentration of reactants and results in lower reaction rates as well as reduced K_{EQ}. However, certain amount of inerts can be beneficial for optimum conversion – e.g. the MTBE production, in which n-butene serves as a coolant for the reactive zone, thereby keeping the temperature of the reactive zone at a level where the equilibrium is favorable for MTBE conversion [13]. In RD processes, the specific reaction rate for the main reaction cannot be too low as that would require large liquid holdups, large amounts of catalyst on each reactive tray and eventually a larger column [19]. Therefore, the reaction rate for the main reaction should be higher than 10^{-5}kmol/kg$_{cat}$.sec (e.g. methyl-acetate hydrolysis) [23]. In RD processes, the desired column temperature should be selected such that the secondary reactions are minimized while the productivity is still sufficiently high. For instance, in the methyl tert-butyl ether (MTBE) process, two consecutive side reactions are present: the irreversible dimerization of isobutene to di-isobutene ($T_b = 101.45°C$) and the reversible dehydration of methanol to dimethyl ether (DME, $T_b = -24.83°C$). Therefore, the purity of the desired products, isobutene and methanol could be reduced due to the by-products formed [25]. The heat of reaction should be lower than the heat of vaporization of key components. A higher heat of reaction results in drying out of trays and reduced conversion.

The last criterion is checking the production rate – if it is above 0.5-1 ktonnes/year then a RD process is economical feasible. For lower production rates it is important to evaluate the gross profit of the process. A gross profit higher than 15% for small scale production is suitable for RD process application (e.g. pharmaceutical industry). Ultimately, if all conditions are fulfilled then RD process is also attractive (e.g. fatty acids esterification to FAME) [15, 18, 22].

4.3.1 Case studies

The four industrial relevant case studies presented here, illustrate the potential applicability range of the proposed methodology. Based also on the previously reported RD studies [5, 6, 15, 17-28], we are also confident that virtually any potential RD application can be quickly and reliably evaluated using this approach that checks if a process is economically attractive – a very important criteria at industrial scale.

4.3.1.1 *Methyl acetate hydrolysis*

During the production of poly vinyl alcohol (PVA), a large quantity of methyl acetate-water mixture (1.68 kg/kg PVA) is produced as by-product [6]. In the industry the mixture of methyl acetate and water is further hydrolyzed to recover the methanol and acetic acid. This process is operated far below critical pressure of the components and the difference in reaction and separation temperatures is less than 50°C. The components present in this process are close boiling components in which methyl acetate is the lightest reactant and forms strong binary azeotrope with methanol as illustrated by the residue curve map (RCM) in figure 4.2 (a) [6, 23]. This thermodynamic behavior dictates that it is very difficult to keep methyl acetate in the reactive zone and the relative volatility is less than 1.1 for the binary pair of methyl acetate and water. Hence, it is not likely to obtain high purity methanol in a single RD column. Due to these technical constraints the conventional RD process is not technically feasible, although RD is suitable for the reverse reaction. However, an RD process with the additional distillation columns could be an alternative for this process. Fuchigami developed an RD process using an ion-exchange resin catalyst [30]. The RD column is operated under total reflux to recover methyl acetate from the methyl acetate-methanol azeotrope. The stripping section strips all methyl acetate and the bottom product is essentially free of methyl acetate and contains methanol, water and acetic acid. This bottom product can be easily separated by two additional distillation columns. Another viable alternative is a non-conventional RD process such as reactive dividing-wall column (RDWC) [26].

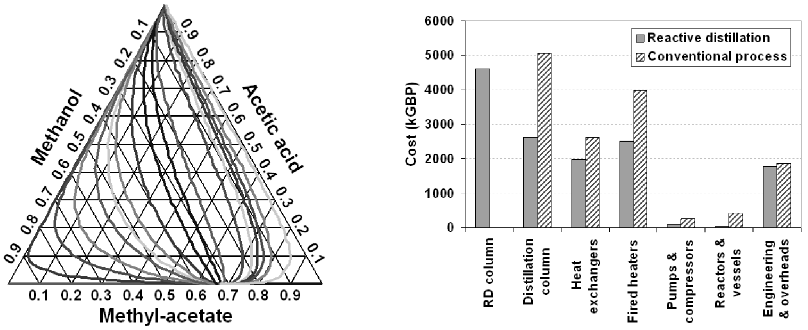

(a) (b)

Figure 4.2: (a) Residue curve map (RCM) of methyl-acetate / methanol / acetic acid (Sundmacher and Kienle, 2003), (b) Cost comparison for a toluene hydro-dealkylation plant [28]

4.3.1.2 *Toluene hydro-dealkylation process*

In the conventional process of hydro-dealkylation (HDA) of toluene to benzene, the reaction requires 20-25 bar and 400°C, whereas the RD column is operated at 30 bar and about 280°C in the reactive zone. Comparison of traditional and RD processes indicates that RD allows significant simplification of the flow sheet with a reduction in the number of distillation columns from five to three as well as the eradication of the reactor vessels. The selectivity of toluene over xylene is improved and by-product formation is reduced by RD compared to the traditional process. However, the optimal reactions vs. separation conditions are significantly different and the pressure required by the RD column is higher. These drawbacks cancel out the overall advantages of the RD process. Figure 4.2 (b) gives a summary of the key capital cost elements for both RD and the conventional process for a design basis of 150 ktones/year xylene and a costing basis in thousands of pounds (kGBP) [28]. The traditional process is dominated by the distillation columns with a significant share of the total spending lying also in the fired heaters and heat exchangers. In the RD process, the capital investment required for all of these is significantly reduced but substantially compensated by the cost of the reactive distillation column. The net effect is that the estimated capital saving is only in the order of 4% well below the 25–50% improvement typically required to drive a new technology development [28]. Therefore, in this case the RD application is not economically attractive in spite of being technically feasible and applicable.

4.3.1.3 *Fatty acid methyl esters (FAME) process*

Fatty acid methyl esters – the main components of biodiesel – can be directly produced by esterification of free fatty acids (FFA) with methanol or bioethanol [15, 18, 22]. Conventionally, biodiesel is produced batch-wise using homogeneous catalysts that have many associated problems (neutralization, separation, salt waste streams). The RD process powered by solid catalysts (Figure 4.3 (a)) offers unique advantages, such as: higher productivity, efficient use of raw materials and equipment, no catalyst related issues, elimination of alcohol excess and recycle, lower capital and operating costs. Figure 4.3 (b) illustrates the composition, temperature and reaction rate profiles along the RD column. High purity products are obtained in the top and the bottom of the RD, while complete conversion of the reactants is achieved. The RD process is technically feasible due to the favorable overlapping of the operating conditions (e.g. temperature, pressure) required for the reaction and separation, respectively. The reaction is slightly exothermal hence the heat of reaction is being used in-situ for the evaporation and removal of products. Moreover, the equilibrium constant, reaction rates and relative volatility are at high levels, while no secondary reactions take place under the design conditions. Remarkably, important energy savings are possible (over 45%) while the capital investment can be reduced by up to 40-60% as compared to conventional processes [22]. Therefore, in this case, the RD process (shown in Figure 4.3) proves to be not only technologically feasible, but at the same time economically attractive – using only ~109 kW·h / ton biodiesel produced in an integrated unit [15].

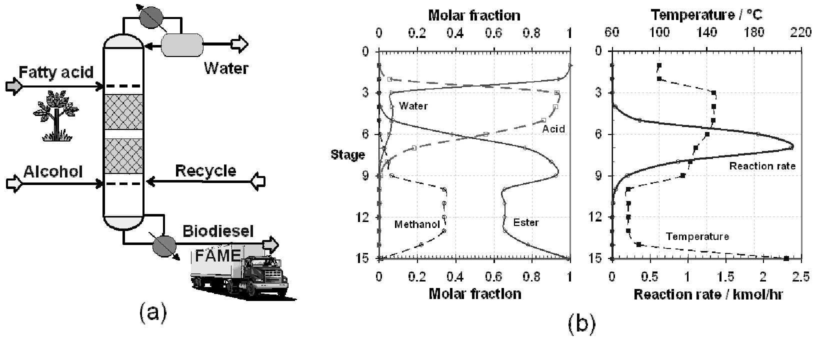

Figure 4.3: (a) RD process for fatty acids esterification, (b) Composition, temperature and reaction rate profiles [22]

4.3.1.4 Unsaturated polyesters synthesis

The synthesis of polyester is carried out with a combination of different anhydrides and diols for varying physical and chemical properties [31]. For this study, the unsaturated polyester synthesis from maleic anhydride and propylene glycol is taken as case study. Maleic anhydride and propylene glycol reacts and produces polyester and water. This is an equilibrium limited process and can be intensified by separating water from the reaction medium which allows shifting equilibrium to product side. Therefore, RD can be an alternative for the traditional batch reactor coupled with distillation column. The process chemistry, kinetic and thermodynamic models and, a comparison of the RD process with the traditional batch reactor process are reported in our earlier work [17, 27, 32]. The boiling point of byproduct (water) is significantly lower than the reaction temperature thus the byproduct can be easily separated at the reaction temperature ranging from 185°C to 270°C. The RD column is operated at 1 bar which is significantly lower than the critical pressure of the components. The polyester is a non-volatile component and water is the lightest component in the mixture of reactants and products. The relative volatility of water is greater than 1.1 with respect to the reactants and polyester. The chemical equilibrium constant over the RD column is ranging from 32 to 62 for given respective reaction temperatures, which refers to the recommended chemical equilibrium constant for the conventional RD process in figure 4.1. The industrial production scale for unsaturated polyesters is 50-150 ktones/year. These important criteria; separation temperature, operating pressure, equilibrium constant and production rate fulfill the requirement of economical feasible RD process. The improvements by RD over the traditional process for the production of unsaturated polyester are significant; the production time is reduced from 12 hours to 1.8 hours (85% reduction) and the required total volume to produce 100 ktones/year is reduced from 152 m^3 to 39 m^3 (74% reduction) [17, 27]. Remarkably, the intensification factors in terms of production time and total volume are about 6 and 4, respectively, which are well above the required intensification factor of 3 to drive new technology.

4.4 Framework for technical evaluation

The development of a realistic process model is the key step in evaluating the feasibility of a reactive distillation process. Moreover, a successful modelling effort requires a complete understanding of both equilibrium and kinetic limits of the process. The equilibrium behavior of most reactive distillation systems varies between two boundaries, corresponding to phase equilibrium and chemical equilibrium control. A residue curve maps (*RCM*) derived from the chemical equilibrium constant and the phase equilibrium for a reactive and non-reactive section of the RD column represents variations of the stationary points (corresponds to pure components and azeotropes) between equilibrium boundaries for given temperature and pressure. Buzad and Doherty [7], Venimadhavan et al. [11] and Okasinski and Doherty [33] have identified that the variations in these singular points can be represented by the Damkohler number (*Da*). The Damkohler number is defined as,

$$Da = \frac{H_0 k_f}{V} \qquad (4.1)$$

where, H_0 is the liquid holdup (mol), k_f is a pseudo-first-order rate constant (1/s) and V is the vapor rate (mol/s). The Damkohler number is the ratio of characteristics residence time (H_0/V) to characteristics reaction time ($1/k_f$). For low values of Da ($Da \leq 0.1$) the reaction rate on each stage is relatively slow compared to the residence time available on each stage, and the system is dominated by phase equilibrium. For large values of Da ($Da > 10$) the reaction rate is fast and chemical equilibrium is approached on the reactive stages. If the Damkohler number does not lie between these values, then the neither phase equilibrium nor the chemical equilibrium is controlling hence the process is kinetically controlled.

Moreover, the combinations of the Damkohler number and the chemical equilibrium constant can be used to perform a preliminary screening of the suitability of the process for an RD application. Reactive distillation is significantly beneficial when the process demonstrates combination of low Da ($Da \leq 0.1$) and high K_{EQ} ($K_{EQ} > 1$) or high Da ($Da > 0.1$) and low K_{EQ} ($K_{EQ} \leq 1$), as proposed by Venimadhavan et al. [11]. The combination of low Da and high K_{EQ} represents a slow forward reaction but a slower reverse reaction leads to high product formation. Reactive distillation offers benefits as long as the required holdup is not too large. The combination of high Da and low K_{EQ} represents a fast product formation but fast reverse reaction leads to little product formation. Reactive distillation is beneficial because the product can be removed quickly from the reactive zone and allows the equilibrium shifts to the product side. Since the product removal rate solely depends on the rate of mass transfer between phases, the process must not be mass transfer controlled. The combination of high Da and high K_{EQ} represents a fast forward reaction and a slower reverse reaction leads to a situation of an instantaneous irreversible reaction therefore a simple reactor is sufficient to carry out the process. For this class of processes, reactive distillation can only be useful compared to a simple reactor, when the higher selectivity of the main reaction over the side reaction is noticed. The reactive stage can be assumed to be at chemical equilibrium and such a reactive stage can be modeled as a vapor-liquid equilibrium stirred tank reactor. Reactive distillation is not beneficial when the process demonstrates a combination of low *Da* and low K_{EQ}. The combination of a low *Da* and a low K_{EQ} represents slow forward reaction and fast reverse reaction which essentially leads to no product formation. This class of processes requires an optimally designed reactor with a large holdup. This technical feasibility analysis of RD process and process limitations based on *Da* and the chemical equilibrium constant is represented in figure 4.4.

Furthermore the working regime of the process must be identified to confirm whether the process is the mass transfer or kinetically controlled, whether the reaction takes place only in the bulk or also in the film. This allows one to determine the requirements of internals for the RD column and the modeling approach that needs to be applied to design the RD process. Identification of the working regime can be performed by using the Hatta number (*Ha*), pseudo-first-order rate constant (k_f) and the product of mass transfer coefficient and interfacial area ($k_L a$). The Hatta number is the ratio of the maximum possible conversion in the film to the maximum diffusion transport through the film. For higher order reactions of two components, the Hatta number is defined as [34],

$$Ha = \sqrt{\frac{\frac{2}{n+1} k_f C_A^{n-1} C_B D_A}{k_L^2}} \tag{4.2}$$

where, n is the order of reaction (-), k_f is the forward reaction rate constant (1/s), C is the concentration (mol/m^3), D is the diffusivity (m^2/s) and k_L is the mass transfer coefficient (m/s). A Hatta number less than 1 represents a slow reactive distillation process and the reactions take place in the bulk. A Hatta number greater than or equal to 1 represents a fast reactive distillation process and the reaction take place in the bulk as well as in the film. This identification of working regime based on the Hatta number is illustrated in figure 4.4. The pseudo-first-order rate constant (k_f) and, the product of mass transfer coefficient and interfacial area ($k_L a$) particularly determine whether the process operates under the slow kinetic regime or slow diffusion regime or slow mixed regime as follows:

Slow reactive distillation process (Ha < 1):

- $k_f < k_L a$: This is a kinetically controlled process. The concentration of all reacting components is significant in the liquid phase. The overall rate is governed by the rate of reaction. Therefore, the design can be improved by a better catalyst or by increasing the liquid holdup. Suitable internals for this class of the process are a catalytic column, tray column (higher liquid holdup by increasing the weir height) and the packed or tray bubble column (where liquid is in continuous phase and vapor is in dispersed phase, allows high liquid holdup). The process requires a model which accounts for reaction kinetics and phase equilibrium. There is no need to account for the rate of mass transfer in the model.

- $k_f > k_L a$: This is a mass transferred controlled process and thus the overall rate is governed by the rate of mass transfer. The design can be improved by better vapor-liquid contactor. The suitable internal for this class of the process is packed column consists of high efficiency packing. The process requires a model which accounts for reaction kinetics, mass transfer between phases and phase equilibrium.

- $k_f = k_La$: This is neither a mass transfer nor a kinetically controlled process and thus the overall rate is governed by both the rate of reaction and mass transfer. The design can be improved by a better catalyst or a vapor-liquid contactor. The suitable internal for this class of the process is a catalytic column or a packed column containing high efficiency packing. The process requires a model which accounts for reaction kinetics, mass transfer between phases and phase equilibrium.

Fast reactive distillation process ($Ha \geq 1$):

- $k_f < k_La$: This describes a fast diffusion rate compared to the kinetic rate in the film. However, this situation can not occur because the Hatta number is greater than or equal to 1.
- $k_f > k_La$: This describes a fast reaction rate compared to the diffusion rate in the film. In this regime the overall rate is only proportional to the surface area per unit volume of a column. A better vapor-liquid contactor improves the design and therefore a packed column with high efficiency contactor is suitable for this process.
- $k_f = k_La$: The overall rate is proportional to the surface area per unit volume of a column and to the square root of the rate constant. A better vapor-liquid contactor and a better catalyst improve the design and therefore a packed column with high efficiency contactor and catalytic column are the suitable internals for this process.

The model for a fast reactive distillation process must account for the phase equilibrium, the rate of reaction and mass transfer in the bulk as well as in the film. The internal and model requirements for different working regimes are summarized in figure 4.4. Technical evaluation of RD can be systematically and quickly performed based on the Damkohler number, the chemical equilibrium constant, the Hatta number, the pseudo-first order rate constant and the product of mass transfer coefficient and the interfacial area.

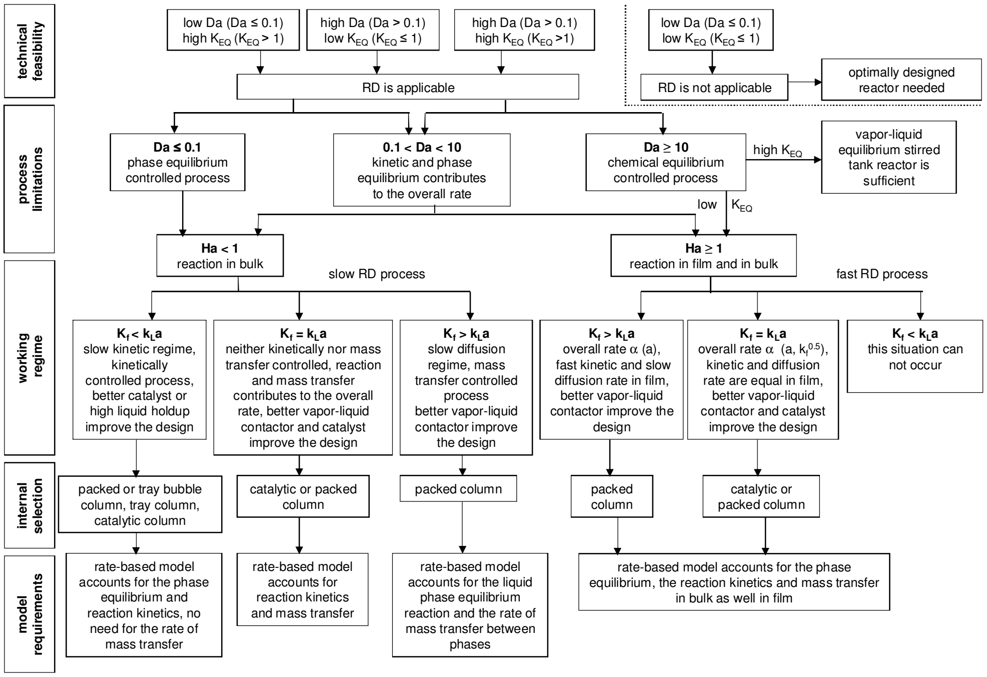
technical feasibility
process limitations
working regime
internal selection
model requirements
low Da (Da ≤ 0.1) high K_EQ (K_EQ > 1)
high Da (Da > 0.1) low K_EQ (K_EQ ≤ 1)
high Da (Da > 0.1) high K_EQ (K_EQ >1)
low Da (Da ≤ 0.1) low K_EQ (K_EQ ≤ 1)
RD is applicable
RD is not applicable
optimally designed reactor needed
Da ≤ 0.1 phase equilibrium controlled process
0.1 < Da < 10 kinetic and phase equilibrium contributes to the overall rate
Da ≥ 10 chemical equilibrium controlled process
high K_EQ
vapor-liquid equilibrium stirred tank reactor is sufficient
low K_EQ
Ha < 1 reaction in bulk
slow RD process
Ha ≥ 1 reaction in film and in bulk
fast RD process
K_f < k_La slow kinetic regime, kinetically controlled process, better catalyst or high liquid holdup improve the design
K_f = k_La neither kinetically nor mass transfer controlled, reaction and mass transfer contributes to the overall rate, better vapor-liquid contactor and catalyst improve the design
K_f > k_La slow diffusion regime, mass transfer controlled process better vapor-liquid contactor improve the design
K_f > k_La overall rate α (a), fast kinetic and slow diffusion rate in film, better vapor-liquid contactor improve the design
K_f = k_La overall rate α (a, k_f^0.5), kinetic and diffusion rate are equal in film, better vapor-liquid contactor and catalyst improve the design
K_f < k_La this situation can not occur
packed or tray bubble column, tray column, catalytic column
catalytic or packed column
packed column
packed column
catalytic or packed column
rate-based model accounts for the phase equilibrium and reaction kinetics, no need for the rate of mass transfer
rate-based model accounts for reaction kinetics and mass transfer
rate-based model accounts for the liquid phase equilibrium reaction and the rate of mass transfer between phases
rate-based model accounts for the phase equilibrium, the reaction kinetics and mass transfer in bulk as well in film

Figure 4.4: A framework for the technical evaluation of reactive distillation processes

4.4.1 Case study: RD process evaluation for unsaturated polyester synthesis

In this section, the reactive distillation process is examined for the synthesis of polyester. Particularly step by step, the technical and economical feasibility, process limitations, working regime, internal and model requirements are identified for the synthesis of unsaturated polyester by RD. The Damkohler number is defined for the synthesis of unsaturated polyester as,

$$Da = k_E C_{COOH}^{n-1} \tau \tag{4.3}$$

where, Da is the Damkohler number, k_E is the forward reaction rate constant of the esterification reaction (mol/kg/s), C_{COOH} is the total concentration of carboxylic acid (mol/kg) and τ is the liquid residence time on each stage (s) and n is the overall order of esterification reaction. For a one stage RD column, the Damkohler number is predicted from eq. (4.3) to be 3.53 at the reference temperature ($T_{ref} = 202^oC$) and when 1.5 hours of residence time is allowed in the RD column. The boiling point of maleic anhydride is selected as reference temperature. The chemical equilibrium constant (K_{EQ}) is about 34 at the given reference temperature. The values of Da and K_{EQ} clearly show that the polyester process is kinetically controlled. Note that different values of Da can be achieved by changing the reaction conditions and by changing the stage hold up and liquid flow rate. The overall conversion in the reactive distillation column is predicted according to,

$$X = 1 - \frac{1}{(1+Da)^N} \tag{4.4}$$

where, X is the conversion of the carboxylic acid, N is the number of stages. For a one stage RD column, a conversion of 78% is predicted from eq. (4.4) at the given reference temperature and a residence time of 1.5 hours is allowed in the column. In order to achieve 96% concentrated polyester, the one stage RD column is extended to a multi-stage RD column. The equilibrium model for the multi-stage RD column was developed in Aspen Custom Modeler (ACM) to evaluate the synthesis of unsaturated polyester [17].

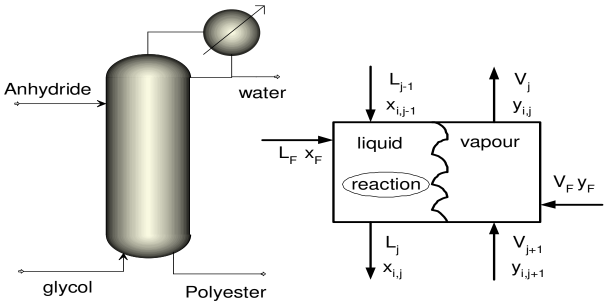

Figure 4.5: Schematic view of the reactive distillation column and the corresponding stage balance

A schematic view of the reactive distillation column is shown in Figure 4.5. The column is operated as a counter current vapor-liquid contactor. The anhydride is fed as liquid at the top of the column and glycol is fed at the bottom of the column as a vapor. The polyester product leaves the column at the bottom and water, glycol and acids leave at the top of the column. A sensitivity analysis is used to obtain the optimal design and operational parameters for this reactive distillation process. These parameters are depicted in table 4.1 [17].

Table 4.1: Summary of parameter settings found from sensitivity analysis

Parameters	values
Required equilibrium reactive stages [-]	20
Required total residence time [hours]	1.8
Reactants ratio [PG:MAD]	1.15:1.0
Liquid feed temperature at the top stage [^{o}C]	185
Vapor feed temperature at the bottom stage [^{o}C]	270
Reflux ratio [mol/mol]	0.3

The reactive distillation process is further evaluated with these parameters to confirm that the RD process is kinetically controlled. The profiles of Da and K_{EQ} over the RD column are shown in figure 4.6 (a)-(b). The Damkohler number is predicted between 0.3 and 1.1 for the given operating conditions at the reactive stages of the RD column. As discussed earlier, the Damkohler number depends on the reaction conditions and the residence time. However, a residence time of 0.09 hour (324 sec) is fixed on each stage, which refers to required residence time of 1.8 hours over the RD column. Thus the Damkohler number for this RD process varies only with the reaction conditions. The chemical equilibrium constant on each reactive stage is significantly high and varies from 32 to 62 in a temperature range from 185°C to 270°C. This combination of Damkohler number and chemical equilibrium constant conclude that the RD process is beneficial over the conventional batch reactor process. Since the Damkohler number is less than 10 and greater than 0.1, the designed RD process is kinetically controlled.

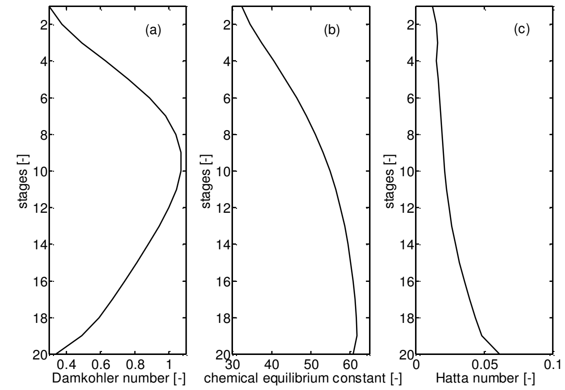

Figure 4.6: RD column profile of (a) Damkohler number (b) chemical equilibrium constant (c) Hatta number

The RD process is further evaluated to assess whether the reactions take place in the liquid film or in the bulk and whether the designed RD process is the mass transfer or kinetically controlled. The propylene glycol is one of the reactants and fed as vapor to the RD column. Hence, this component has to be transferred from the vapor phase to the liquid phase. The Hatta number for propylene glycol is redefined from eq. (4.2) as,

$$Ha = \sqrt{\frac{k_E C_{PG} D_{PG}}{k_{L,PG}^2}} \tag{4.5}$$

where, k_E is the forward rate constant of the esterification reaction (mol/kg/s), C_{PG} is the concentration of propylene glycol in the liquid phase (mol/kg), D_{PG} is the diffusivity of propylene glycol (m^2/s), $k_{L,PG}$ is the mass transfer coefficient of propylene glycol (m/s). The Hatta number is predicted to be 0.012 at the reference temperature from eq. (4.5) indicating that the reaction takes place only in the bulk for this RD process. Furthermore, the Hatta number profile is calculated along the RD column for the operating conditions depicted in table 4.1. It can be noticed from figure 4.6 (c) that the Hatta number is ranging from 0.012 at the top of the column to 0.06 at the bottom of the column. This confirms that the designed RD column is kinetically controlled and that the reaction takes place only in the bulk of the liquid on each reactive stage.

The liquid holdup and interfacial area available for mass transfer depend strictly on 1) the surface area provided by the internals per unit column volume and 2) whether the liquid phase is dispersed or continuous. Therefore, the RD process is evaluated for two different scenarios of phase inversion as follows,

- *Liquid in dispersed phase and vapor in continuous phase:* This scenario leads to traditional column internals for the RD column such as a packed column and a tray column in which the liquid holdup is rather low compared to the vapor holdup, but these internals provides better mass transfer.
- *Liquid in continuous phase and vapor in dispersed phase:* This scenario leads to a column filed with liquid and vapor passing through the column as bubbles. For this class of internals the liquid holdup is significantly higher than vapor holdup but the mass transfer is limited by the interfacial area available from the vapor bubbles. However, the mass transfer and vapor holdup can be increased by using packing or partition trays.

Table 4.2: Influence of column internals on reaction rate, mass transfer and liquid holdup

Configurations	Phase		K_EC_{COOH} at T_{ref} (1/hr)	k_La at T_{ref} (1/hr)	h_L [%]
	liquid	vapor			
Packed column (Metal pall ring)	Dispersed	Continuous	5.5	4780	13
Sieve tray column	Dispersed	Continuous	5.5	2450	25
Bubble column	Continuous	Dispersed	5.5	80	85
Packed bubble column (Metal pall ring)	Continuous	Dispersed	5.5	160	75
Sieve bubble tray column	Continuous	Dispersed	5.5	130	73

The reaction rate (k_EC_{COOH}) in (1/hr), mass transfer (k_La) in (1/hr) and liquid hold up (h_L) in (%) for the different column internals are depicted in table 4.2. It can be noticed from table 4.2 that the mass transfer is significantly higher compared to the reaction rate for all column internals. This is expected because the Damkohler number is less than 10 and the Hatta number is less than 1 for the unsaturated polyester process. This concludes that the RD process for the unsaturated polyester synthesis is in the slow kinetic regime and reactions only takes place in the liquid bulk. The process can be improved by selecting the internals which provides significant liquid holdup or a catalytic column. Since a catalytic process is not yet identified for the synthesis of unsaturated polyesters, provision of higher liquid holdup on the reactive stages is the best option to speed up the reaction rate. Comparison of the different internals in table 4.2 clearly shows that the bubble column provides the maximum liquid holdup. However, the mass transfer is lower in the bubble column. The mass transfer between two phases can be significantly increased when using the packing or partition trays in the bubble column. The comparison of different internals shows that the bubble column consisting of partition trays or packing is one of the best internal for this process, as high holdups can be achieved in the bubble column and provision of partition trays and packing improves the mass transfer.

4.5 Conclusions

The novel methodology proposed in this chapter is very effective in evaluating systematically and quickly the economical and technical feasibility of RD processes, determining also the boundary conditions of the process (e.g. relative volatilities, target purities, equilibrium conversion and equipment restriction).

Several industrially relevant processes were successfully used as case studies to validate the proposed framework: di-methyl carbonate (DMC), methyl acetate hydrolysis, toluene hydro-dealkylation, fatty acid methyl esters synthesis, and the production of unsaturated polyesters. Using the evaluating methodology, one can rapidly scan and decide on the viability of the RD option, based on either technical or economical criteria.

Provided that RD is an economically attractive option, the technical evaluation framework described in this chapter can be effectively used to determine the key process parameters and limitations, working regime, selection of internals, as well as the model requirements for the rigorous simulation of the reactive distillation process. This approach is based only on dimensionless numbers such as Damkohler and Hatta numbers, along with the kinetic, thermodynamic and mass transfer limits.

References

[1] J. Harmsen, Reactive distillation: The front-runner of industrial process intensification: A full review of commercial applications, research, scale-up, design and operation, Chemical Engineering and Processing, 46 (2007) 774.

[2] J. Harmsen, Process intensification in the petrochemicals industry: Drivers and hurdles for commercial implementation, Chemical Engineering and Processing: Process Intensification, 49 (2010) 70.

[3] C. Noeres, E.Y. Kenig, A. Górak, Modelling of reactive separation processes: reactive absorption and reactive distillation, Chemical Engineering and Processing, 42 (2003) 157.

[4] A. Stankiewicz, Reactive separations for process intensification: an industrial perspective, Chemical Engineering and Processing, 42 (2003) 137.

[5] R. Taylor, R. Krishna, Modelling reactive distillation, Chemical Engineering Science, 55 (2000) 5183.

[6] K. Sundmacher, A. Kienle, Reactive distillation- status and future directions, Willey-VCH, 2003.

[7] G. Buzad, M.F. Doherty, Design of three-component kinetically controlled reactive distillation columns using fixed-points methods, Chemical Engineering Science, 49 (1994) 1947.

[8] A.R. Ciric, D. Gu, Synthesis of nonequilibrium reactive distillation processes by MINLP optimization, AIChE Journal, 40 (1994) 1479.

[9] J.R. Jackson, I.E. Grossmann, A disjunctive programming approach for the optimal design of reactive distillation columns, Computers & Chemical Engineering, 25 (2001) 1661.

[10] J. Gangadwala, A. Kienle, U.-U. Haus, D. Michaels, R. Weismantel, Global Bounds on Optimal Solutions for the Production of 2,3-Dimethylbutene-1, Industrial & Engineering Chemistry Research, 45 (2006) 2261.

[11] G. Venimadhavan, G. Buzad, M.F. Doherty, M.F. Malone, Effect of kinetics on residue curve maps for reactive distillation, AIChE Journal, 40 (1994) 1814.

[12] R. Baur, A.P. Higler, R. Taylor, R. Krishna, Comparison of equilibrium stage and nonequilibrium stage models for reactive distillation, Chemical Engineering Journal, 76 (2000) 33.

[13] A. Higler, R. Krishna, R. Taylor, Nonequilibrium cell model for multicomponent (reactive) separation processes, AIChE Journal, 45 (1999) 2357.

[14] A.M. Katariya, R.S. Kamath, K.M. Moudgalya, S.M. Mahajani, Non-equilibrium stage modeling and non-linear dynamic effects in the synthesis of TAME by reactive distillation, Computers & Chemical Engineering, 32 (2008) 2243.

[15] A.A. Kiss, Separative reactors for integrated production of bioethanol and biodiesel, Computers & Chemical Engineering, 34 (2010) 812.

[16] J. Peng, T. F. Edgar, R. Bruce Eldridge, Dynamic rate-based and equilibrium models for a packed reactive distillation column, Chemical Engineering Science, 58 (2003) 2671.

[17] M. Shah, E. Zondervan, A.B. de Haan, Development of a model for the synthesis of unsaturated polyester by reactive distillation, in: Distillation Absorption 2010, Eindhoven, The Netherlands, 2010, pp. 247-252.

[18] A.C. Dimian, C.S. Bildea, F. Omota, A.A. Kiss, Innovative process for fatty acid esters by dual reactive distillation, Computers & Chemical Engineering, 33 (2009) 743.

[19] D.B. Kaymak, W.L. Luyben, Effect of the Chemical Equilibrium Constant on the Design of Reactive Distillation Columns, Industrial & Engineering Chemistry Research, 43 (2003) 3666.

[20] D.B. Kaymak, W.L. Luyben, Quantitative comparison of dynamic controllability between a reactive distillation column and a conventional multi-unit process, Computers & Chemical Engineering, 32 (2008) 1456.

[21] E. Kenig, K. Jakobsson, P. Banik, J. Aittamaa, A. Górak, M. Koskinen, P. Wettmann, An integrated tool for synthesis and design of reactive distillation, Chemical Engineering Science, 54 (1999) 1347.

[22] A.A. Kiss, C.S. Bildea, Integrated reactive absorption process for synthesis of fatty esters, Bioresource Technology, 102 (2011) 490.

[23] Y.-D. Lin, J.-H. Chen, J.-K. Cheng, H.-P. Huang, C.-C. Yu, Process alternatives for methyl acetate conversion using reactive distillation. 1. Hydrolysis, Chemical Engineering Science, 63 (2008) 1668.

[24] W.L. Luyben, C.C. Yu, Reactive distillation design and controll, Wiley, 2008.

[25] Z. Qi, A. Kienle, E. Stein, K.D. Mohl, A. Tuchlenski, K. Sundmacher, MTBE Decomposition in a Reactive Distillation Column, Chemical Engineering Research and Design, 82 (2004) 185.

[26] S. Sander, C. Flisch, E. Geissler, H. Schoenmakers, O. Ryll, H. Hasse, Methyl Acetate Hydrolysis in a Reactive Divided Wall Column, Chemical Engineering Research and Design, 85 (2007) 149.

[27] M. Shah, E. Zondervan, A.B. de Haan, Reactive distillation: An attractive alternative for the synthesis of unsaturated polyester, in: 10th International Workshop on Polymer Reaction Engineering, Hamburg, Germany, 2010.

[28] E.H. Stitt, Reactive distillation for toluene disproportionation: a technical and economic evaluation, Chemical Engineering Science, 57 (2002) 1537.

[29] F.H. Cao, D. Fang, D. Liu, W. Ying, Catalytic esterification of carbon dioxide and methanol for the preparation of dimethyl carbonate, Fuel chemistry division preprints, 74 (2002) 295-297.

[30] Y. Fuchigami, Hydrolysis of methyl acetate in distillation column packed with reactive packing of ion exchange resin, Journal of chemical engineering of Japan, 23 (1990) 354-359.

[31] E.E. Parker, Unsaturated polyesters, Industrial & Engineering Chemistry, 58 (1966) 53.

[32] M. Shah, E. Zondervan, A.B. de Haan, Modelling and simulation of an unsaturated polyester process, Journal of applied sciences, 10 (2010) 2551-2557.

[33] M.J. Okasinski, M.F. Doherty, Design Method for Kinetically Controlled, Staged Reactive Distillation Columns, Industrial & Engineering Chemistry Research, 37 (1998) 2821.

[34] C. Roizard, G. Wild, Mass transfer with chemical reaction: the slow reaction regime revisited, Chemical Engineering Science, 57 (2002) 3479.

Chapter 5

Gas holdup, mass transfer and axial dispersion in the bubble column with and without internals

In this chapter, the gas holdup, axial liquid dispersion and mass transfer are extensively studied for the packed, trayed and empty bubble column. Four different types of structured packings (Super-Pak, Flexipac, Mellapak and Gauze) and two types of perforated partition trays (with 25% and 40% tray open area) are used to characterize the packed and trayed bubble column, respectively. It is observed that the gas holdup and mass transfer characteristics of packed and trayed bubble columns are found to be superior to those of the empty bubble columns and the axial dispersion coefficients are much lower. The effect of liquid and gas flow rates, liquid phase viscosity and, packing and tray is discussed in detail in this chapter. Moreover, experimental data of the packed, trayed and empty bubble column are correlated by dimensionless numbers. Empirical correlations for the gas holdup, Bodenstein number (for the axial dispersion coefficient) and Stanton number (for the volumetric mass transfer coefficient) as a function of the Froude and Gallilei dimensionless numbers are proposed.

5.1 Introduction

Bubble columns are intensively used as multiphase contactors and reactors in chemical, petrochemical, biochemical and metallurgical industries [1, 2]. They are used especially in chemical processes involving reactions such as oxidation, chlorination, alkylation, polymerization, hydrogenation, and in the manufacture of synthetic fuels by gas conversion processes and in the biochemical processes such as fermentation and biological wastewater treatment [2, 3]. Bubble column reactors owe their wide application area due to a number of advantages such as the absence of moving parts, simple design and implementation, low maintenance and operating costs, large interfacial area, excellent heat and mass transfer between two phases and capability to easily change the residence times [4, 5]. However, bubble columns suffer from one severe drawback: substantial back-mixing prevails in both the liquid and gas phase. Although large axial back mixing is advantageous in a process that requires good heat and mass transfer capabilities, the reactants and products are diluted which further decreases the reaction driving force. Hence the reactor volumetric productivity is reduced [6]. This back-mixing can be reduced considerably by introducing a packing or partition trays into the bubble column [4, 7-9]. Packed bubble columns have proven advantages over empty bubble columns: reduction in axial-mixing, enhanced gas holdup and improved mass transfer characteristics [10, 11]. This is due to the bubble-disintegrating features offered by the packed bubble column. However, application of solid packing into the bubble column reduces liquid throughput. In order to maintain the advantages of applying packing, it is desirable to use a packing of high porosity [4]. A structured packing may serve this purpose. The installation of perforated partition plates divides the whole column into multiple stages so that column is configured as a multistage continuous stirred tank reactor (CSTR) [6]. Moreover, sectioning of the bubble column provides uniform distribution of liquid and gas over the entire column and their characteristics remains identical in each stage of column [6, 12, 13].

The hydrodynamic characteristics of structured packings are governed by the size of the packing channels and not by the column diameter [14, 15]. Moreover, the hydrodynamic characteristics of a trayed bubble column are not similar to the empty bubble column because of the redistribution of gas [14, 15]. Therefore, experiments need to be performed in a pilot column containing these internals to obtain correlation for the gas holdup, axial dispersion coefficient and volumetric mass transfer coefficient. The scale up of a bubble column strongly depends on accurate estimation of gas holdup, axial dispersion and mass transfer parameters. These parameters depend on the column diameter for the empty bubble column [2, 16] and the hydraulic diameter of packing ($d_h = 4\varepsilon/a$) for the packed bubble column [7, 14]. Rendtorff Birrer et al. [7] have concluded that the smaller the ratio of ε/a, the higher will be the maximal attainable gas holdup. The number and position of trays, the tray hole diameter and the open area of the partition plates influence the characterization of the trayed bubble column [6, 12]. Furthermore, the gas holdup, axial dispersion and mass transfer also strongly depend on the liquid and gas flow velocities, the liquid phase viscosity and, the liquid and gas phase density.

Many publications dealing with these parameters have been reported. The empirical or semi-empirical equations for these parameters reported by several authors are reviewed in the literature [2-4, 6, 8-10, 12, 13, 15, 17-22]. The proposed equations were derived for the air-water system applied in empty bubble columns, in randomly packed bubble columns or in trayed bubble columns. Only a few authors have studied the effect of viscosity on these parameters and the prediction of these parameters for structured packing. Rendtorff Birrer et al. [7] and Khamadieva et al. [11] have respectively studied the gas holdup and mass transfer characteristics for a high-viscous (1-510 mPas) liquid system in the packed bubble column containing structured packing. Urseanu et al. [14] studied the hydrodynamics and mixing properties in structured catalytic bubble column reactors working with the air-water system. Kemoun et al. [18] have compared the attained gas holdup in a trayed bubble column with an empty bubble column and they concluded that the gas holdup is identical in both configurations. Contradicting to this finding, Alvare et al. [12] and Thaker et al. [22] have found that the attained gas holdup is higher in the trayed bubble column compared to the empty bubble column. Moreover, Alvare et al. [12] have studied the effects of tray hole diameter and open area of partition trays on the gas holdup and they concluded that the gas holdup is strongly affected by the tray hole diameter compared to the open area of tray. Alvare et al. [8] have found that the axial back mixing is more influenced by the open area of partition trays than the tray hole diameter. Dreher et al. [23] have concluded that the liquid back mixing strongly depends on the tray open area and is independent of the column diameter. Moreover, the mass transfer is higher in the trayed bubble column than in the empty bubble column [21, 22]. All of the proposed correlations for these parameters are derived from semi-batch operations or a co-currently operated bubble column. Therefore, the application of these correlations for a counter-currently operated bubble column is not straight forward.

As discussed in chapter 4, the bubble column is the potential device for producing unsaturated polyesters by the reactive distillation. Moreover, introduction of packing or partition trays in the bubble column significantly improves the unsaturated polyester process. But considering the lack of information about the behavior of counter-currently operated bubble columns in the presence of structured packing or partition trays and in the viscous system, a systematic investigation on the gas holdup, axial dispersion and mass transfer in the packed bubble column and the trayed bubble column is undertaken in this work. Moreover, experiments are also performed with the empty bubble column for comparison under the comparable operating conditions. The experimental data are used to derive the correlations for these parameters. The derived correlations are based on dimensionless numbers which can be considered as a useful tool for scale up of the bubble column with or without internals.

5.2 Experimental

5.2.1 Experimental setup

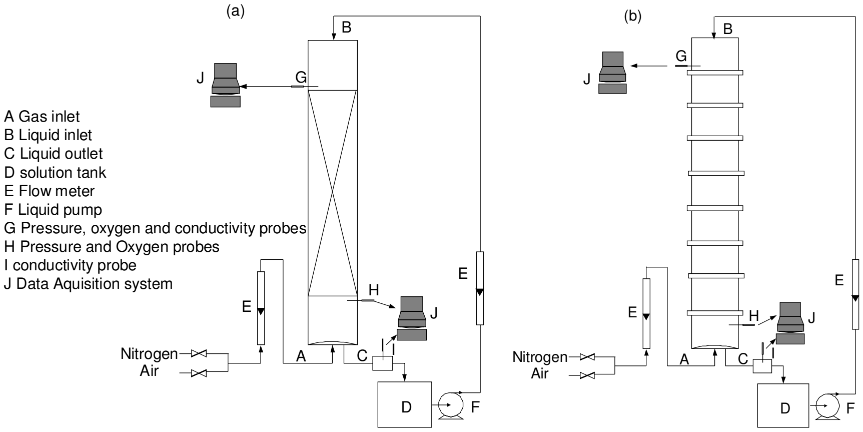

Figure 5.1: Schematic of the used column setup for performing holdup, axial dispersion and mass transfer experiments (a) packed bubble column (b) trayed bubble column

The experimental setup consists of a vertical bubble column made of Plexiglas is used for studying the gas holdup, axial dispersion and mass transfer characteristics. The column is 29 *cm* in diameter and 200 *cm* in height, operated with counter-current gas and liquid flow. A perforated plate is placed at the bottom of the column for uniform distribution of the gas bubbles. The sparger of this perforated plate has 0.05 *cm* diameter holes which are placed in a triangular pitch of 0.7 *cm*. Figure 5.1 (a) shows schematic view of bubble column containing structured packing. The different types of structured packings used in the present work and their packing characteristics are summarized in table 5.1. Figure 5.1 (b) shows a schematic view of the bubble column containing partition trays. The trayed bubble column has nine stage units with a total of 8 trays. The height of each stage is 15 cm. Two different types of partition trays are used; 1) tray with a tray hole diameter of 0.8 *cm* and tray open area (OA) of 25%, and 2) tray with a tray hole diameter of 0.8 *cm* and tray open area (OA) of 40%.

Polyethylene glycol solutions are used to perform experiments at various liquid viscosities and tap water is used to perform experiments at a viscosity of 1 *mPas*. The viscosity of polyethylene glycol solutions is measured by a Ubbelohde viscometer (type - I up to 10 mm^2/s, type - Ic up to 30 mm^2/s and type - II up to 100 mm^2/s kinematic viscosity) and the density by a digital density meter DMA 4500. Compressed air is used to perform experiments for the gas holdup and axial dispersion measurements. Oxygen free nitrogen is used to perform the mass transfer experiments. The gas flow rate is automatically controlled by a Brooks MT 3903 controller and the liquid flow rate is manually adjusted and measured with a Brooks MT 3809 volumetric flow meter. The pressure difference is measured by two pressure sensors (supplied by Endress & Hauser, model PMC131 – A1F1A2K) placed at the top and bottom section of packed bubble or trayed bubble column. Conductivity probes (supplied by Mettler Toledo, model InPro 7100) are placed at the top section and at the exit of the bubble column to measure the conductivity of the tracer (sodium chloride) during the residence time distribution (RTD) experiments. Similarly, oxygen probes (supplied by Mettler Toledo, model InPro 6800) are mounted at the top and bottom section to measure the oxygen concentration in the liquid during the mass transfer experiments. The experiments are performed at various viscosities ranging from 1-50 *mPas*, gas flow rates ranging from 5-25 m^3/h and liquid flow rates ranging from 0.120-0.480 m^3/h. In total 30 experiments consisting of various combinations of liquid flow, gas flow and liquid viscosity are performed for each structured packing, each type of partition tray and the empty bubble column.

Table 5.1: Packing characteristics

Packing	Mellapak	Gauze	Flexipac	Super-Pak
Specific surface area, a, (m^2/m^3)	250	471	225	250
Void fraction, ε_p, (-)	0.97	0.90	0.99	0.98
Hydraulic diameter, D_h, *(cm)*	1.57	0.75	1.77	1.54
Chanel side, S_c, *(cm)*	2.0	0.9	2.1	-
Channel height, H_c, *(cm)*	1.0	0.8	1.3	-
Channel base, B_c, *(cm)*	3.0	1.0	3.0	-
Height of packed section, H_p, *(cm)*	1.49	1.53	1.45	1.41

5.2.2 Methods

5.2.2.1 Gas holdup

The average gas holdup is determined using the pressure sensors mounted at the top and bottom section of the packed or trayed bubble column. After achieving a constant liquid level in the column and, steady gas and liquid flows, the pressure difference between these two points is recorded. The average holdup value from pressure difference measurement is calculated from [4],

$$\frac{dh}{dz} = 1 - \varepsilon_l = \varepsilon_g \tag{5.1}$$

where ε_l is the liquid holdup and ε_g is the gas holdup.

5.2.2.2 Residence time distribution (RTD)

The RTD experiments are performed to estimate the axial dispersion coefficient. RTD is usually studied by injecting a tracer as an impulse input or step input in the liquid inlet stream in the case of co- or counter current operation or added directly to the top of the column in the case of semi batch operation and obtaining the output concentration of tracer at the exit of column [24]. One main disadvantage with these two methods is the difficulty in achieving a homogeneous dispersion of tracer in the radial direction of column. To overcome the maldistribution of tracer over the column cross-section, a liquid pool of 10 *cm* height is applied above the packing or partition tray in which a pulse of tracer is introduced. The inlet concentration of tracer for the packed or trayed bubble column is measured in the liquid pool by a conductivity probe as a function of time. Campos et al. [25] and Therning et al. [24] proposed a similar approach to perform the RTD experiments. After achieving a constant liquid level in the column and, steady gas and liquid flows, 0.5 *l* sodium chloride (NaCl) solution is fed as tracer. Since the gas and liquid are fed counter - currently and the liquid is fed at the top of column, the tracer is injected at the top of the column. Ideally the outlet concentration of the tracer should be measured at the bottom of the column. However, due to the very dynamic behavior of the gas bubbles introduced by the sparger at the bottom of column, the conductivity of the tracer could not be measured without significant noise. Therefore, the conductivity probe is placed outside the column and conductivity is measured in the outlet liquid stream. In order to estimate accurately the axial dispersion of the packed bubble column, the liquid pool below the packed section is modeled as a continuous stirred tank reactor (CSTR) and incorporated in the axial dispersion model (ADM). The conductivity data is recorded online (at time intervals of 1 *s*) through the data acquisition system.

5.2.2.3 Volumetric mass transfer coefficient

The volumetric mass transfer coefficient is determined with the dynamic oxygen desorption method [4]. Oxygen is desorbed by introducing nitrogen instead of air in the bubble column and the oxygen concentration is measured as a function of time at the bottom of the packed or tray bubble column by an oxygen probe. The response time is less than 1 *s* and recorded online through the data acquisition system. The liquid is recycled during the course of the experiment. The amount of liquid in the solution tank is kept at least 5 times that of the liquid holdup of the column to avoid recycling of oxygen free liquid. In most of the literature, the volumetric mass transfer coefficient is determined by assuming an ideal mixing of the liquid phase in the bubble column. However, the gas phase always has significant effect on the dispersion in the liquid phase which is the cause of non-ideal flow in the bubble column. Hence, in order to introduce the effect of dispersion on the volumetric mass transfer coefficient (k_La), a one dimensional axial dispersion model (ADM) superimposed with the mass transfer rate derived by applying a differential mass balance in the bubble column is used. Furthermore, the oxygen concentration is also measured at the top of the column to analyze the concentration difference over the column during the mass transfer experiment.

5.3 Results and discussion

5.3.1 Gas holdup

5.3.1.1 Effect of packing, liquid and gas properties

The attained gas holdup in the packed bubble column with different types of structured packings, trayed bubble column with different types of trays and the empty bubble column is compared in figure 5.2 (a)-(c). The gas holdup is always significantly higher in the trayed and packed bubble column compared to the empty bubble column. The gas holdup increase in the presence of trays can be due to the reduction of liquid circulation velocity and the increase in the gas phase resistance time within the stages [12, 15]. In addition, the redistribution of the gas phase in each stage can also reduce the overall bubble size and the bubble coalescence rate [12, 13]. Hence, the gas holdup in the trayed bubble column is higher compared to the empty bubble column. An increase in the tray open area increases the total amount of energy dissipated due to the larger number of holes in the tray. Thus, the gas holdup attained with the tray open area of 40% is higher than tray open area of 25%. Alvare et al. [12] also found an increase in the gas holdup with an increase in the tray open area.

The introduction of a packing prevents a rapid escape of gas bubbles from the column because the packing provides a tortuous path to the gas bubbles. Hence, the effective traveling distance for the gas bubble in the packed bubble column is higher than the empty bubble column, which leads to a significant increase in gas holdup. Moustiri et al. [26] have shown that the packing causes bubble breakup and because of this less large bubbles are formed in the packed bubble column compared to the empty column, although the column is operated at high gas velocity (the churn turbulent regime). Rendtorff Birrer et al. [7] have shown that the smaller the ratio of void fraction to surface area per unit volume (ε/a) is, the higher is the attained gas holdup. Since the hydraulic diameter of the packing is a direct function of ε/a, it can be shown that the higher the hydraulic diameter of the packing, the lower is the attained gas holdup. The Gauze packing has the lowest hydraulic diameter therefore the attained gas holdup is the highest compared to the other packings. Although the hydraulic diameter of Mellapak and Super-Pak is identical, the attained gas holdup in Mellapak is higher than Super-Pak. This can be because of different geometry features of these packings. The Mellapak is made from corrugated sheets and the discrete crimped channels thereby provide a tortuous path for the gas bubbles that reduces the effective rise velocity of the bubble. In contrast the Super-Pak consists of a sinusoidal wave type open structure and provides no directional change to the liquid and gas flow. Hence, the effective rise velocity of the bubbles will be significantly higher in Super-Pak compared to Mellapak.

Moreover, the hydraulic diameter of Flexipac is higher than Mellapak therefore the attained gas holdup in Flexipac is lower compared to Mellapak.

Figure 5.2 (a) shows the influence of gas velocity on the gas hold up at a superficial liquid velocity of 0.10 *cm/s* and for a liquid viscosity of 25 *mPas*. As expected, the gas velocity increases the gas holdup. It can be also seen that at low gas velocities (bubbly flow regime) the effect of the gas velocity on gas holdup is more pronounced than at high gas velocities (churn-turbulent regime). At low gas velocities, the diameter of bubbles is small and uniform causing them to travel upwards without major coalescences. At high gas velocities, significantly more bubbles are formed which eventually increases the coalescence between the bubbles and thereby forms bigger bubbles. Hence, although more bubbles are formed at high velocity which should lead to higher gas holdup, the bigger bubble which rise faster level off the linear increase in the gas holdup with respect to the gas velocity.

Figure 5.2 (b) shows the influence of liquid velocity on the gas holdup at a superficial gas velocity of 6.31 *cm/s* and a liquid viscosity of 25 *mPas*. The gas holdup is not significantly altered by the liquid velocity. Only a slight reduction in the gas holdup is noticed when liquid velocity is increased. We postulate that an increase in the liquid velocity might increase friction force between liquid and gas bubbles in counter-current flow and thereby bigger bubbles are formed. Hence, the gas holdup is reduced. Figure 5.2 (c) shows the influence of liquid viscosity on the gas holdup at a superficial gas velocity of 6.31*cm/s* and a superficial liquid velocity of 0.10 *cm/s*. An increase in the liquid viscosity reduces the gas holdup. This can be due to an increase in the viscous force which results in bigger bubble formation and thus higher rising velocities and lower gas holdup [9].

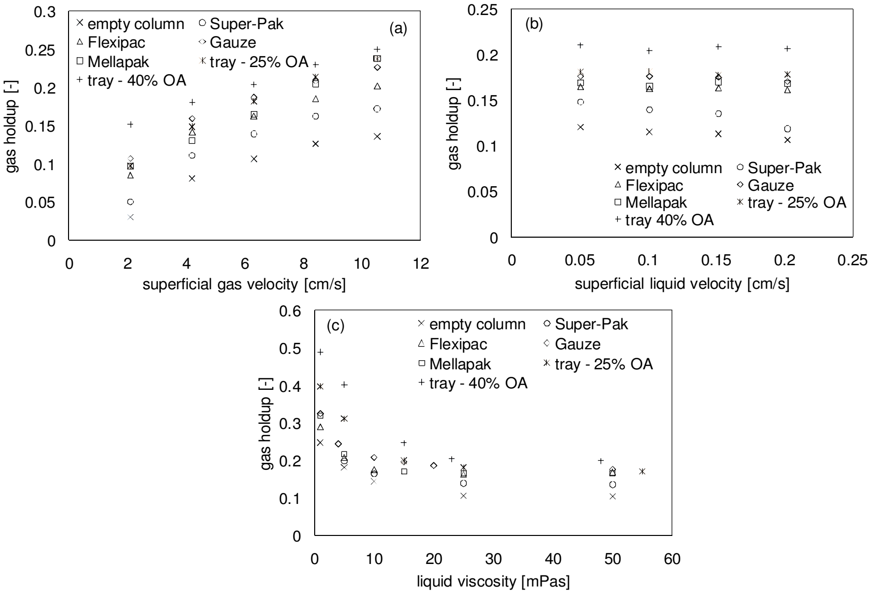

Figure 5.2: (a) Effect of gas velocity (b) effect of liquid velocity (c) effect of liquid viscosity on the gas holdup in the empty, packed and trayed bubble column

5.3.1.2 gas holdup correlations

Since the gas holdup is influenced by gas, liquid, type of partition tray and type of packing, the gas holdup is correlated as a function of the superficial gas and liquid velocities, liquid density, liquid viscosity, tray and packing properties. The other physical properties such as gas density, gas viscosity and surface tension are not varied and therefore have not been taken into account. Gas holdup data obtained in the empty bubble column can be correlated by using one of the three types of correlations proposed in the literature. The first type correlates the gas holdup directly to the gas velocity as homographic function [2, 3, 7, 9, 10]. The second type correlates the gas holdup as a function of the slip velocity between the gas and the liquid phase [2, 27]. The third type is the gas holdup correlated with dimensionless numbers [2, 28]. In this work the gas holdup correlation is expressed as function of Froude and Gallilei dimensionless numbers. Alternatively the Reynolds number can be used to describe the liquid phase. Since the gas density and viscosity are not varied and the density of gas remarkably influences the gas holdup [18, 24, 29], the Reynolds number cannot be used to describe the gas phase in the present work. The Froude number ($u_g^2/g/D$) at the gas side represents the balance between gas momentum and the gravitational force, and the Froude number ($u_l^2/g/D$) at the liquid side represents the balance between the liquid inertia force and the gravitational force. Moreover, the Gallilei number ($g\rho^3D^3/\mu^2$) represents the balance between the liquid inertia forces to the viscous forces. Hence, the usage of these dimensionless numbers completely describes the forces acting in the two phase bubble column. The following correlation for gas holdup is proposed [2, 12],

$$\varepsilon_g = AFr_g^{\alpha} Fr_l^{\beta} Ga^{\gamma} \tag{5.2}$$

The magnitude of the coefficients A, α, β and γ represents the effect of the dimensionless groups on the overall gas holdup. To account for the effect of different packing structures on the gas holdup, these dimensionless numbers are based on the hydraulic diameter of packing. For an empty bubble column these dimensionless numbers are based on the diameter of column. For a trayed bubble column these dimensionless numbers are based on the tray hole diameter. In addition, to include the effect of the tray open area on the gas holdup, eq. (5.2) is extended with tray open area (OA) as [12],

$$\varepsilon_g = AFr_g^{\alpha} Fr_l^{\beta} Ga^{\gamma} OA^{\lambda} \tag{5.3}$$

The coefficients in eq. (5.2) and (5.3) are estimated by fitting the experimental gas hold up data in MATLAB by conducting non-linear regression analysis. For the empty bubble column the resulting gas holdup correlation is:

$$\varepsilon_g = 0.072 Fr_g^{0.224} Fr_l^{-0.018} Ga^{0.087} \tag{5.4}$$

To obtain the gas holdup correlation for the packed bubble column, first the coefficients α, β, γ of the empty bubble column were tried and only the coefficient A was fitted. However, the mean relative error between the experimental and predicted gas holdup value appeared more than 35%. Hereafter, each of these coefficients was sequentially fitted while the other coefficients kept equal to those determined for the empty bubble column. However, it was found that the mean relative error is more than 18%, which can be due to the fact that all the coefficients are contributing in more or less in the same range to the gas holdup correlation. Therefore, all four coefficients fitted to the experimental data yielding the following correlation for the packed bubble column:

$$\varepsilon_g = 0.178 Fr_g^{0.243} Fr_l^{-0.002} Ga^{0.074} \tag{5.5}$$

For the trayed bubble column the gas holdup correlation become:

$$\varepsilon_g = 0.289 Fr_g^{0.349} Fr_l^{-0.0013} Ga^{0.142} OA^{0.565} \tag{5.6}$$

Table 5.2: Parameters with their 95% confidence intervals

Empty bubble column	Packed bubble column	Tray bubble column
A: 0.072 ± 0.015	A: 0.178 ± 0.014	A: 0.289 ± 0.0136
α: 0.224 ± 0.015	α: 0.243 ± 0.018	α: 0.349 ± 0.074
β: -0.018 ± 0.011	β: -0.002 ± 0.0003	β: -0.0013 ± 0.001
γ: 0.087 ± 0.004	γ: 0.074 ± 0.005	γ: 0.142 ± 0.0184
		λ: 0.565 ± 0.0145

The values of the coefficients in eq. (5.4), (5.5) and (5.6) with their 95% confidence intervals are depicted in table 5.2. The mean relative error between the experimental and the predicted overall gas holdup for the empty bubble column from eq. (5.4) is 5%, for the packed bubble column from eq. (5.5) is 9% and for the trayed bubble column from eq. (5.6) is 10%.

Furthermore, the sensitivity of the empty bubble column correlation coefficients on the gas holdup is investigated by changing one of the coefficients and keeping other coefficients constant. The sensitivity parameter is the average of the change in the gas holdup with respect to the change in coefficient over n number of experiments. This sensitivity parameter is defined as,

$$S = \frac{\sum_n \left(\frac{y(b+\Delta b) - y(b)}{\Delta b} \right)}{n} \tag{5.7}$$

where b refers to the coefficients (A, α, β and γ) used in eq. (5.4), y (in this case $y = \varepsilon_g$) refers to a parameter for which sensitivity is determined, n is the number of experiments performed at various operating conditions and S is the sensitivity parameter. For 10% change in the estimated value of one of the coefficients, the found sensitivity parameter for the coefficient A is 1.90, for the coefficient α is 0.85, for the coefficient β is 2.0 and for the coefficient γ is 3.34. The value of these coefficients is in the same range and hence indicates that the change in these coefficients contributes in the same order of magnitude to the change in gas holdup.

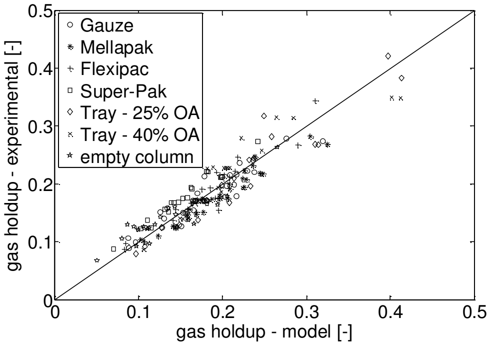

Figure 5.3: Parity plot of the experimental gas holdup and the gas holdup estimated from eq. (5.4), (5.5) and (5.6) for the empty, packed and trayed bubble column, respectively

A good agreement between the experimental overall gas holdup and the estimated values from the empirical expression can be seen in figure 5.3. The negative power on the liquid side Froude number and the positive power on the gas side Froude number are in agreement with the fact that the gas holdup decreases with an increase in the liquid flow rate and increases with an increase in the gas flow rate. Since the Froude number is proportional to the square of the superficial velocity and the power of the liquid side Froude number is significantly smaller than the gas side Froude number, it indicates that the gas holdup is more influenced by the gas velocity rather than the liquid velocity. Moreover, the Gallilei number is inversely proportional to the square of the liquid viscosity. Therefore comparison of the coefficient of the liquid side and gas side Froude number with the Gallilei number indicates that the liquid viscosity has a more pronounced effect compared to the liquid flow rate and a less pronounced effect compared to the gas flow rate on the gas holdup. Comparison of the liquid side Froude number coefficient of the empty bubble column with the packed and trayed bubble column indicates that the effect of liquid velocity on the gas holdup is a factor 10 lower in the packed and trayed bubble column. The positive coefficient of the tray open area in eq. (5.6) indicates that the gas holdup increases with the tray open area.

5.3.2 Axial dispersion

5.3.2.1 Axial dispersion model (ADM)

For the estimation of the axial dispersion coefficient, an ADM is used in the present study. Since the radial dispersion can be assumed to be negligible [24], and the liquid and gas flows are steady, a one dimensional ADM is valid. The partial differential equation describing the concentration of tracer with time over the length of the packed, trayed or empty bubble column is given by,

$$\frac{\partial C}{\partial t} = D_{ax} \frac{\partial^2 C}{\partial Z^2} - U_{l_{eff}} \frac{\partial C}{\partial Z} \tag{5.8}$$

where, C is the tracer concentration, Z is the vertical position, D_{ax} is the axial dispersion coefficient and $U_{l_{eff}}$ is the effective liquid velocity defined as the ratio of superficial liquid velocity to the liquid holdup ($U_l/(1-\varepsilon_g)$). Since the volume of the liquid pool applied above the top section of the packed and trayed bubble column is maximum 5% of total volume of the column, the liquid pool can be assumed well mixed. Therefore, the inlet tracer concentration to the packed or trayed bubble column can be considered equal to the tracer concentration in the liquid pool. The tracer concentration in the liquid pool (C_{top}) is measured by the conductivity sensor as a function of time. For the given assumptions, eq. (5.8) can be solved subject to the following boundary conditions:

At $t = 0,\ 0 \le Z \le L,\ C = 0$ (5.9)

At $t > 0,\ Z = 0,\ C = C_{top}$ (5.10)

At $t>0,\ Z = L,\ \dfrac{\partial C}{\partial Z} = 0$ (5.11)

Since the tracer concentration is measured in the outlet liquid stream and the liquid pool is present under the packed section of the packed bubble column, the liquid pool is modeled as a CSTR to calculate the tracer concentration at the bottom of the packed section. In this case, it is assumed that there is only convective mass transport in the liquid pool and the mass transport between the packed section and the liquid pool at the boundary is due to dispersion and convection. A model to determine the concentration of tracer at the bottom of the packed section from the tracer concentration measured at the outlet liquid stream can therefore be written as,

$$V_p \frac{\partial C_P}{\partial t} = U_{l_{eff}} A(C_B - C_P) - D_{ax} A \frac{\partial C_P}{\partial Z} \tag{5.12}$$

where, C_B is the concentration at the boundary, C_p is the concentration in the liquid pool, V_p is the volume of liquid pool and A is the cross sectional area. This model is solved in MATLAB with the axial dispersion coefficient as the parameter to calculate. The axial dispersion coefficient is determined by nonlinear least square fitting obtained by minimizing the sum of squares of error. The error corresponds to the difference between the tracer concentration predicted from the model and measured experimentally over the time period. The dimensionless tracer concentration (C_{top}) measured experimentally just above the packed section (Z = 0) is shown in figure 5.4 which provides the top boundary condition for ADM. Moreover, the dimensionless concentration of tracer measured experimentally in the outlet liquid stream is compared with the predicted concentration by ADM in figure 5.4. Figure 5.4 shows that the experimental data are satisfactory regressed by using the ADM.

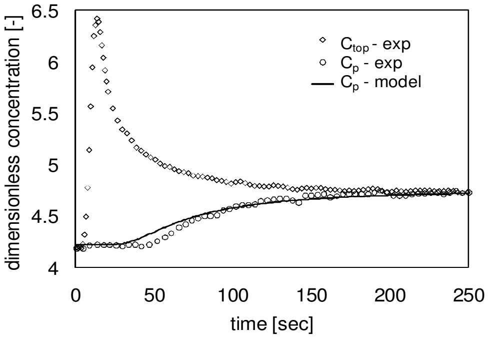

Figure 5.4: The dynamic tracer response profiles. The experimental data of tracer in this figure are taken from the RTD experiments performed at gas velocity of 6 *cm/s*, the liquid velocity of 0.5 *cm/s* and the liquid viscosity of 25 *mPas* for the bubble column packed with Flexipac.

5.3.2.2 Effect of gas, liquid and packing properties

The influence of gas velocity on the axial dispersion coefficient at a superficial liquid velocity of 0.10 *cm/s* and for a liquid viscosity of 25 *mPas* is shown in Figure 5.5 (a). The axial dispersion coefficient increases with an increase in the gas velocity which indicates that the liquid phase is agitated. In accordance with the gas holdup profiles, increase in gas velocity increases the gas holdup and thereby induces more liquid circulation which results in an increase in the liquid dispersion. Moreover at high gas velocities, the axial dispersion coefficient is significantly higher in the empty bubble column compared to the packed and trayed bubble column, which indicates that the packing and partition trays significantly reduces the liquid dispersion compared to the empty bubble column. Figure 5.5 (b) shows the influence of the liquid velocity on the liquid dispersion at a superficial gas velocity of 6.31 *cm/s* and for a liquid viscosity of 25 *mPas*. The axial dispersion coefficient decreases with an increase in the liquid velocity because an increase in the liquid velocity reduces the residence time of liquid in the column which leads to increased plug flow behavior. This effect is most pronounced for the empty bubble column.

Figure 5.5 (c) shows the influence of the liquid viscosity on the liquid dispersion at a superficial gas velocity of 6.31 *cm/s* and a superficial liquid velocity of 0.10 *cm/s*. The axial dispersion coefficient decreases as the liquid viscosity increases because an increase in the liquid viscosity results in more viscous force and thereby reduces the liquid circulation. Moreover with an increase in the liquid viscosity, the reduction in liquid dispersion is higher in the packed and trayed bubble column compared to the empty bubble column. Depending on the operating condition of packed bubble column, the liquid dispersion is reduced for Super-Pak by factor 1.16-1.55 (15-36%), Gauze by factor 1.82-2.0 (43-47%), Mellapak by factor 1.13-2.21 (37-54%) and Flexipac 1.9-3.0 (47-57%). As discussed earlier, Super-Pak consists of an open structure that does not prevent the liquid circulation as compared to other packings, which results in modest reduction of the liquid dispersion. In contrast, the discrete crimped channels of Mellapak and Flexipac significantly prevent the liquid circulation therefore the liquid dispersion is reduced strongest in this packings compared to the other packings. Trays with a smaller open area offer more resistance to the gas-liquid flow compared to the trays with a bigger open area and thus the axial dispersion is reduced more in the trayed bubble column with tray open area of 25%. The trayed bubble column with a tray open area of 40% reduces the liquid dispersion by factor 2–2.5 (47-60%) and the trayed bubble column with a tray open area of 25% reduces the liquid dispersion by factor 2.5-3.0 (55-65%).

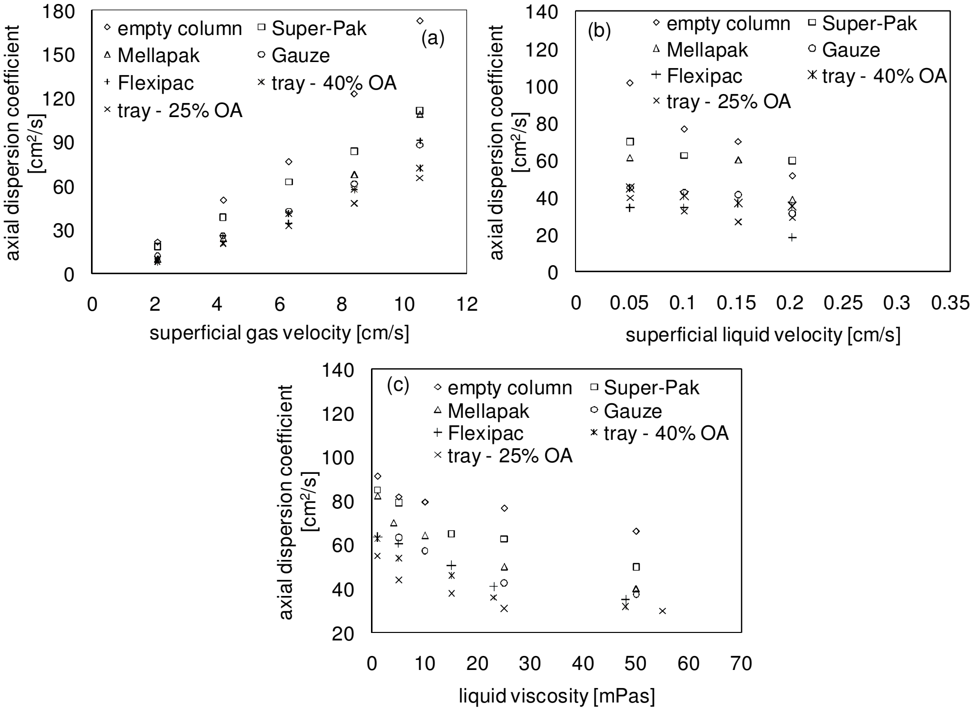

Figure 5.5: (a) Effect of gas velocity (b) effect of liquid velocity (c) effect of liquid viscosity on the axial dispersion coefficient in the packed, trayed and empty bubble column

5.3.2.3 *Axial dispersion correlation*

The experimental observations show that the liquid dispersion is influenced by the liquid velocity, the gas velocity, the liquid viscosity, and the type of tray and packing. As discussed earlier, the gas density, the gas viscosity and the liquid surface tension are not varied therefore the influence of these parameters on the liquid dispersion could not be described. A dimensionless correlation is proposed which accounts for the effect of the studied parameters on the axial dispersion. For a two-phase system, the Bodenstein dimensionless number can be used to describe the liquid dispersion [16]. The Bodenstein number is defined as,

$$Bo = \frac{U_l D}{(1-\varepsilon_g) D_{ax}} \qquad (5.13)$$

where D refers to the diameter of the empty bubble column, the hydraulic diameter of packing for the packed bubble column and the tray hole diameter for the trayed bubble column. An empirical correlation of the Bodenstein number as function of Froude and Gallilei dimensionless numbers for the empty and packed bubble column is proposed as [16],

$$Bo = A Fr_g^{\alpha} Fr_l^{\beta} Ga^{\gamma} \qquad (5.14)$$

The magnitude of the coefficients A, α, β and γ represents the effect of dimensionless groups on the Bodenstein number and thereby on the liquid dispersion. An empirical correlation of the Bodenstein number for the trayed bubble column is proposed as,

$$Bo = A Fr_g^{\alpha} Fr_l^{\beta} Ga^{\gamma} OA^{\lambda} \qquad (5.15)$$

which also includes the effect of the tray open area on the axial dispersion. The coefficients in eq. (5.14) and (5.15) are estimated by fitting the experimental data in MATLAB by conducting non-linear regression analysis. For the empty bubble column, the liquid dispersion correlation is:

$$Bo = 1.5 Fr_g^{-0.740} Fr_l^{0.560} Ga^{-0.016} \qquad (5.16)$$

The value of coefficients in eq. (5.16) with their 95% confidence intervals is depicted in table 5.3. The mean relative error between the experimental and the predicated Bodenstein number is 13%.

A sensitivity analysis is performed using eq. (5.7) for 10% change in the value of coefficient of eq. (5.16). The sensitivity parameter for the coefficient A is 0.049, for the coefficient α is 0.80, for the coefficient β is 0.73 and for the coefficient γ is 1.65. These sensitivity parameters indicate that the correlation for the Bodenstein number is more sensitive to the change in liquid viscosity compared to the liquid and gas velocities. For the packed bubble column the liquid dispersion correlation is:

$$Bo = 2.64 Fr_g^{-0.714} Fr_l^{0.810} Ga^{-0.020} \qquad (5.17)$$

The liquid dispersion correlation for the trayed bubble column according to eq. (5.15) is:

$$Bo = 0.165 Fr_g^{-0.581} Fr_l^{0.526} Ga^{-0.053} OA^{-0.370} \qquad (5.18)$$

The value of the coefficients in eq. (5.17), (5.18) with their 95% confidence intervals is depicted in table 5.3. The mean relative error between the experimental and the predicted Bodenstein number for the packed bubble column from eq. (5.17) is 16% and for the trayed bubble column from eq. (5.18) is 10%.

Table 5.3: Parameters with their 95% confidence intervals

Empty bubble column	Packed bubble column	Tray bubble column
A: 1.5 ± 0.045	A: 2.64 ± 0.14	A: 0.165 ± 0.074
α: -0.740 ± 0.080	α: -0.714 ± 0.017	α: -0.581 ± 0.024
β: 0.560 ± 0.043	β: 0.810± 0.082	β: 0.526 ± 0.037
γ: -0.016 ± 0.006	γ: -0.020 ± 0.003	γ: -0.053 ± 0.003
		λ: -0.370 ± 0.085

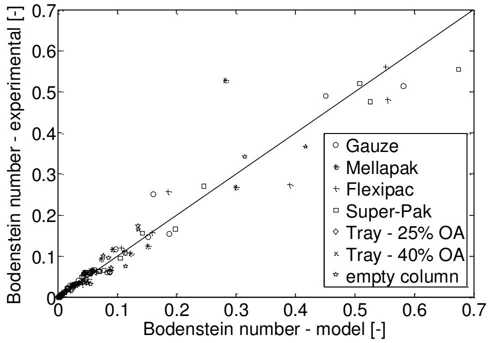

Figure 5.6: Parity plot of the calculated Bodenstein number from experimental data and estimated from eq. (5.16), (5.17) and (5.18) for the empty, packed and trayed bubble column, respectively

Figure 5.6 shows a good agreement between the experimental and the estimated values of the Bodenstein number. The axial dispersion coefficient is inversely proportional to the Bodenstein number and, the gas and liquid velocity is directly proportional to the Froude number. Thus, the positive power on the liquid side Froude number and the negative power on the gas side Froude number in eq. (5.16), (5.17) and (5.18) are in agreement with the fact that the axial liquid dispersion decreases with an increase in the liquid flow rate and increases with an increase in the gas flow rate. Moreover, the Gallilei number is inversely proportional to the square of the liquid viscosity and the coefficient of the Gallilei number in eq. (5.16), (5.17) and (5.18) is negative which indicates that the liquid dispersion decreases with an increase in the liquid viscosity. The negative power of the tray open area in eq. (5.18) is in agreement with the fact that the axial dispersion coefficient increases with the tray open area.

5.3.3 Mass transfer coefficient

5.3.3.1 Model

The volumetric mass transfer coefficient is estimated by using a one dimensional ADM. The differential equation describing the concentration of oxygen with time and over the length of column is given by [28],

$$\frac{\partial C_{O_2}}{\partial t} = D_{ax}\frac{\partial^2 C_{O_2}}{\partial Z^2} - U_{l_{eff}}\frac{\partial C_{O_2}}{\partial Z} - K_L a(C_{O_2} - C^*_{O_2}) \qquad (5.19)$$

where, C_{O_2} and $C^*_{O_2}$ are the oxygen concentration respectively at any time and at equilibrium, $K_L a$ is the liquid-side mass transfer coefficient, Z is the vertical position, D_{ax} is the axial dispersion coefficient and $U_{l_{eff}}$ is the effective liquid velocity. Eq. (5.19) is solved by using the boundary conditions described in eq. (5.9) to eq. (5.11). This model is solved in MATLAB with the liquid-side mass transfer as the parameter to determine. The liquid-side mass transfer coefficient is determined by nonlinear least square fitting through minimizing the sum of squares of error. The error corresponds to the difference between the oxygen concentration predicted from the model and measured experimentally over the time period. Figure 5.7 shows a representative example for the comparison of the oxygen concentration predicted using the ADM and experimental data. The experimental data shown in figure 5.7 are for the mass transfer experiments performed at gas velocity of 6.31 *cm/s*, 0.10 cm/s liquid velocity and the liquid viscosities of 25 *mPas* in the bubble column packed with Flexipac. It can be seen from the figure 5.7 that the experimental data are satisfactorily fitted by the proposed model with simultaneous estimation of the liquid-side mass transfer coefficient.

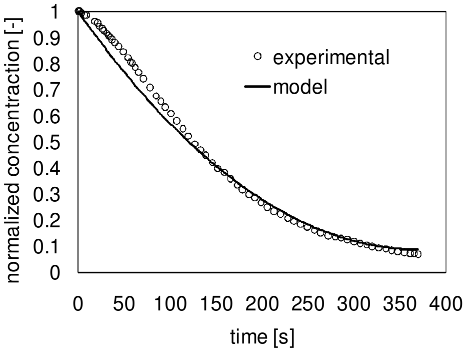

Figure 5.7: Comparison of normalized oxygen concentration estimated using the proposed model and experimental data.

5.3.3.2 *Effect of gas, liquid and packing properties*

The effect of the superficial gas velocity on the volumetric mass transfer coefficient for the empty, packed and trayed bubble column at a superficial liquid velocity of 0.10 *cm/s* and for a liquid viscosity of 25 *mPas* is shown in Figure 5.8 (a). It can be seen from this figure that the volumetric mass transfer coefficient increases with an increase in the gas flow rate. This can be attributed to an increase in the gas holdup. The effect of superficial liquid velocity on the volumetric mass transfer coefficient for the empty, packed and trayed bubble column at a superficial gas velocity of 6.31 *cm/s* and for a liquid viscosity of 25 *mPas* is shown in Figure 5.8 (b). It can be seen from the figure that the increase in superficial liquid velocity marginally enhances the volumetric mass transfer coefficient.

This can be due to higher turbulence caused by an increase in the superficial liquid velocity [21, 30]. Therefore the gas-liquid interface resistance is reduced and thereby mass transfer is increased [21, 30]. The volumetric mass transfer coefficient decreases with an increase in the liquid viscosity in the empty, packed and trayed bubble column as shown in Figure 5.8 (c). The values of volumetric mass transfer coefficients at various liquid viscosities, at a superficial gas velocity of 6.31 *cm/s* and at a superficial liquid velocity of 0.10 *cm/s* are shown in Figure 5.8 (c). An increase in the liquid viscosity increases the gas-liquid interface resistance and thereby reduces the mass transfer.

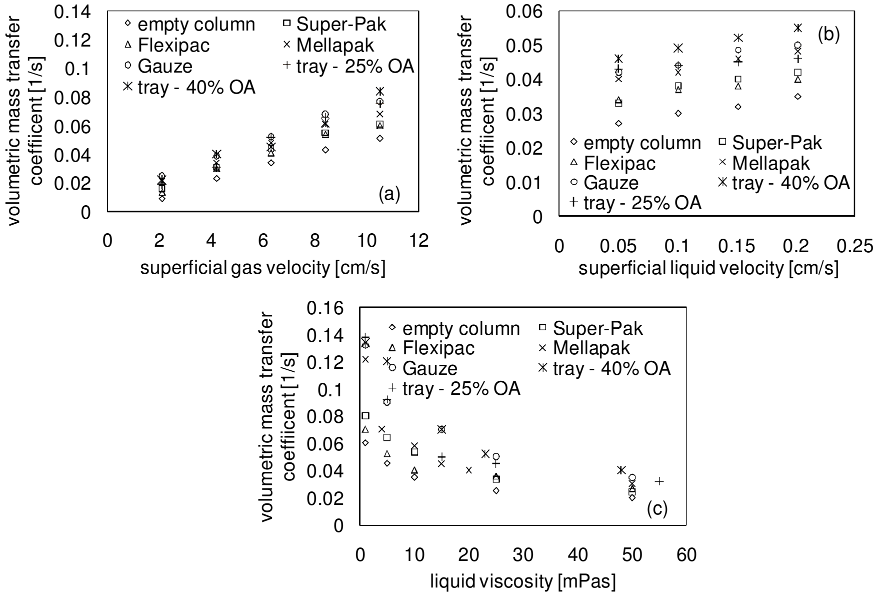

Figure 5.8: (a) Effect of gas velocity (b) effect of liquid velocity (c) effect of liquid viscosity on the volumetric mass transfer coefficient in the packed, trayed and empty bubble column

It can be seen from Figure 5.8 that the volumetric mass transfer coefficient is higher for the trayed and packed bubble column compared to the empty bubble column. This can be attributed to the higher value of interfacial area and the higher gas holdup that is achieved in packed and trayed bubble column. A bubble column equipped with a gauze packing offers the highest volumetric mass transfer coefficient compared to other packings because the Gauze packing provides the highest surface area per unit volume compared to other packings. In contrast, Flexipac provides the lowest surface area per unit volume compared to other packings and thereby the lowest volumetric mass transfer coefficient is obtained in Flexipac. Depending on the operating condition of the packed bubble column, the volumetric mass transfer coefficient is increased for Flexipac by a factor 1.17-1.5 (15-33%), Super-Pak by a factor 1.20-1.75 (16-44%), Mellapak by a factor 1.3-2.4 (25-58%) and Gauze by a factor 1.5-2.8 (33-65%). In the trayed bubble column, the volumetric mass transfer coefficient is increased by a factor 1.3-2.11 (25-53%) for a tray open are of 25% and by a factor 1.3-2.5 (25-60%) for a tray open area of 40%. A higher volumetric mass transfer coefficient is achieved with a tray open area of 40% compared to a tray open area of 25%. This is due to the fact that the attained gas holdup is higher in the tray with an open area of 40% compared to 25%.

5.3.3.3 Volumetric mass transfer correlations

The liquid side mass transfer coefficient is estimated from experiments performed at various gas and liquid flow rates, and the liquid viscosities. The effect of these parameters on the volumetric mass transfer coefficient can be correlated by the Stanton dimensionless number as a function of the Froude and Gallilei dimensionless numbers [11, 31]. The Stanton number is defined as

$$St = \frac{K_L a D}{U_l} \tag{5.20}$$

where D refers to the diameter of the empty bubble column, the hydraulic diameter of packing for the packed bubble column and the tray hole diameter for the trayed bubble column. An empirical correlation for the empty and packed bubble column is proposed as[11, 31],

$$St = AFr_g^{\alpha} Fr_l^{\beta} Ga^{\gamma} \tag{5.21}$$

The value of the coefficients in eq. (5.21) represents the effect of Froude and Gallilei numbers on the Stanton number and thereby on the volumetric mass transfer coefficient. An empirical correlation for the trayed bubble column is proposed as,

$$St = AFr_g^{\alpha} Fr_l^{\beta} Ga^{\gamma} OA^{\lambda} \tag{5.22}$$

which also accounts for the effect of the tray open area on the volumetric mass transfer coefficient. The correlations for the empty, packed and trayed bubble column are determined by fitting experimental data in MATLAB by conducting non-linear regression analysis. For the empty bubble column, the volumetric mass transfer coefficient correlation is: $St = 0.0029 Fr_g^{0.301} Fr_l^{-0.511} Ga^{0.120}$ (5.23)

The value of coefficients in eq. (5.23) with their 95% confidence intervals is depicted in table 5.4. The mean relative error between the experimental and the predicated Stanton number is 14%. The sensitivity analysis is performed using eq. (5.7) for a 10% change in the value of coefficient of eq. (5.23). The sensitivity parameter for the coefficient A is 3475, for the coefficient α is 59, for the coefficient β is 227 and for the coefficient γ is 241. These sensitivity parameters indicate that the correlation for Stanton number is more sensitive to the change in the coefficient A compared to other coefficients. For the packed bubble column the volumetric mass transfer coefficient correlation is:

$$St = 0.01 Fr_g^{0.425} Fr_l^{-0.374} Ga^{0.121} \tag{5.24}$$

The volumetric mass transfer coefficient correlation for trayed bubble column according to eq. (5.22) is:

$$St = 0.0012 Fr_g^{0.465} Fr_l^{-0.564} Ga^{0.153} OA^{0.428} \tag{5.25}$$

The value of the coefficients in eq. (5.24), (5.25) with their 95% confidence intervals is depicted in table 5.4. The mean relative error between the experimental and the predicated Stanton number for the packed bubble column from eq. (5.24) is 17% and for the trayed bubble column from eq. (5.25) is 13%.

Table 5.4: Parameters with their 95% confidence intervals

Empty bubble column	Packed bubble column	Tray bubble column
A: 0.0029 ± 0.0009	A: 0.01 ± 0.002	A: 0.0012 ± 0.0007
α: 0.301 ± 0.017	α: 0.425 ± 0.064	α: 0.465± 0.048
β: -0.511 ± 0.059	β: -0.374 ± 0.017	β: -0.564 ± 0.043
γ: 0.120 ± 0.017	γ: 0.120 ± 0.009	γ: 0.153 ± 0.014
		λ: -0.428 ± 0.011

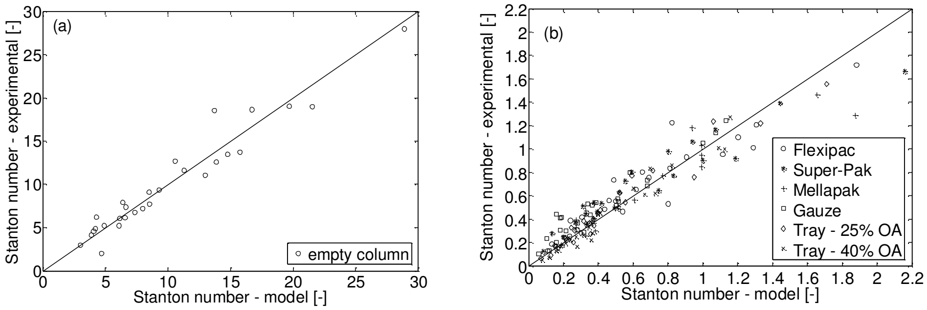

Figure 5.9: Parity plot of the Stanton number calculated from experimental data versus estimated from the model for the empty (a) and packed and trayed (b) bubble column

Figure 5.9 shows a good agreement between the experimental and the estimated values of Stanton number. The volumetric mass transfer coefficient is proportional to the Stanton number and, the gas velocity is directly proportional to the Froude number. Hence, the positive power of the gas side Froude number in eq. (5.23), (5.24) and (5.25) is in agreement with the fact that the volumetric mass transfer coefficient increases with an increase in the gas velocity. Although the Stanton number in eq. (5.23), (5.24) and (5.25) is proportional to the negative power of the liquid side Froude number and thereby the liquid velocity, the volumetric mass transfer coefficient increases with an increase in the liquid velocity because the liquid velocity appears in denominator of the Stanton number as well. Moreover, the positive power of the Gallilei number supports that the volumetric mass transfer coefficient decreases with an increase in the liquid viscosity. The positive power of the tray open area in eq. (5.25) is in agreement with the fact that the volumetric mass transfer coefficient increases with the tray open area.

5.4 Conclusions

The effect of gas and liquid flow rates, and the liquid phase viscosity on the gas holdup, liquid dispersion and mass transfer in the packed, trayed and empty bubble column is systematically investigated. The packed and trayed bubble columns improve the gas holdup and mass transfer compared to the empty bubble column and reduces the axial dispersion significantly. Particularly, the Gauze packing improves the gas holdup and mass transfer and, sufficiently reduces the axial dispersion. In contrast, Super-Pak offers only a modest improvement because of its open structure. Comparison of the experimental data of the packed and trayed bubble column indicates that the partition trays improve the bubble column in the same order as packing. The gas holdup, axial dispersion and mass transfer depend more strongly on the gas velocity compared to the liquid velocity. The liquid viscosity also significantly influences these parameters and therefore the empirical correlations obtained from the air-water system cannot be applied for the viscous system. Empirical correlations for these parameters based on Bodenstein, Stanton, Froude and Gallilei dimensionless numbers were proposed and validated.

References

[1] S. Degaleesan, M. Dudukovic, Y. Pan, Experimental study of gas-induced liquid-flow structures in bubble columns, AIChE Journal, 47 (2001) 1913.

[2] N. Kantarci, F. Borak, K.O. Ulgen, Bubble column reactors, Process Biochemistry, 40 (2005) 2263.

[3] Y.T. Shah, B.G. Kelkar, S.P. Godbole, W.D. Deckwer, Design parameters estimations for bubble column reactors, AIChE Journal, 28 (1982) 353.

[4] B. Bhatia, K.D.P. Nigam, D. Auban, G. Hebrard, Effect of a new high porosity packing on hydrodynamics and mass transfer in bubble columns, Chemical Engineering and Processing, 43 (2004) 1371.

[5] A. Shaikh, M.H. Al-Dahhan, A Review on Flow Regime Transition in Bubble Columns, International Journal of Chemical Reactor Engineerign, 5 (2007) R1.

[6] Y. Wu, Z.-M. Cheng, Z.-B. Huang, Backmixing Reduction of a Bubble Column by Interruption of the Global Liquid Circulation, Industrial & Engineering Chemistry Research, 48 (2009) 6558.

[7] F. Rendtorff Birrer, U. Böhm, Gas-liquid dispersions in structured packing with high-viscosity liquids, Chemical Engineering Science, 59 (2004) 4385.

[8] J. Alvaré, M.H. Al-Dahhan, Liquid phase mixing in trayed bubble column reactors, Chemical Engineering Science, 61 (2006) 1819.

[9] K. Niranjan, V.G. Pangarkar, Gas holdup and mixing characteristics of packed bubble columns, The Chemical Engineering Journal, 29 (1984) 101.

[10] S.B. Sawant, V.G. Pangarkar, J.B. Joshi, Gas hold-up and mass transfer characteristics of packed bubble columns, The Chemical Engineering Journal, 18 (1979) 143.

[11] R. Khamadieva, U. Böhm, Mass transfer to the wall of a packed and unpacked bubble column operating with Newtonian and non-Newtonian liquids, Chemical Engineering Journal, 116 (2006) 105.

[12] J. AlvarÃ©, M.H. Al-Dahhan, Gas Holdup in Trayed Bubble Column Reactors, Industrial & Engineering Chemistry Research, 45 (2006) 3320.

[13] M. Vinaya, Y.B.G. Varma, Some aspects of hydrodynamics in multistage bubble columns, Bioprocess and Biosystems Engineering, 13 (1995) 231.

[14] M.I. Urseanu, J. Ellenberger, R. Krishna, A structured catalytic bubble column reactor: hydrodynamics and mixing studies, Catalysis Today, 69 (2001) 105.

[15] A.A. Youssef, M.H. Al-Dahhan, Impact of Internals on the Gas Holdup and Bubble Properties of a Bubble Column, Industrial & Engineering Chemistry Research, 48 (2009) 8007.

[16] S. Moustiri, G. Hebrard, S.S. Thakre, M. Roustan, A unified correlation for predicting liquid axial dispersion coefficient in bubble columns, Chemical Engineering Science, 56 (2001) 1041.

[17] D.-H. Lee, J.R. Grace, N. Epstein, Gas holdup for high gas velocities in a gas–liquid cocurrent upward-flow system, The Canadian Journal of Chemical Engineering, 78 (2000) 1006.

[18] A. Kemoun, B. Cheng Ong, P. Gupta, M.H. Al-Dahhan, M.P. Dudukovic, Gas holdup in bubble columns at elevated pressure via computed tomography, International Journal of Multiphase Flow, 27 (2001) 929.

[19] A. Shaikh, M. Al-Dahhan, Development of an artificial neural network correlation for prediction of overall gas holdup in bubble column reactors, Chemical Engineering and Processing, 42 599.

[20] K. Shimizu, S. Takada, K. Minekawa, Y. Kawase, Phenomenological model for bubble column reactors: Prediction of gas hold-ups and volumetric mass transfer coefficients, Chemical Engineering Journal, 78 (2000) 21.

[21] B.C. Meikap, G. Kundu, M.N. Biswas, Mass Transfer characteristics of a counter current multi-stage bubble column scrubber, Journal of Chemical Engineering of Japan, 37 (2004) 1185.

[22] K. Thaker, D.P. Rao, Effects of Gas Redispersion and Liquid Height on Gas-Liquid Hydrodynamics in a Multistage Bubble Column, Chemical Engineering Research and Design, 85 (2007) 1362.

[23] A.J. Dreher, R. Krishna, Liquid-phase backmixing in bubble columns, structured by introduction of partition plates, Catalysis Today, 69 (2001) 165.

[24] P. Therning, A. Rasmuson, Liquid dispersion and gas holdup in packed bubble columns at atmospheric pressure, Chemical Engineering Journal, 81 (2001) 69.

[25] J.B.L.M. Campos, J.R.F.G. de Carvalho, A new experimental technique to study backmixing in packed bubble columns, Chemical Engineering Science, 47 4063.

[26] S. Moustiri, G. Hebrard, M. Roustan, Effect of a new high porosity packing on hydrodynamics of bubble columns, Chemical Engineering and Processing, 41 (2002) 419.

[27] V.P. Chilekar, C. Singh, J.v.d. Schaaf, B.F.M. Kuster, J.C. Schouten, A Gas hold-up model for slurry bubble columns, AIChE Journal, 53 (2007) 1687.

[28] C.M.R. Madhuranthakam, Q. Pan, G.L. Rempel, Hydrodynamics in Sulzer SMX Static Mixer with Air/Water System, Industrial & Engineering Chemistry Research, 48 (2008) 719.

[29] P. Therning, A. Rasmuson, Liquid dispersion, gas holdup and frictional pressure drop in a packed bubble column at elevated pressures, Chemical Engineering Journal, 81 (2001) 331.

[30] T. Seno, S. Uchida, S. Tsuyutani, Mass transfer in countercurrent and cocurrent bubble columns, Chemical Engineering & Technology, 13 (1990) 113.

[31] A. Lakota, Impact of structured packing on bubble column mass transfer characteristics evaluation., Acta Chimica Slovenica, 50 (2003) 771-776.

Chapter 6

Validation of the reactive distillation concept and model by pilot plant testing

This chapter discusses the experimental pilot plant validation of the reactive distillation process for the polyester synthesis. Two different configurations are investigated: 1) a reactive distillation column and 2) a reactive distillation column coupled with a pre-reactor. For the first configuration, we have demonstrated that mostly monoesters are formed in the reactive distillation column. For the second configuration, we have demonstrated that the polyesters are formed in the reactive distillation column. The extended rate-based model developed in chapter 3 is used to simulate the pilot reactive distillation column. The model adequately describes the experimental data obtained from the pilot plant. Moreover, the product specification of polyester produced in the reactive distillation column is compared with the polyester produced in industry. It is found that the product specifications of the polyester produced in the reactive distillation column comparable to that of the polyester produced in industry.

6.1 Introduction

In chapter 3, the simulation results demonstrated that reactive distillation is a promising alternative for polyester synthesis. The production time was reduced by 85% and the required volume to produce 100 ktonnes/year polyester was reduced by 74%. Moreover, the reactive distillation model predicted the polymer attribute, isomerization and saturation composition of the polymer in the range of industrial production data of the polyester process. Although the ideal reaction temperature of the polyester process is between 210°C and 220°C (to avoid the degradation of reactants and products) [1], the reaction temperature of the reactive distillation was varied between 185°C and 270°C. It was assumed that there is no possibility of destruction of unsaturated acid in the reactive distillation process due to the short residence time requirement and the free acid (or anhydride) only being present in the 3 top stages of the reactive distillation column, where the reaction temperature remains between 185°C and 210°C as shown in figure 3.8 of chapter 3.

It is important to demonstrate with experiments that the polyesters can be produced in a reactive distillation column and the assumption given for operating the reactive distillation column at temperatures higher than 220°C is reasonable. This chapter discusses the experiments carried out in the pilot reactive distillation column. The polyester produced in the pilot plant is compared with the polyester produced in industry. Moreover, the experimental results are compared with the simulation results to check the validity of the developed model in chapter 3. The model adequately describes the experimental data obtained from the pilot plant. Moreover, it is found that the product specifications of the polyester produced in the reactive distillation column are comparable to those of the polyester currently produced in the traditional industrial batch-reactor setup.

6.2 Experimental

6.2.1 Configurations

The reaction between maleic anhydride and propylene glycol is taken as a model reaction system for the synthesis of unsaturated polyesters. Two configurations are investigated:

Configuration 1: This configuration represents the polyester synthesis in a reactive distillation column by feeding maleic anhydride as a liquid at the top of the column and propylene glycol as a vapor at the bottom of the column. A schematic view of this configuration is shown in figure 6.1 (a).

Configuration 2: This configuration represents the polyester synthesis in a reactive distillation column by feeding monoesters as a liquid at the top of the column and propylene glycol as a vapor at the bottom of the column. In this case, propylene glycol acts as a stripping agent. The monoesters are prepared in a batch reactor by mixing maleic anhydride and propylene glycol in the ratio of 1.0:1.15. A schematic view of this configuration is shown in figure 6.1 (b).

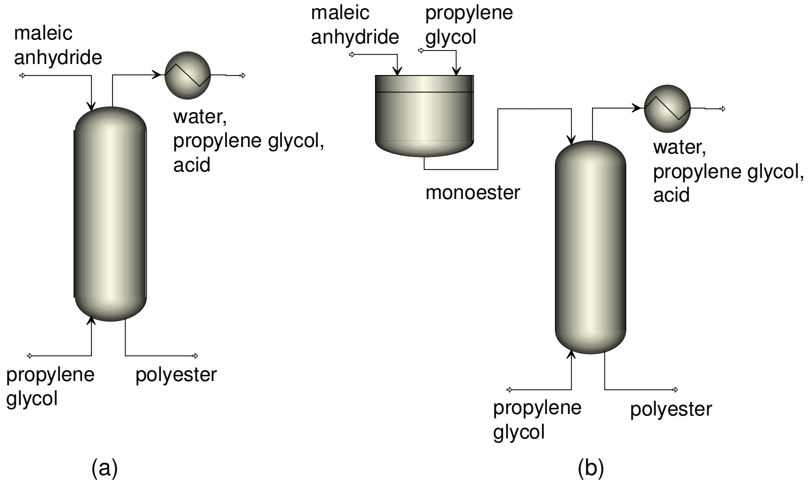

Figure 6.1: Schematic view of configuration 1; reactive distillation column (a) and configuration 2; reactive distillation column coupled with a pre-reactor (b)

6.2.2 Experimental setup

A schematic view of the pilot plant setup is given in figure 6.2 and the picture of pilot plant setup is given in figure 6.3. The column has an inner diameter of 50 *mm* and a height of 1.7

meter. The column is made from stainless steel and contains an outer jacket for circulating hot oil. The column is equipped with 7 units of Sulzer BX packing and the total packed section height is 1.19 *meter*. Along the column, 8 temperature sensors are mounted to measure the temperature profile and 8 samples points are available to collect samples. The liquid holdup inside the column is monitored by differential pressure measurement over the column. Two differential pressure transmitters (GE Sensing LX8381) are placed: 1) to measure the pressure difference over the packed section 2) to measure the pressure difference in the bottom section of the column. Four tanks of 50 *liters* are used for storage. The tanks contain a level controller and a temperature sensor. In addition, the tanks for anhydride and the bottom product storage are equipped with an agitator and an outer jacket for heating or cooling. Two heating thermostats (supplied by LAUDA, model E200) are used to heat the storage tanks. The heating thermostats (supplied by LAUDA, model Proline P5) are used for heating the column up to the required temperature. A condenser containing a helical tube of 6 *meter* is connected to the column to condense the vapor leaving the column. The temperature of the condenser is controlled by a cooling thermostat (supplied by Julabo, model F25). The reactants are fed to the column by a magnetic gear pump (supplied by Bronkhorst, model MZR-7255). The mass flow rates of reactants are controlled by a Coriolis mass flow controller (supplied by Bronkhorst, model M53-RAD-220-B). The evaporator – aSTEAM DV1C supplied by aDROP Feuchtemeztechnik GmbH is used to vaporize the glycol. The flow rate of vapor leaving the column is controlled with a mass flow controller which is regulated by pressure measurement. The pilot plant set up is monitored and controlled by a custom made graphical interface in LabVIEW.

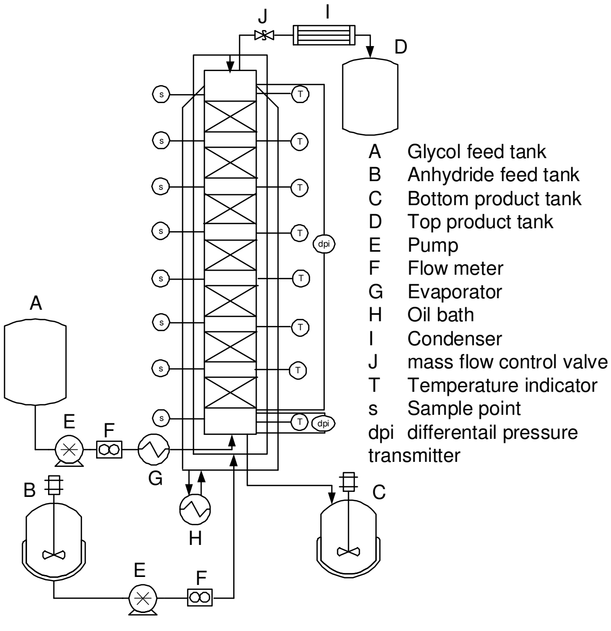
J
I
D
A
E
F
G
B
H
C
E
F
s
T
dpi
A Glycol feed tank
B Anhydride feed tank
C Bottom product tank
D Top product tank
E Pump
F Flow meter
G Evaporator
H Oil bath
I Condenser
J mass flow control valve
T Temperature indicator
s Sample point
dpi differentail pressure transmitter

Figure 6.2: Schematic of the reactive distillation pilot plant setup

6.2.3 Experimental procedure

The column is heated to the required isothermal temperature in both configurations. The temperature difference between the top and bottom section of the column is maximum ± 3°C. The column is operated at 1 *bar* in both configurations. After achieving the isothermal operation and setting the required pressure in the column, propylene glycol is fed to the column via the evaporator where propylene glycol is vaporized. The evaporator is equipped with an additional heater to keep the vapor temperature above the dew point. The evaporator requires at least 30 minutes for complete evaporation of propylene glycol. The propylene glycol lines from the evaporator to the column are also traced up to 300°C to avoid condensation of the propylene glycol vapor. After achieving a constant vapor flow rate and an isothermal temperature in the column, the liquid is fed at the top of the column. The liquid feed line is passing through the column jacket to heat up the liquid feed to the column temperature. In case of the first configuration, maleic anhydride is preheated up to 90°C in the storage tank to liquefy maleic anhydride. In case of the second configuration, monoesters are prepared in the storage tank by mixing maleic anhydride and propylene glycol in the molar ratio of 1.0:1.15 at 90°C. This storage tank acts as a pre-reactor since this tank is equipped with an agitator and, an outer jacket for heating and cooling. The distillate samples are collected at the outlet of the condenser. The samples are collected at various points along the length of the column in case of first configuration. In case of the second configuration, due to the high viscosity of the liquid flowing inside the column, the samples could not be collected from the 1.5 *mm* sample lines mounted on the column. Therefore, the samples are collected from the liquid stream leaving the bottom of column.

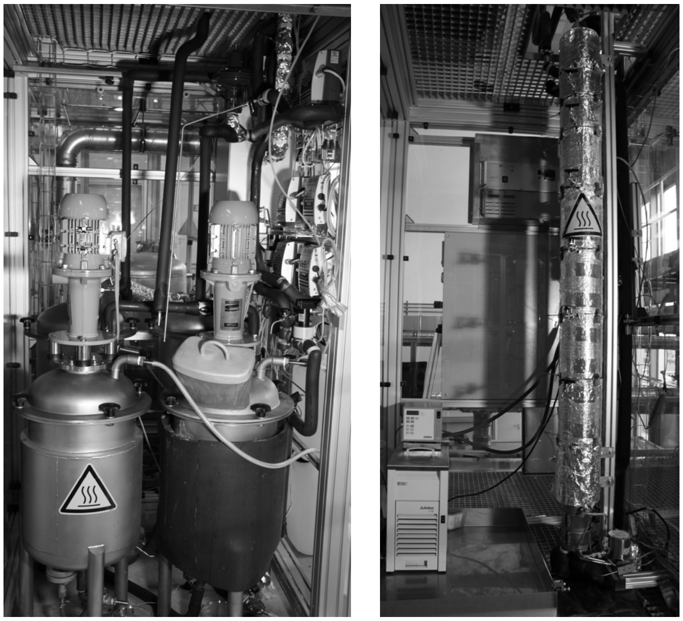

Figure 6.3: Pilot plant setup

6.2.4 Analytical methods

The acid number is defined as the amount of milligrams of potassium hydroxide (KOH) required for neutralizing the free or unreacted carboxyl groups in 1 *gram* of a sample. It is determined by the following formula:

$$AN = \frac{V_t.N.MW_{KOH}}{W} \tag{6.1}$$

where, V_t is the volume of the titer (KOH), N and MW_{KOH} are the normality and the molecular weight of the titer, respectively. W is the weight of a sample. The isomerization and saturation concentration of a sample is measured by the ^{1}H-NMR. The ^{1}H-NMR spectrum is recorded on a Varian VXR 400 spectrometer. A sample is dissolved in dimethyl sulfoxide (d6-DMSO) in 5 *mm* NMR tubes and Tetra methyl silane (TMS) is used as internal standard for quoting chemical shifts in all spectra. The molecular weight distribution is measured using Gel permeation chromatography (GPC). The calibration of GPC is performed by using polystyrene standards and Tetrahydrofuran (THF) is used as solvent to dissolve the sample. The quantity of water in the distillate is measured by Karl Fischer titration with a 652 KF Coulometer.

6.2.5 Pilot plant modeling

The reactive distillation column is modeled as a packed column containing the Sulzer BX packing. The extended rate-based model developed in chapter 3 is used to simulate the column. Since the polyesterfication process involves autocatalytic reactions, the reactions take place throughout in the column. The kinetic and thermodynamic models and their parameters from chapter 2 are used. The liquid holdup, pressure drop and mass transfer are calculated using the correlation for Sulzer BX packing as proposed by Bravo et al. [2]. The axial dispersion coefficient is calculated using the correlation as proposed by Kushalkar et al. [3].

6.3 Results and discussion

6.3.1 Configuration 1

In this configuration, the reactions between maleic anhydride and propylene glycol in the reactive distillation column are investigated. The column is operated counter-currently with maleic anhydride (MAD) fed as liquid at the top of the column and propylene glycol (PG) fed as vapor at the bottom of the column. The liquid to vapor feed ratio is 1.0:1.15. Since the liquid feed (maleic anhydride) tube passes through the column jacket, the preheated maleic anhydride is further heated up to the column temperature. The boiling point of maleic anhydride is 202°C and the boiling point of propylene glycol is 188°C. To prevent extreme vaporization of maleic anhydride in the liquid feed line and extreme condensation of propylene glycol at the bottom of the column, the column should be operated around 195°C. The operating parameters are listed in table 6.1.

Table 6.1: Operating parameters of experiments

Temperature (^oC)	Pressure (bar)	MAD flow rate (kg/hr)	PG flow rate (kg/hr)
195	1	2.12	1.98

After operating the column for two hours at steady liquid and vapor flows, and steady column temperature, samples are taken from the liquid feed stream tube, the liquid stream leaving the bottom of column and, the sample points at 1.2 *m* and 1.45 *m* of the column. The acid value of the samples is determined by titration. The conversion of the carboxylic acid is determined from the acid value as,

$$X = \frac{AV_{MAD} - AV_{product}}{AV_{MAD}} \tag{6.2}$$

where, AV_{MAD} and $AV_{product}$ are the acid value of maleic anhydride (reactant) and the product produced in the reactive distillation column, respectively. The acid value of pure maleic anhydride is 572 mg/g.

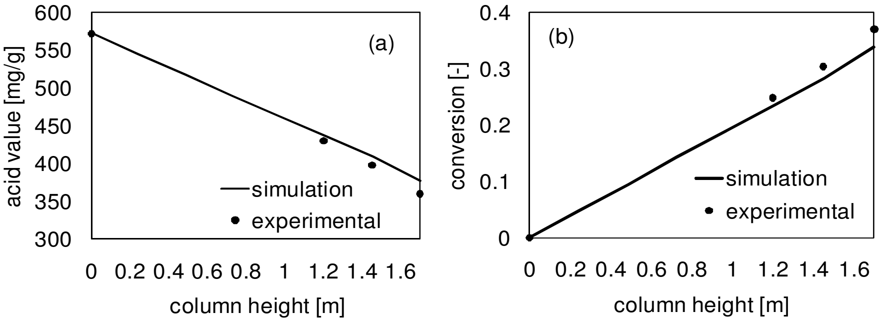

Figure 6.4: Acid value (a) and conversion (b) profiles over the column height

The experimental acid value and the conversion are compared with the simulation results in figure 6.4 (a) and 6.4 (b), respectively. It can be seen from figure 6.4 (a) and 6.4 (b) that the model discussed in chapter 3 accurately predicts the performance of the pilot reactive distillation column. Moreover, the maleic anhydride acid value of 572 *mg/g* has decreased to 360 *mg/g* in the product leaving at the bottom of the column; indicating that 37% conversion is achieved. The mean relative error between experimental and simulated acid value is 5% and the mean relative error between experimental and simulated conversion is 9%. The model predicts 14% liquid holdup in the column. Moreover, the residence time of the liquid is calculated from the liquid holdup and the liquid flow rate, which is approximately 0.32 hours (19 minutes). Due to the short liquid residence time of approximately 0.32 hours and the relatively low column temperature of 195°C, a maximum conversion of 37% is achieved. Due to the lower conversion achieved in the pilot reactive distillation column, mostly monoesters have been formed.

6.3.2 Configuration 2

The column is operated counter-currently with the monoester fed as a liquid at the top of the column and propylene glycol fed as vapor at the bottom of the column. The monoesters are prepared in the storage tank at 90°C by mixing maleic anhydride and propylene glycol in the ratio of 1.0:1 .15. Due to the formation of monoester in the storage tank, the acid value of the mixture is reduced from 572 *mg/g* of maleic anhydride (reactant) to 264 *mg/g* after 1 hour of mixing. The acid value of the monoester reduces further with the reaction time, which can be seen in figure 6.5. The monoesters of variable acid value are fed to the column and the measured acid value of the monoester is used to calculate the conversion achieved in the reactive distillation column as,

$$X = \frac{AV_{monoester} - AV_{product}}{AV_{MAD}} \tag{6.2}$$

where, $AV_{monoester}$ and $AV_{product}$ are the acid value of monoester and the product produced in the reactive distillation column, respectively.

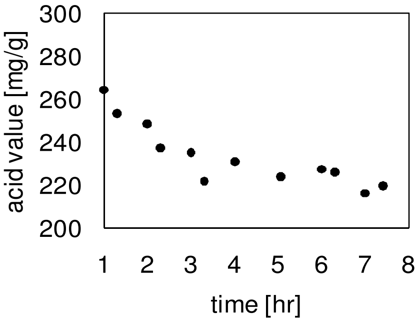

Figure 6.5: An acid value of the monoester in the liquid feed stream

Table 6.2: Operating parameters of experiments

Exp. no.	Temperature (°C)	Pressure (bar)	Monoester flow rate (kg/hr)	PG flow rate (kg/hr)	Acid value of monoester (mg/g)
E1	195	1	1.5	0.25	250
E2	200	1	1.5	0.25	237
E3	230	1	1.5	0.25	235
E4	250	1	1.5	0.25	217
E5	230	1	1.5	0.5	224
E6	230	1	1.5	0.75	224
E7	250	1	1.5	0.5	224
E8	250	1	1.5	0.75	216

To validate the reactive distillation model and, to quantify the influence of the temperature and the glycol vapor feed flow rate on the polyesters synthesis, in total 8 experiments with varying operating conditions were performed. The experimental operating conditions are listed in table 6.2. After operating the column at steady liquid and vapor flows and steady column temperature, samples were taken at 15 minutes intervals from the liquid feed stream, the liquid stream leaving at the bottom of column and the distillate.

The acid values of the bottom product at different operating conditions of the reactive distillation column are shown in figures 6.6 (a)-(c). It can be seen from figure 6.6 that the acid value for different samples of the bottom product at the particular operating condition are constant, which confirms that the samples were taken when the column was operating under steady-state conditions. It can be seen from figure 6.6 (a) that the acid value of the bottom product reduces with an increase in the temperature of the column, which indicates that a higher conversion is achieved by operating the column at higher temperature. Figures 6.6 (b) and (c) show that the acid value of the bottom product reduces with an increase in the glycol vapor feed flow rate, which indicates that a higher conversion is achieved with an increase in the glycol vapor feed flow rate.

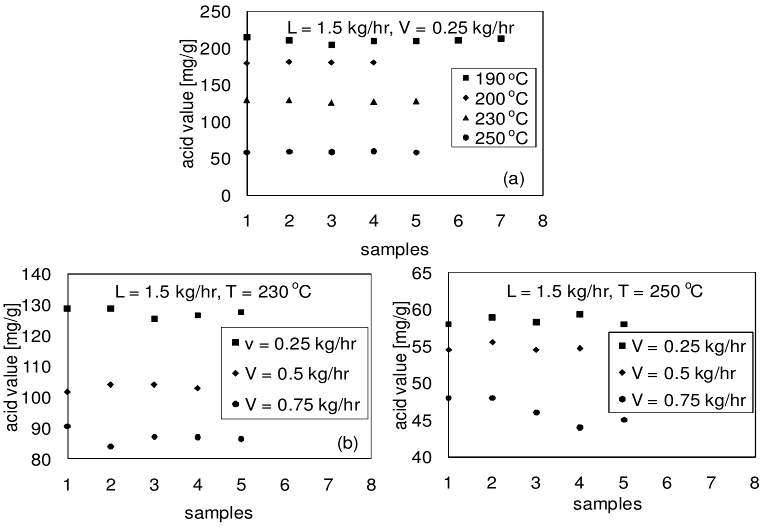

Figure 6.6: An acid value of the bottom product leaving the column for experiments E1, E2, E3, E4 (a), for experiments E3, E5, E6 (b) and for experiments E4, E7, E8

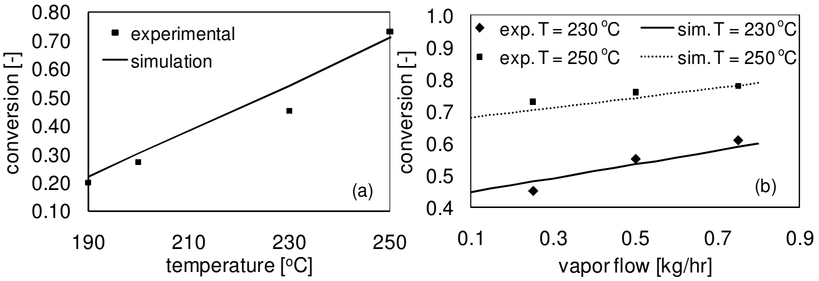

Figure 6.7: Conversion as function of temperature for experiments E1 to E4 (a) and conversion as function of glycol vapor feed rate for experiments E3 to E8 (b)

The conversion of carboxylic acid in the reactive distillation column for different operating conditions is shown in figures 6.7 (a) and (b). Figure 6.7 (a) shows the influence of column temperature on the conversion for experiments E1, E2, E3 and E4. It can be seen that the conversion increases significantly with an increase in the column temperature. A conversion of 21% is achieved at a column temperature of 190°C which increases up to 73% at a column temperature of 250°C. The conversion versus the glycol vapor feed flow rate is shown in figure 6.7 (b) for the experiments performed at the monoester feed flow of 1.5 *kg/hr* and, at 230°C (exp. E3, E5 and E6) and 250°C (exp. E4, E7 and E8). At both temperatures the conversion increases with an increase in the glycol vapor feed flow rate. From figures 6.7 (a) and (b), it can be seen that a conversion of > 70% is achieved at a column temperature of 250°C and a conversion of > 45% is achieved at a column temperature of 230°C. Figures 6.7 (a) and (b) also indicate that the model adequately predicts the experimental data. The mean relative error between experimental and predicted conversion from the model is 9%.

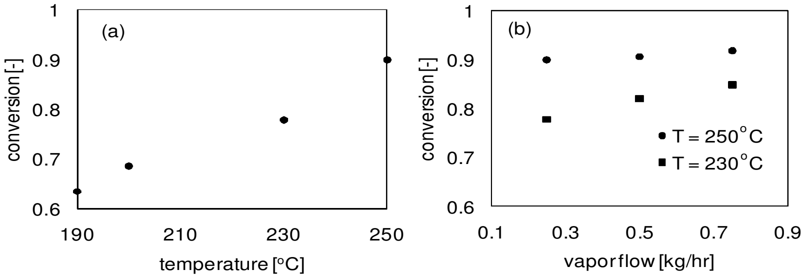

Figure 6.8: Overall conversion as a function of temperature for experiments E1 to E4 (a) and overall conversion as function of glycol vapor feed rate for experiments E3 to E8 (b)

It should be noted that the conversion shown in figures 6.7 (a) and (b) is calculated from the acid values of the monoester and the bottom product. Thus, this conversion refers to the conversion achieved in the reactive distillation column. The overall conversion should be calculated from the acid value of the reactant (maleic anhydride) and the bottom product according to eq. (6.2) as shown in figure 6.8. Figures 6.8 (a)-(b) show that a minimum conversion of 90% is achieved at a column temperature of 250°C and a minimum conversion of 77% is achieved at a column temperature of 230°C. The model predicts 16% liquid holdup in the column. Moreover, the residence time of the liquid is calculated from the liquid holdup and the liquid flow rate, which is approximately 0.55 hours (32 minutes). This indicates that 90% conversion is achieved within 0.55 hours at a temperature of 250°C in the reactive distillation column coupled with the pre-reactor; which confirms the polyester formation in the reactive distillation column.

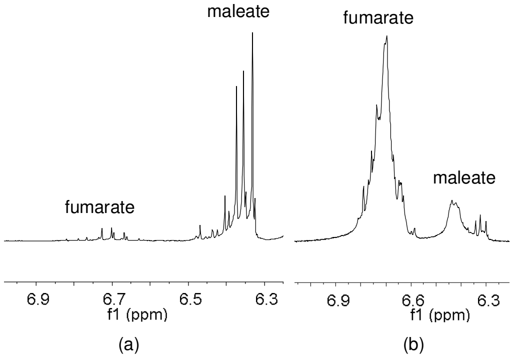

Figure 6.9: ^{1}H-NMR spectra of maleate-fumarate isomerization in the liquid feed (a) and the bottom product (b)

Furthermore, the isomerization and saturation fraction of the liquid feed and the bottom product has been determined by ^{1}H-NMR. For experiment E4, figure 6.9 shows an illustrative example for determination of the isomerized fraction in the liquid feed and the bottom product from ^{1}H-NMR spectra. The maleate-formed acid and ester compounds appear at peaks from 6.3 *ppm* to 6.5 *ppm* and the fumarate-formed acid and ester compounds appear at the peaks from 6.6 *ppm* to 6.9 *ppm* [4]. The peaks for maleate and fumarate compounds are well separated from each other, and their area can be easily determined. The area of an NMR peak is directly proportional to the number of protons causing the peak [4]; thus the relative concentrations of maleate and fumarate present in the sample can be easily determined. The isomerization percentage at various temperatures in the bottom product is shown in figure 6.10 (a). It can be seen that the bottom product contains 83% of isomerized compounds when the column is operated at 250°C and 79% of isomerized compounds when the column is operated at 230°C. The mean relative error between experimental and predicted isomerization percentage from the model is 12%.

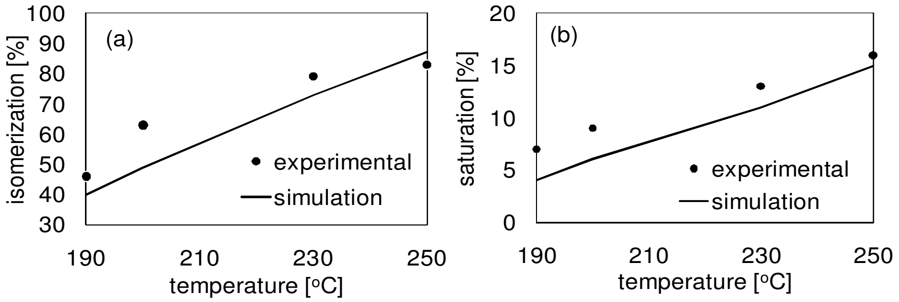

Figure 6.10: Isomerization percentage (a) and saturation percentage (b) in the bottom product for experiments E1 to E4

The concentrations of the unsaturated and saturated compounds are also determined from the ^{1}H-NMR peak. Furthermore, the saturation fraction is calculated from the concentration of unsaturated and saturated compounds present in the sample. Then the percentage change in the saturation fraction of the bottom product is calculated with respect to the saturation fraction of the liquid feed. The bottom product obtained at 230^{o}C and 250^{o}C contains 12% and 17% saturated compounds, respectively as shown in figure 6.10 (b). The mean relative error between the experimental and predicted saturation percentages from the model is 22%. For experiment E4; the number-average molecular weight (M_n) and the degree of polymerization (DP) are experimentally determined by GPC, and further compared with the simulation results in table 6.3. The model predicted the polymer attributes accurately as can be seen from table 6.3.

Table 6.3: Polymer attributes of a bottom product for experiment E4

Product specifications	experimental	simulation
Number-average-molecular weight [-]	1404	1497
Degree of polymerization [-]	8.89	9.47

The acid value, conversion, isomerization and saturation percentages and polymer attributes of the bottom product produced at a column temperature of 250^{o}C are compared with polyester typically produced in an industrial setup in table 6.4. The conversion achieved in the reactive distillation column at 250^{o}C is close to the conversion achieved in the industrial polyester process. Moreover, the isomerization and saturation fraction of the bottom product is in the range of the polyester produced in industry. The number-average molecular weight and the degree of polymerization of the bottom product produced in the reactive distillation column are lower compared to the polyester produced in industry. This is due to lower conversion that was achieved in the pilot reactive distillation column. The polymer attributes of polyester produced in the reactive distillation column are expected to be similar to the polyester produced in industry, if a conversion of 95% is achieved in the reactive distillation column.

Table 6.4: Comparison of product specification

Product specifications	bottom product produced at 250^{o}C	Polyester product produced in industry [5-8]
Acid value [mg/g]	58	25
Conversion [-]	90	95
Isomerization [%]	83	90-95
Saturation [%]	17	15-20
Number-average-molecular weight [-]	1404	3100
Degree of polymerization [-]	8.89	25

The colors of the liquid feed sample, the bottom product and the top product sample are shown in figure 6.11. It can be seen that the color of the liquid feed and the bottom product are similar. However, the color of bottom product is a little darker yellow compared to the pale yellow color of monoester feed. Since the bottom product sample is taken in open air, an oxidation reaction may have occurred which influenced the color of the bottom product. Moreover, the distillate is colorless which indicates that a good separation took place in the column.

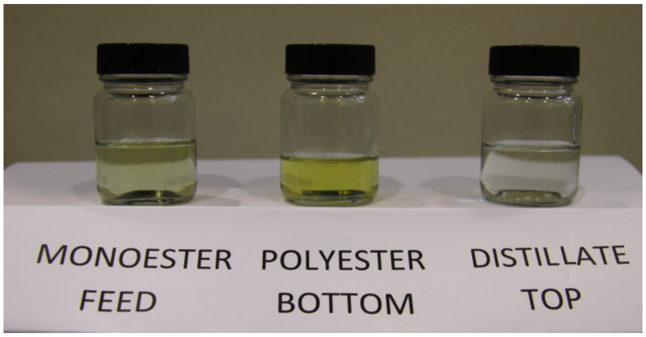

Figure 6.11: Color of sample taken from feed, bottom and top products for experiments E4

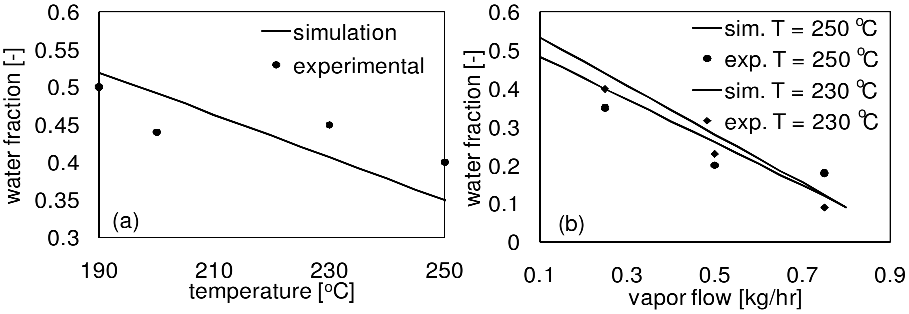

Figure 6.12: Water fraction in the distillate as a function of column temperature for experiments E1 to E4 (a) and glycol vapor feed rate for experiments for E3 to E8 (b)

The experimentally determined water fraction of the distillate is compared with the predicted water fraction of the distillate from the model as shown in figure 6.12. It can be seen that the model predicted the water fraction of distillate within the range of experimental data. The mean relative error between experimental and predicted water fraction from model is 14%.

6.4 Conclusions

In this chapter, polyester synthesis is successfully executed in a pilot reactive distillation column equipped with Sulzer BX gauze packing. Two different configurations were investigated: 1) a reactive distillation column and 2) a reactive distillation column coupled with a pre-reactor. Due to a relatively short residence time of 0.32 hours and an operating temperature of 190°C in case of the first configuration, a maximum conversion of 37% was achieved; which indicates monoester formation in the reactive distillation column. In the case of the second configuration, a 90% conversion is achieved within 0.55 hours at a temperature of 250°C in the reactive distillation column coupled with a pre-reactor; which confirms the polyester formation in the reactive distillation column. The extended rate-based model developed in chapter 3 was used to simulate the pilot reactive distillation column. The model predicted the experimental data (acid value, conversion, isomerization and saturation fraction, number-average molecular weight, the degree of polymerization and water fraction in the distillate) adequately (5-22%). Moreover, the product specifications of the polyester produced at 250°C in the reactive distillation column is in the range of polyesters produced in the traditional industrial setup. Furthermore, the discoloration of the polyester was hardly noticed even though the column was operated at 250°C. From this experimental validation of the reactive distillation process for polyester synthesis, it is concluded that the polyester can be produced in a reactive distillation column in a short residence time with comparable product specifications as the polyester produced in industry.

References

[1] E.E. Parker, Unsaturated polyesters, Industrial & Engineering Chemistry, 58 (1966) 53.

[2] J.L. Bravo, J.A. Rocha, J.R. Fair, A comprehensive model for the performance of columns containing structured packings, in: I. ChemE. Symp. Ser., 1992, pp. A439.

[3] K.B. Kushalkar, V.G. Pangarkar, Liquid holdup and dispersion in packed columns, Chemical Engineering Science, 45 (1990) 759.

[4] L.G. Curtis, D.L. Edwards, R.M. Simons, P.J. Trent, P.T. Von Bramer, Investigation of Maleate-Fumarate Isomerization in Unsaturated Polyesters by Nuclear Magnetic Resonance, I&EC Product Research and Development, 3 (1964) 218.

[5] J. Korbar, J. Golob, A. Šebenik, Process of unsaturated polyester resin synthesis on a laboratory and industrial scale, Polymer Engineering & Science, 33 (1993) 1212.

[6] R. Jedlovčnik, A. Šebenik, J. Golob, J. Korbar, Step-growth polymerization of maleic anhydride and 1,2-propylene glycol, Polymer Engineering & Science, 35 (1995) 1413.

[7] S.S. Feuer, T.E. Bockstahler, C.A. Brown, I. Rosenthal, Maleic-Fumaric Isomerization in Unsaturated Polyesters, Industrial & Engineering Chemistry, 46 (1954) 1643.

[8] A. Fradet, E. Marechal, Study on models of double bond saturation during the synthesis of unsaturated polyesters, Die Makromolekulare Chemie, 183 (1982) 319.

Chapter 7

Evaluation of configuration alternatives for the multi-product polyester synthesis by reactive distillation

The aim of this chapter is to find the best suitable internal and feed configurations of the reactive distillation process for the unsaturated polyester synthesis. Moreover, multi-product simulations are performed to find the operational parameters for producing different grades of polyester in the same equipment. Finally, the product transition time during product changeover is determined. The criteria to select the best configuration are the minimum requirement of volume and energy to produce 100 ktonnes/year polyester. From simulations, it is found that the configuration which contains the reactive stripping section as a packed or trayed bubble column and the reactive rectifying section as a packed column requires minimum volume and energy to produce 100 ktonnes/year polyester. With respect to the feed configuration, the feeding of monoesters to the reactive distillation column significantly intensifies the polyester process as compared to an anhydrous reactant fed to the column. Moreover, the product transition time in this configuration is also significantly reduced compared to the other configurations.

7.1 Introduction

In chapter 3, the equilibrium and the rate-based models required to study the feasibility of reactive distillation for unsaturated polyesters synthesis were developed. The simulation results demonstrated that reactive distillation is a promising alternative for polyesters synthesis. In chapter 6, the experimental validation of the reactive distillation concept and the rate-based model were discussed. From this experimental validation, it is concluded that the polyester can be produced in a reactive distillation column employing a short residence time with comparable product specifications as the polyester produced in industry. Moreover, the model predicted the experimental data adequately.

In this chapter, the best suitable internal and feed configuration for the reactive distillation column are investigated. The best internal and feed configurations are selected on the basis of criteria that it requires minimum volume and energy to produce 100 *ktonnes/year* polyester. In the first part of this chapter, several possible internals are investigated. After finding the best internal for the reactive distillation column, several possible feed configurations are investigated from which the best feed configuration is identified. Then, the multi-product simulations are performed to produce two different grades of polyester in the same equipment. In particular, steady state simulations are carried out to find the operational parameters to produce different grades of polyester in the same equipment. In order to determine the product transition time during the product changeover in different configurations, dynamic simulations for grade switching are performed. Moreover, the required product transition time in different configurations are compared to determine the configuration which requires a minimum product transition time.

7.2 Internal configuration

In chapter 3, the simulation results demonstrated that at least 1.8 to 2.0 hours of liquid residence time are required to achieve the desired conversion. Moreover, in chapter 4 the simulation results showed that the reactive distillation process for the synthesis of unsaturated polyester is kinetically controlled and that therefore a high liquid holdup is required to enhance the rate of reaction. Traditional internals such as packed columns and tray columns provide a lower liquid holdup compared to the vapor holdup, but these internals provide a better mass transfer. In contrast, packed bubble columns and trayed bubble columns provide a higher liquid holdup compared to the vapor holdup, but the mass transfer is limited by the interfacial area available from the vapor bubbles. In order to achieve a separation with high purity, a better mass transfer is required in the non-reactive section of the column. In order to achieve an enhanced rate of reaction, a higher liquid holdup is required in the in the reactive-section of the column.

Since the polyester process involves autocatalytic reactions, the reactions will take place throughout the column. The reaction rates depend on the temperature, pressure and concentration of the reactants. Since the temperature and concentration of the reactants are significantly lower in the rectifying section compared to the stripping section of the column, significantly slower reactions take place in the rectifying section. Therefore, the provision of higher liquid holdup to enhance the reaction rate is not required in the rectifying section of the column. However, a better mass transfer is required to separate highly pure water in the distillate. Therefore, the packed column configuration (liquid as dispersed phase and vapor as continuous phase) is recommended for the rectifying section of the column. In the stripping section of the column, the temperature and concentration of the reactants are high. Therefore the reactions take place mostly in the stripping section of the column. Hence, the provision of higher liquid holdup will enhance the rate of reaction in the stripping section of the column. With respect to this analysis, four internal configurations are selected for the reactive distillation column;

- RD1: rectifying section as a packed column and stripping section as a packed bubble column
- RD2: rectifying section as a packed column and stripping section as a trayed bubble column
- RD3: rectifying section as a packed column and stripping section as a tray column
- RD4: rectifying and stripping sections as a packed column

A schematic representation of the reactive distillation column with the four different internal scenarios is shown in figure 7.1. Four heat exchangers are attached to the reactive distillation column; 1) for heating the liquid feed up to the required temperature (HEX1), 2) for obtaining the superheated vapor of glycol (HEX2), 3) condensing the vapor leaving at the top of the reactive distillation column (HEX3) and 4) for cooling down the product leaving at the bottom of the column (HEX4).

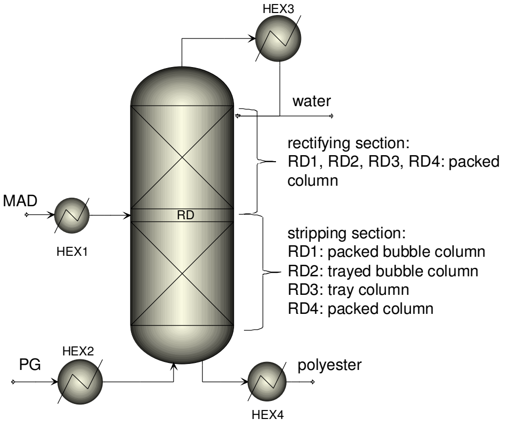

Figure 7.1: Schematic representation of the column with the different internal scenarios.

The extended rate-based model proposed in chapter 3 is used to simulate the column. This model is developed in Aspen custom modeler (ACM). The components, properties, thermodynamics are defined by the problem definition file of Aspen plus/property plus. The non-conventional component properties are estimated by Aspen property plus. The kinetic and thermodynamic models and their parameters are used from shah et al. [1]. For all configurations, the reactive distillation column is designed to produce 100 *ktonnes/year* polyester with an acid value of 25 *mg/g*, to achieve the carboxylic acid conversion of 95.62% and to achieve the water purity in the distillate of 99.5%.

7.2.1 Configurations RD1 and RD2

For these configurations, Mellapak 250Y is used as a structured packing in the rectifying section of the column. The liquid holdup, pressure drop and mass transfer in the rectifying section are calculated using the correlation for Mellapak 250Y packing as proposed by Bravo et al. [2]. These correlations are included in appendix A1. In configuration RD1, Flexipac 2X is used as a structured packing in the stripping section of the column. In configuration RD2, a sieve tray with a tray open area of 25% and a tray hole diameter of 0.8 cm is used in the stripping section of the column. The developed correlations for the liquid holdup, mass transfer and liquid back mixing of packed bubble columns and trayed bubble column in chapter 5 are used to simulate the stripping section of the configurations RD1 and RD2, respectively.

The liquid to vapor feed ratio needs to be selected on the basis of kinetics and hydrodynamics (weeping, flooding and entrainment) requirements. Since the reactive stripping section of the RD1 and RD2 configurations are operated respectively as a packed bubble column and a trayed bubble column, the reactive distillation column needs to satisfy only the kinetics requirements. For these configurations, the liquid to vapor feed molar ratio is found to be 1.0:1.20. The higher vapor (glycol) feed flow is required because 15-20% of the glycol is consumed in the double bond saturation reaction. This feed molar ratio is close to the optimum feed molar ratio (1.0:1.15) found from the calculation with the equilibrium model in chapter 3. For 100 *ktonnes/year* productivity, the required liquid feed flow rate is 7000 *kg/hr* and the required vapor feed flow rate is 6544 *kg/hr*. For these configurations, the total 20 reactive stripping stages are required to achieve 95.62% conversion of carboxylic acid and total 9 reactive rectifying stages are required to achieve 99.5% pure water in the distillate. The stages are numbered from top to bottom. That means the rectifying stages are the stages from 1 to 9 and the stripping stages are the stages from 10 to 29. The liquid is fed at 10th stage and vapor is fed at 29th stage.

For these configurations, the column diameter needs to be selected in such a way that slug formation is avoided. To avoid slug formation, the column diameter needs to be larger than 0.30 *m* for any superficial vapor velocity [3]. The diameter and height of the column is designed such that the reactive stripping section is operated in the heterogeneous bubble region for which the superficial vapor velocities range from 0.12-0.18 *m/s*. The designed diameter and height of the reactive stripping section are given in table 7.1. The rectifying section is designed for a flooding factor of 0.4. The pressure drop is 0.177 *kPa/m* in the rectifying section of the column. The height of the rectifying section depends on the separation efficiency. From the simulations, the height of the rectifying section is calculated to be 2.5 *m* to separate pure water (99.5%) at the top. Since the reactive stripping section is operated as a packed or trayed bubble column and the rectifying section is operated as a packed column in these configurations, it is obvious that the liquid holdup is significantly higher in the reactive stripping section than in the reactive rectifying section. Moreover, the liquid holdup in the rectifying section solely depends on the liquid reflux rate and the condensation rate of the vapor in the rectifying section. Since a very low reflux ratio is required to separate pure water in the distillate, the liquid reflux flow is low. Therefore, the liquid holdup in the rectifying section is low as well. The achieved liquid holdup in the stripping and rectifying sections is depicted in table 7.1.

Since the liquid feed contains pure maleic anhydride, the liquid feed temperature is set to 185°C below the boiling temperature (202°C) of maleic anhydride to avoid extreme vaporization of maleic anhydride. Since the heat is provided in the column through the heat supply from the feed, the vapor feed temperature is selected in such a way that sufficient heat is provided in the column to heat up the material. Moreover, the distillate temperature is set to 99°C. From simulation, the required temperature of vapor feed is found to be 300°C and the temperature of the bottom product leaving the column is found to be 272°C. It is noted that the product is cooled down in the traditional batch process up to 185°C at the end of batch and before blending with Styrene. Therefore, the product leaving the bottom of the column is cooled down from 272°C to 185°C. The energy required for heating the liquid and vapor feeds, cooling the top and bottom products leaving the column is depicted in table 7.1. From simulation, the energy required to produce 100 *ktonnes/year* polyester is found to be 242 *kWh/ton*.

7.2.2 Configurations RD3 and RD4

7.2.2.1 Configuration RD3

Mellapak 250Y is used as a structured packing in the rectifying section of the column and sieve trays with a tray hole diameter of 0.005 *m* are used in the stripping section of the column. The liquid holdup, pressure drop and mass transfer in the rectifying section are calculated using the correlation for Mellapak 250Y packing as proposed by Bravo et al. [2]. These correlations are included in appendix A1. The liquid holdup and pressure drop in the stripping section are calculated using the correlation proposed by Bennett et al. [4], the mass transfer is calculated using the correlation proposed by Chan and Fair [5] and the liquid back mixing is calculated using the correlation proposed by Zuiderweg [6] for sieve tray columns. These correlations are included in appendix A2.

The diameter and the height of the column, the liquid and vapor flow rate are designed in such a way that weeping, flooding and entrainment are avoided in the column. A non-reactive tray distillation column usually operates at higher superficial vapor velocities (1-3 *m/s*) and in the spray or froth region to increase the throughput and vapor-liquid mass transfer area. Moreover, there is no need to aim for the maximum liquid holdup in a conventional distillation column. The situation with respect to the reactive stripping section is quite different. The reaction takes place in the liquid phase and in order to enhance the rate of reaction, high liquid holdup and high residence time are required. Since one of the reactants (glycol) is fed as a vapor, sufficient vapor residence time is required to allow the condensation of this reactant. Therefore, the preferred regime for operation is the bubbly flow regime, which allows to operate the column at much lower superficial vapor velocities (0.05-1 *m/s*). However, the superficial vapor velocities should be higher than the vapor velocity where weeping starts to occur. The Froude number describes the situation of weeping [7, 8]. Weeping occurs at a Froude number lower than 0.5 [7]. Therefore, the reactive stripping section is designed in such a way that the Froude number is larger than 0.5 on each tray employing superficial vapor velocities of 0.48-0.6 *m/s*.

For the conventional non-reactive tray distillation column, a tray spacing of at least 0.5 *m* is recommended to minimize liquid entrainment from tray to tray. This is indeed required when a tray column is operated in the spray or froth region at significantly higher superficial velocities. However, the designed reactive stripping section is operated in the bubbly flow region and at a much lower superficial vapor velocity. Therefore, a tray spacing of 0.2 *m* can be chosen for the reactive stripping section. The entrainment mass flow rate is calculated according to correlation given by Bennett et al. [7]. The entrainment mass flow rate ranges from 216 *kg/hr* to 360 *kg/hr* in the reactive stripping section, which is only 3% of the liquid mass flow rate on each tray.

The liquid holdup on each tray depends on the weir height. An increase in weir height increases the liquid holdup on each tray. However, an increase in the liquid holdup increases the pressure drop on each tray as well and thereby increases the chance of flooding. Therefore, it is required that the weir height, column diameter and superficial gas velocity are iteratively calculated in a way that no weeping and flooding occur, and the column operates under reasonable pressure drop. For a superficial vapor velocity of 0.48-0.6 *m/s*, the required weir height is 0.1 *m*, the required column diameter is 1.84 *m* and in total 90 trays are required for the reactive stripping section of the column to produce 100 *ktonnes/year* polyester. It is noted that more trays are required because only a maximum of 18% liquid holdup is achieved in the stripping section to carry out the reaction. The pressure drop on each tray is about 0.853 *kPa* and the flooding factor is about 0.5 at the bottom of the stripping section and 0.2 at the top of the stripping section of the column. This indicates that the reactive stripping section is operated below the flooding level and the pressure drop on each tray is between the typical pressure drop values of 0.3 to 1.0 *kPa* for a sieve tray column.

For given superficial vapor velocities, the liquid to vapor feed (glycol) molar ratio is about 1.0:1.40, which is higher than the minimum required for kinetics. Therefore, it is obvious that the vapor leaving the reactive stripping section has a higher glycol concentration. For 100 *ktonnes/year* productivity, the required liquid feed flow rate is 7000 *kg/hr* and the required vapor feed flow rate is 7609 *kg/hr*. To separate pure water (99.5%) in the distillate, a reflux ratio of 1.1 and a rectifying section of 3.0 *m* height are required. Moreover, the diameter of the rectifying section is found to be 0.9 *m* for a flooding factor of 0.4 and the pressure drop of 0.066 *kPa/m*. Due to the fact that a higher reflux ratio is required in this configuration compared to the configurations RD1 and RD2, a higher liquid holdup is obtained in the rectifying section. The temperature of the liquid feed is 185°C, the temperature of vapor feed is 300°C and the temperature of distillate is 99°C. The product leaving the bottom of the column has a temperature of 259°C which is further cooled down to 185°C. The energy required for heating the liquid and vapor feed, cooling the top and bottom products leaving the column is depicted in table 7.1. From simulation, the energy required to produce 100 *ktonnes/year* polyester is found to be 276 *kWh/ton*.

Table 7.1: Process design for configurations RD1, RD2, RD3 and RD4

	RD1	**RD2**	**RD3**	**RD4**
Stripping section				
Height of the reactive stripping section [m]	4	4	18	14
Diameter of the reactive stripping section [m]	2.82	2.8	1.84	2.64
Liquid holdup on the reactive stripping stages [%]	62-68	70-77	16-21	14-16
Rectifying section				
Height of the reactive rectifying section [m]	2.5	2.5	3.0	2.5
Diameter of the reactive rectifying section [m]	0.54	0.6	0.9	0.5
Liquid holdup on the reactive rectifying stages [%]	2	2	6-10	2
Reflux ratio [-]	0.32	0.34	1.1	0.2
Distillate rate [kmol/hr]	60	60	56	63
Energy requirements				
MAD heating duty (HEX1) [KW]	402	402	402	402
PG evaporation duty (HEX2) [KW]	2465	2465	2866	2465
Condenser heat duty (HEX3) [KW]	-909	-911	-1345	-856
Bottom product cooling heat duty (HEX4) [KW]	-607	-607	-512	-621
Energy requirements per ton polyester product [kWh/ton]	242	242	276	242

7.2.2.2 *Configuration RD4*

Mellapak 250Y is used as a structured packing in the rectifying and stripping section of the column. The liquid holdup, pressure drop and mass transfer in the rectifying and stripping section are calculated using the correlation for Mellapak 250Y packing as proposed by Bravo et al. [2] and the axial dispersion coefficient is calculated using the correlation proposed by Kushalkar and Pangarkar [9]. These correlations are included in appendix A1.

The diameter of the reactive stripping section is designed such that the flooding and a substantial pressure drop are avoided. It is noted that the height of the reactive stripping section depends on the total volume required to produce 100 *ktonnes/year* polyester with 95.62% conversion of carboxylic acid and not on the height equivalent to theoretical plate (HETP). The diameter of the reactive stripping section is found to be 2.64 *m* for a flooding factor of 0.4 and the pressure drop of 0.42 *kPa/m*. This indicates that the reactive stripping section is operated well below the flooding condition and the typically highest allowed pressure drop of 1.2 *kPa/m*. Moreover, a reactive stripping section of 14 *m* in height is required. The liquid holdup is about 15-21% in the reactive stripping section of the column.

The liquid to vapor feed molar ratio is 1.0:1.20, which is the kinetically required liquid to vapor feed molar ratio to achieve the desired conversion. With respect to the feed molar ratio and the diameter of the stripping section, the superficial vapor velocities ranges from 0.13-0.20 *m/s*, which is significantly lower than the vapor velocity at flooding (0.62-1.38 *m/s*). To separate pure water (99.5%) at the distillate, a reflux ratio of 0.2 and the rectifying section of 2.5 *m* in height are required. Moreover, the diameter of the rectifying section is 0.5 *m* for a flooding factor of 0.3 and the pressure drop of 0.2 *kPa/m*. The achieved liquid holdup in the stripping and rectifying sections is depicted in table 7.1. The temperature of the liquid feed is 185^{o}C, the temperature of vapor feed is 300^{o}C and the temperature of distillate is 99^{o}C. The product leaving the bottom of the column has temperature of 274^{o}C which is further cooled to 185^{o}C. The energy required for heating the liquid and vapor feeds, cooling the top and bottom products leaving the column is depicted in table 7.1. From simulation, the energy required to produce 100 *ktonnes/year* polyester is found to be 242 *kWh/ton*.

7.2.3 Comparison of internal configurations

In this section, the total volume and energy required to produce 100 *ktonnes/year* polyester in the reactive distillation column for four different configurations (RD1, RD2, RD3 and RD4) are compared. From figure 7.2, it is noticed that the configurations RD1 and RD2 require similar volumes to produce 100 *ktonnes/year* polyester. The configuration RD4 requires the highest volume to produce 100 *ktonnes/year* polyester due to the lowest achieved liquid holdup. The configuration RD3 provides a lower liquid holdup than the configurations RD1 and RD2 but provides a higher liquid holdup than configuration RD4. Therefore, the volume required to produce 100 *ktonnes/year* polyester is higher than the configurations RD1 and RD2, and lower than the configuration RD4.

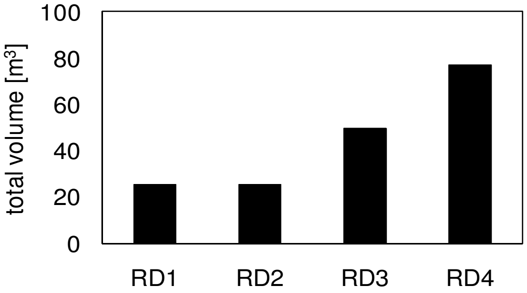

Figure 7.2: Total volume required to produce 100 *ktonnes/year* polyester

The energy required to produce 100 *ktonnes/year* polyester for the configurations RD1, RD2, RD3 and RD4 is depicted in table 7.1. It is found that the energy needed for configurations RD1, RD2 and RD4 is similar and about 242 *kWh/ton*. The configuration RD3 uses slightly more energy compared to the other configurations. This is due to the fact that the vapor feed flow rate is higher in the configuration RD3. Hence, the required heat to obtain the vapor feed is higher and thereby the overall energy required to produce 100 *ktonnes/year* polyester is higher. It is noted that the energy requirement can be further reduced by applying the heat integration between the heat exchangers required for heating and cooling.

With respect to the total volume and energy required to produce 100 *ktonnes/year* polyester, the configurations RD1 and RD2 intensifies the polyester synthesis more compared to the other configurations. Since RD1 and RD2 need similar energy and there is no substantial difference in the required volume, it is recommended to choose one of them on the basis of investment cost and the product transition time. It is obvious that trays are much cheaper and easy to install than packings therefore configuration RD2 can be a much better option. However in section 7.4, the configuration RD1 and RD2 are compared for the product transition time and the better option is identified.

7.3 Feed configuration

In this section, the different feed configurations are explored and from these configurations the best feed configuration is identified on the basis of volume and energy required to produce 100 *ktonnes/year* polyester. From the best suitable internal configurations RD1 and RD2, RD1 is used in this section. That means the reactive stripping section of the column is modeled as a packed bubble column and the reactive rectifying section is modeled as a packed column. There are three possibilities to feed the reactants;

- RD1: One of the reactants (maleic anhydride) is fed as liquid at the top of the reactive stripping section and the other reactant (propylene glycol) is fed as vapor at the bottom of the column.
- RD5: Both reactants (maleic anhydride and propylene glycol) are fed stoichiometrically as liquid mixture at the first stage of the reactive stripping

section. The excess of propylene glycol is fed as vapor at the bottom of the column to strip out the water and to provide heat to the column.

- RD6: Monoester is fed as liquid at the first stage of the reactive stripping section and the propylene glycol is fed as vapor at the bottom of the column. In this case, propylene glycol acts as stripping agent and provides the heat to the column. The monoester is separately synthesized by mixing maleic anhydride and propylene glycol in a pre-reactor.

The results of configuration RD1 were discussed in previous section. The results of configurations RD5 and RD6 are discussed in this section. In configuration RD1, the heat required for the reactive distillation column is provided by feeding the superheated propylene glycol (at 300^{o}C) and the pre-heated liquid (at 185^{o}C). From simulations, we concluded that the provided heat is sufficient to obtain the desired temperature profile along the column. In the case of configuration RD5, both reactants (maleic anhydride and propylene glycol) are fed as liquid at the first stage of the reactive stripping section. Therefore, there is no kinetic requirement to feed a significant amount of glycol at the bottom of the column as a vapor. However, to increase the stripping rate of water, a certain glycol vapor feed is beneficial. When a very low propylene glycol (912 *kg/hr*) is fed as a vapor at the bottom of the column, the heat supplied to the reactive distillation column is not sufficient because the maximum liquid feed temperature can be 185^{o}C in order to keep both reactants below their boiling points. Therefore, a longer residence time of 5.5 hours is required to obtain the desired conversion (95.62%). When a very large amount of propylene glycol (4489 *kg/hr*) is fed to the column as a vapor, the required volume of the column increases due to the accommodation of excess glycol vapor. The required volume to produce 100 ktonnes/year polyester is about 74 m^3 which is by factor 2.89 times higher than the configuration RD1. Furthermore, the provision of excess propylene glycol at the bottom of the column leads to dilution of the product with unreacted propylene glycol in the stripping section. The reboiler cannot be attached to the column to provide the vapor and heat inside the column because heating of the main product (polyester) in the reboiler can degrade the polyester product. Hence, the heat can only be provided to the column either by feeding the pre-heated liquid and vapor or by heating the column through an outer jacket. However, to control the temperature profile of 185^{o}C-250^{o}C along the reactive stripping section through an outer jacket is very difficult. Therefore the option of heat supply through an outer jacket is ruled out. From this analysis, it is concluded that the configuration RD5 has limitations to provide sufficient energy to heat up the column. Moreover, in any case of heat provision, the configuration RD5 requires either a longer residence time or a larger volume to produce 100 *ktonnes/year* polyester. The provided solution by this configuration is far away from the advantages gained by configuration RD1.

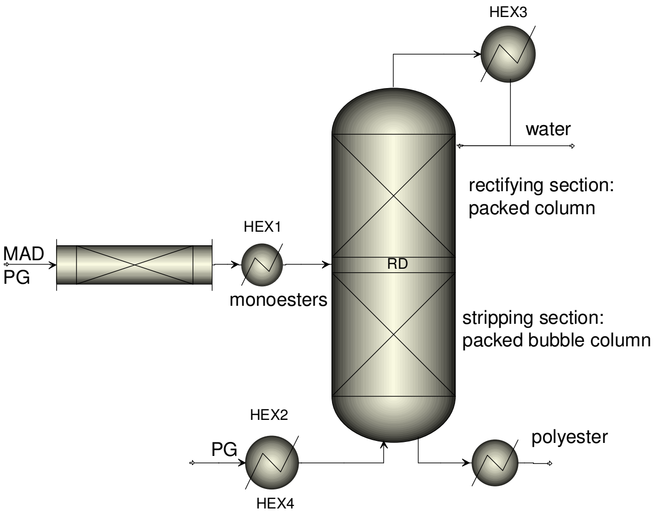

Figure 7.3: Schematic representation of the reactive distillation column coupled with pre-reactor (configuration RD6)

The limitations of configuration RD5 can be overcome by configuration RD6. A schematic view of the configuration RD6 is shown in figure 7.3. An equimolar ratio of maleic anhydride and propylene glycol are fed to a pre-reactor in which they are mixed, heated and reacted. The monoesters are formed upon the ring opening reaction. This is a very fast exothermic reaction and a maximum 10 minutes of residence time is required to complete the reaction. The monoesters are heated further to 250°C and then fed to the first stage of the reactive stripping section. The advantage of this configuration over configuration RD5 is that the liquid feed can be heated to a temperature higher than 185°C due to the higher boiling point of the monoester. Hence in this configuration, more heat can be provided through the liquid feed to the column. Moreover, in this configuration, it can be possible that no excess glycol vapor is required to provide the heat to the column.

Since the reaction kinetics for the ring opening reaction are not known, the volume of pre-reactor is calculated based on the assumed residence time (10 minutes) to produce monoesters. The process design parameters for the reactive distillation column are determined from simulations and depicted in table 7.2. The total volume required to produce 100 *ktonnes/year* polyester is 14.35 m^3 and the energy required to produce 100 *ktonnes/year* polyester is 210 *kWh/ton*. The required volume is reduced by a factor 1.77 (43%) in configuration RD6 compared to configuration RD1. Moreover, the required energy is also reduced by 13% in configuration RD6 compared to configuration RD1.

Table 7.2: Process design for configuration RD6

	RD6
Pre-reactor	
Liquid feed (MAD) flow rate [kg/hr]	5540
Liquid feed (PG) flow rate [kg/hr]	4300
Liquid feed (MAD and PG) temperature [^oC]	55
Temperature of monoesters leaving the reactor [^oC]	185
Residence time in the reactor [hour]	0.17
Volume of the reactor [m^3]	1.3
Reactive distillation column	
Feed parameters	
Flow rate of monoester feed [kg/hr]	9840
Temperature of monoester feed [^oC]	250
Vapor feed (PG) flow rate [kg/hr]	2815
Vapor feed (PG) temperature [^oC]	255
Stripping section	
Height of the reactive stripping section [m]	4
Diameter of the reactive stripping section [m]	2.0
Liquid holdup on the reactive stripping stages [%]	59-70
Temperature of bottom product leaving the column [^oC]	257
Rectifying section	
Height of the reactive rectifying section [m]	2.5
Diameter of the reactive rectifying section [m]	0.5
Liquid holdup on the reactive rectifying stages [%]	3
Reflux ratio [-]	0.58
Distillate rate [kmol/hr]	44.5
Distillate temperature [^oC]	99
Energy requirements	
Heat duty for pre-reactor [KW]	756
Heat duty for monoester feed (HEX1) [KW]	745
PG evaporation duty (HEX2) [KW]	988
Condenser heat duty (HEX3) [KW]	-796
Bottom product cooling heat duty (HEX4) [KW]	-498
Production rate of polyester [tones/hr]	11.82
Energy requirements per ton polyester product [kWh/ton]	210

Furthermore, this most intensified configuration - RD6 is compared with the traditional batch reactor process. The required volume and the production time in a batch reactor process are discussed in chapter 3. The batch reactor process requires 623 *kWh/ton* to produce 100 *ktonnes/year* polyester. The energy usage is calculated based on the heat load required per batch of polyester production. The required volume is reduced from 152 m^3 to 14.35 m^3, the production time is reduced from 12 hours to 0.8 hour and the needed energy is reduced from 623 *kWh/ton* to 210 *kWh/ton* to produce 100 *ktonnes/year* polyester by configuration RD6 as compared to the traditional batch reactor process. In configuration RD6, the energy usage is significantly lower compared to the traditional batch reactor process due to two reasons: 1) In the designed continuous reactive distillation process, a better heat transfer is achieved due to direct heat transfer from super heated feed. In the batch reactor process, the heat is transferred through a jacket heating, where heat transfer strictly depends on heat transfer coefficient of liquid phase, thermal conductivity of wall and surface area available of heat transfer. 2) In a batch reactor process, the significant heat is consumed for heating up a reactor in each batch. However in configuration RD6, such heat consumption does not exist due to continuous operation. In conclusion, the required volume is reduced by a factor 10 (90%), the production time is reduced by a factor 15 (93%) and the required energy is reduced by a factor 3 (66%) in configuration RD6.

7.4 Multi-product simulation

In this section, three configurations RD1, RD2 and RD6 are simulated for multi-product production. The polyester of grade P_1 is produced from the reactants maleic anhydride and propylene glycol. The polyester of grade P_2 is produced from the reactants maleic anhydride, phthalic anhydride and propylene glycol. In previous sections 7.2 and 7.3, all configurations are designed to produce the polyester of grade P_1. The reaction conditions to produce the polyester of grade P_2 are similar to those of grade P_1. This suggests that both grades P_1 and P_2 can be produced in the same equipment. Therefore, the design found for the configurations RD1, RD2 and RD6 to produce the polyester of grade P_1 is used to produce the polyester of grade P_2. Moreover in this section, the operational parameters are determined to achieve the polyester of grade P_2 with an acid value of 25 *mg/g*, to achieve the carboxylic acid conversion of 95.62% and to achieve the water purity of 99.5% in the distillate.

Table 7.3: Operational parameters for configurations RD1, RD2 and RD6 to produce the polyester of grade P_2

	RD1	**RD2**	**RD6**
Pre-reactor			
Liquid feed (MAD) flow rate [kg/hr]	-	-	2354
Liquid feed (PAD) flow rate [kg/hr]	-	-	3553
Liquid feed (PG) flow rate [kg/hr]	-	-	3653
Liquid feed temperature [^{o}C]	-	-	55
Temperature of monoesters leaving the reactor [^{o}C]	-	-	185
Reactive distillation column			
Liquid feed (MAD) flow rate [kg/hr]	2630	2630	-
Liquid feed (PAD) flow rate [kg/hr]	3970	3970	-
Monoester feed flow rate [kg/hr]	-	-	9560
Temperature of monoester feed [^{o}C]	185	185	250
Vapor feed (PG) flow rate [kg/hr]	5707	5935	2815
Vapor feed (PG) temperature [^{o}C]	300	300	250
Reflux ratio [-]	0.52	0.72	0.94
Distillate rate [kmol/hr]	46	43	37
Productivity [ktones/year]	92.41	91.04	90.92

In configuration RD1 and RD2, the maleic anhydride and phthalic anhydride are fed as liquid mixture at the first stage of stripping section and propylene glycol is fed as a vapor at the bottom of the column. In configuration RD6, the mixture of maleic anhydride, phthalic anhydride and propylene glycol is fed to a pre-reactor. The produced monoesters in a pre-reactor are fed to the first stage of the reactive stripping section. Moreover, the vapor of propylene glycol is fed at the bottom of the column. For all configurations, the molar ratio of maleic anhydride to phthalic anhydride is 1.0:1.0. The reaction kinetics for the phthalic anhydride and propylene glycol system is used from Salmi et al. [10] and the reaction kinetics for the maleic anhydride and propylene glycol is used from Shah et al. [1]. The operational parameters found from simulations for the configurations RD1, RD2 and RD6 are given in table 7.3. It is noted that due to slower reaction kinetics of the phthalic anhydride and propylene glycol system, the productivity of the polyester of grade P_2 is less than the productivity of the polyester of grade P_1.

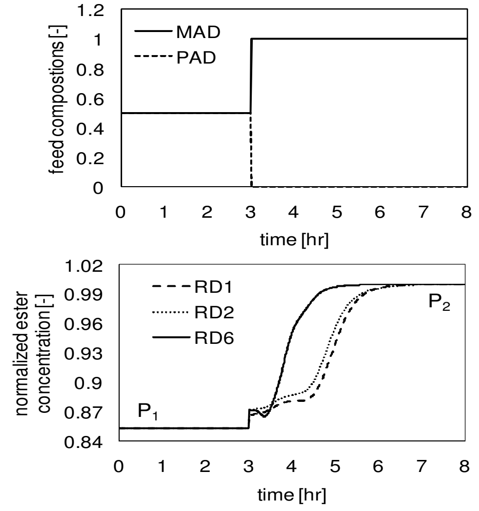

Figure 7.4: Dynamic profile of product changeover from grade P1 to grade P2

Furthermore, the dynamic simulation of product changeover is performed to determine the product transition time. This dynamic simulation of product changeover from grade P_1 to grade P_2 in the configurations RD1, RD2 and RD6 is shown in figure 7.4. From these dynamic simulations, the product transition time is found to be 3.5 hours for the configuration RD1, 3.3 hours for the configuration RD2 and 2 hours for the configuration RD6, which shows that the product transition time is reduced by a factor 1.75 (43%) in configuration RD6 as compared to RD1 and RD2. It can be seen from figure that the polyester grades are more quickly switched in the configuration RD6 as compared to the configurations RD1 and RD2. This is due to the fact that the vapor flow rate in configuration RD6 is much lower than the configurations RD1 and RD2. Thus, the configuration RD6 provides a better plug flow behavior compared to the configuration RD1. Moreover, the configuration RD2 requires slightly lower product transition time as compared to the configuration RD1.

7.5 Conclusions

In this chapter, the best suitable internal and feed configurations for the polyester process are identified. With respect to the internal configuration, the configuration which contains the reactive stripping section as a packed or trayed bubble column and the reactive rectifying section as a packed column requires minimum volume and energy to produce 100 *ktonnes/year* polyester. With respect to the feed configuration, the feeding of monoesters to the reactive distillation column significantly intensifies the polyester process compared to an anhydrous reactant fed to the column. Moreover, the product transition time in this configuration is also significantly lower compared to the other configurations. As compared to all other configurations, the configuration where a reactive distillation column is coupled with a pre-reactor intensifies the polyester process in all domains of structure, energy and time and provides the best solution for continuous production.

References

[1] M. Shah, E. Zondervan, A.B. de Haan, Process modeling for the synthesis of unsaturated polyester, Polymer Engineering & Science, 2011, DOI: 10.1002/pen.22038

[2] J.L. Bravo, J.A. Rocha, J.R. Fair, A comprehensive model for the performance of columns containing structured packings, in: I. ChemE. Symp. Ser., 1992, pp. A439.

[3] N. Kantarci, F. Borak, K.O. Ulgen, Bubble column reactors, Process Biochemistry, 40 (2005) 2263.

[4] D.L. Bennett, R. Agrawal, P.J. Cook, New pressure drop correlation for sieve tray distillation columns, AIChE Journal, 29 (1983) 434.

[5] H. Chan, J.R. Fair, Prediction of point efficiencies on sieve trays. 1. Binary systems, Industrial & Engineering Chemistry Process Design and Development, 23 (1984) 814.

[6] F.J. Zuiderweg, Sieve trays: A view on the state of the art, Chemical Engineering Science, 37 (1982) 1441.

[7] D.L. Bennett, D.N. Watson, M.A. Wiescinski, New correlation for sieve-tray point efficiency, entrainmnt, and section efficiency, AIChE Journal, 43 (1997) 1611.

[8] M.J. Lockett, S. Banik, Weeping from sieve trays, Industrial & Engineering Chemistry Process Design and Development, 25 (1986) 561.

[9] K.B. Kushalkar, V.G. Pangarkar, Liquid holdup and dispersion in packed columns, Chemical Engineering Science, 45 (1990) 759.

[10] T. Salmi, E. Paatero, P. Nyholm, M. Still, K. Narhi, Kinetics of melt polymerization of maleic acid phthalic acids with propylene glycol, Chemical Engineering Science, 49 (1994) 5053.

Chapter 8

Conclusion and Outlook

8.1 Conclusion

The goal of the thesis is to develop a reactive distillation process for the production of unsaturated polyester from anhydrides and glycols and to evaluate its attractiveness compared to the traditional production process. To achieve this, five objectives are formulated in this work:

- develop reliable dynamic and steady state models for the reactive distillation process
- provide the validation of the concept that the polyester can be produced in the reactive distillation column by conducting experiments at the reactive distillation pilot plant
- validate the developed model with experimental results of the reactive distillation pilot plant
- obtain the model parameters such as gas holdup, mass transfer coefficient and liquid back mixing by conducting experiments
- identify the best internal and feed configurations of the reactive distillation process, which require a minimum volume and energy requirement to produce unsaturated polyester combined with a minimum product transition time during the product changeover.

The first step was to develop a process model for the synthesis of unsaturated polyester in order to validate the kinetic and thermodynamic models. We found that the polymer NRTL model significantly improved the prediction capability of the process model compared to the ideal-behaviour modeling. The behaviour of the model system, the polyesterification of the unsaturated carboxylic acid and two side reactions, isomerization and double bond saturation are reliably predicted. We concluded that the process model which consists of kinetics with changing rate order connected with the polymer NRTL thermodynamic model give a better representation of the industrial unsaturated polyester process. This validated kinetic and thermodynamic models and their parameters were further used to simulate the reactive distillation process.

In the second step a reactive distillation model for the unsaturated polyester process was formulated. The model predicts the polymer attribute, isomerization and saturation composition of the polymer in the range of industrial polyester production data. The reactive distillation process with the best operating and design parameters was compared with the batch reactor process. It is found that the reactive distillation process has distinct advantages over the traditional batch reactor process. A 7% higher equilibrium conversion is achieved in the reactive distillation process compared to the batch reactor process. The required residence time is only 1.8-2 hours compared to 12 hours of batch time in the conventional process.

Then the traditional rate-based model was extended to account for the axial dispersion. The predictions of the extended model were compared with the traditional rate-based and equilibrium models. The simulation results demonstrated that the axial dispersion significantly influences the reactive distillation process and cannot be neglected. The extended model predicts lower conversion in a highly dispersed system, as compared to a low dispersed one. Moreover, it predicts that the product transition time is significantly increased at high liquid back mixing. Undesired product is formed at >1.5 times larger amounts in higher dispersed systems compared to less dispersed ones.

Furthermore on the basis of current research work and literature review, a novel methodology is proposed which is very effective in evaluating systematically and quickly the economical and technical feasibility of RD processes, determining also the boundary conditions of the process (e.g. relative volatilities, target purities, equilibrium conversion and equipment restriction). Using the evaluating methodology, one can rapidly scan and decide on the viability of the RD option, based on either technical or economical criteria. Provided that RD is an economically attractive option, the technical evaluation framework described in this thesis can be effectively used to determine the key process parameters and limitations, working regime, selection of internals, as well as the model requirements for the rigorous simulation of the reactive distillation process. From the technical evaluation of the reactive distillation process for the unsaturated polyester synthesis, we concluded that this process is kinetically controlled and the bubble column could be the potential device for producing unsaturated polyesters by the reactive distillation.

In the next step, the effect of gas and liquid flow rates, and the liquid phase viscosity on the gas holdup, liquid dispersion and mass transfer in the packed, trayed and empty bubble column was systematically investigated. The packed and trayed bubble columns improve the gas holdup and mass transfer compared to the empty bubble column and reduces the axial dispersion significantly. Particularly, the Gauze packing improves the gas holdup and mass transfer and, sufficiently reduces the axial dispersion. In contrast, Super-Pak offers only a modest improvement because of its open structure. Comparison of the experimental data of the packed and trayed bubble column indicates that the partition trays improve the bubble column in the same order as packing. The gas holdup, axial dispersion and mass transfer depend more strongly on the gas velocity compared to the liquid velocity. The liquid viscosity also significantly influences these parameters and therefore the empirical correlations obtained from the air-water system cannot be applied for the viscous system. Empirical correlations for these parameters based on Bodenstein, Stanton, Froude and Gallilei dimensionless numbers were proposed and validated.

Afterwards, polyester synthesis was successfully executed in a pilot reactive distillation column equipped with Sulzer BX gauze packing. Two different configurations were investigated: 1) a reactive distillation column and 2) a reactive distillation column coupled with a pre-reactor. Due to a relatively short residence time of 0.32 hours and an operating temperature of 190^{o}C in case of the first configuration, a maximum conversion of 37% was achieved; which indicates monoester formation in the reactive distillation column. In the case of the second configuration, a 90% conversion is achieved within 0.55 hours at a temperature of 250°C in the reactive distillation column coupled with a pre-reactor; which confirms the polyester formation in the reactive distillation column. The extended rate-based model was used to simulate the pilot reactive distillation column. The model predicted the experimental data (acid value, conversion, isomerization and saturation fraction, number-average molecular weight, the degree of polymerization and water fraction in the distillate) adequately (5-22%). Moreover, the product specifications of the polyester produced at 250°C in the reactive distillation column is in the range of polyesters produced in the traditional industrial batch reactor setup. Furthermore, discoloration of the polyester was hardly noticed even though the column was operated at 250°C. From this experimental validation of the reactive distillation process for polyester synthesis, it is concluded that the polyester can be produced in a reactive distillation column in a short residence time with comparable product specifications as the polyester produced in industry.

Finally, the validated model was used to find the best suitable internal and feed configurations of the reactive distillation process for the unsaturated polyester synthesis. With respect to the internal configuration, the configuration which contains the reactive stripping section as a packed or trayed bubble column and the reactive rectifying section as a packed column requires minimum volume and energy to produce 100 ktonnes/year polyester. With respect to the feed configuration, we concluded that the feeding of monoesters to the reactive distillation column significantly intensifies the polyester process as compared to an anhydrous reactant fed to the column. Moreover, the product transition time in this configuration is also significantly lower compared to the other configurations. As compared to all other configurations, the configuration where a reactive distillation column coupled with a pre-reactor intensifies the polyester process the most and provides the best solution for continuous production.

In conclusion, a reactive distillation column coupled with pre-reactor is the most promising alternative to continuously produce unsaturated polyesters. It requires a factor 10 (90%) lower volume, a factor 15 (93%) lower production time and a factor 3 (66%) lower energy as compared to the traditional batch reactor process to produce 100 ktonnes/year of polyester. Hence, the reactive distillation process improves the unsaturated polyester synthesis in all domains of structure, energy and time compared to the traditional batch reactor process coupled with a distillation column.

8.2 Outlook

In this research work, we concluded that the reactive distillation is an attractive alternative for the polyester synthesis. The main focus is on the development and validation of the reactive distillation process for the production of unsaturated polyester from maleic anhydride and propylene glycol. The multi-product production is demonstrated by producing two different grades of polyester from maleic anhydride, phthalic anhydride and propylene glycol. The polyester of grade P_1 is produced from maleic anhydride and propylene glycol and the polyester of grade P_2 is produced from the maleic anhydride, phthalic anhydride and propylene glycol. For grade P2, the proportion of maleic anhydride to phthalic anhydride is kept similar. In industry, various grades of polyester are produced by changing the proportion of maleic anhydride to phthalic anhydride. Moreover, the ethylene glycol is also used to produce various grades of polyester. Therefore, it is recommended to carry out further research in this direction to determine the operating parameters of the reactive distillation process for producing various grades of polyester. Moreover in this research work, the product transition time during the grade changeover is only determined by applying a step change in the feed compositions and the liquid and vapor feed flows. Therefore, it is recommended to carry out further research to find the optimal product changeover strategy which ultimately reduced the product transition time and the undesired product formation during the grade changeover. To verify this, the existing pilot plant should be adapted in such a way that the optimal product changeover strategy can be tested. Apart from this, the polyester synthesis involves autocatalytic reaction and acid acts as a catalyst in this system. Therefore, the provision of acid based heterogeneous catalyst inside the reactive distillation column could further intensify the polyester synthesis. However, no heterogeneous catalyst is found for the polyester synthesis in literature. Therefore, further research in this direction is recommended.

Appendix A

A1: Correlations for packed columns

The liquid holdup, pressure drop and mass transfer correlations for Mellapak 250Y packing are from Bravo et al. [1].

Liquid holdup:

$$h_L = h_t h_p A_t \tag{1}$$

Pressure drop per unit height of the packing:

$$\frac{\Delta P}{\Delta Z} = \frac{\Delta P_d}{\Delta Z}\left(\frac{1}{1-(0.614+71.35S)h_t}\right)^5 \tag{2}$$

Binary mass transfer coefficient for the liquid:

$$k_i^L = 2\sqrt{\frac{D_i^L u_{Le}}{\pi S C_E}} \tag{3}$$

Fractional holdup:

$$h_t = \left(4\frac{F_t}{S}\right)^{2/3}\left(\frac{3\mu^L u_s^L}{\rho_t^L g_{eff}\varepsilon \sin\theta}\right)^{1/3} \tag{4}$$

Correction factor for total holdup due to effective wetted area:

$$F_t = \frac{29.12(We_L Fr_L)^{0.15} S^{0.359}}{\mathrm{Re}_L^{0.2}\,\varepsilon^{0.6}(\sin\theta)^{0.3}(1-0.93\cos\gamma)} \tag{5}$$

Effective gravity:

$$g_{eff} = g\left(\frac{\rho_t^L-\rho_t^V}{\rho_t^L}\right)\left(1-\frac{\Delta P/\Delta Z}{\Delta P/\Delta Z_{flood}}\right) \tag{6}$$

Froude number for the liquid:

$$Fr_L = \frac{(u_s^L)^2}{Sg} \tag{7}$$

Reynolds number for the liquid:

$$\mathrm{Re}_L = \frac{u_s^L S \rho_t^L}{\mu^L} \tag{8}$$

Superficial liquid and vapor velocities:

$$u_s^L = \frac{L}{\bar{\rho}^L A_t}, \qquad u_s^V = \frac{V}{\bar{\rho}^v A_t} \tag{9}$$

Effective liquid velocity through the channel:

$$u_{Le} = \frac{u_s^L}{\varepsilon h_t \sin\theta} \tag{10}$$

Weber number for the liquid:

$$We_L = \frac{\left(u_s^L\right)^2 \rho_t^L S}{\sigma} \tag{11}$$

Dry pressure drop per unit height of packing:

$$\frac{\Delta P_d}{\Delta Z} = \frac{0.177\rho_t^V}{S\varepsilon^2(\sin\theta)^2}\left(u_s^V\right)^2 + \frac{88.774\mu^V}{S^2\varepsilon\sin\theta}u_s^V \tag{12}$$

Total interfacial area for mass transfer:

$$a^I = a_e A_t h_p \tag{13}$$

Effective surface area per unit volume of the column:

$$a_e = F_t F_{se} a_p \tag{14}$$

List of symbols

A_t	cross-sectional area of the column (m^2)
a^I	Total interfacial area for mass transfer (m^2)
a_e	effective surface area per unit volume of the column (m^2/m^3)
a_p	specific area of the packing (m^2/m^3)
CE	correction factor for surface renewal (-)
D_i^L	diffusivity of the liquid (m^2/s)
Fr_L	Froude number for the liquid (-)
F_{se}	factor for surface enhancement (-)
F_t	correction factor for total holdup due to effective wetted area (-)

g	gravitational constant (m/s^2)
g_{eff}	effective gravity (m/s^2)
h_p	height of the packed section (m)
h_L	volumetric liquid holdup (m^3)
h_t	fractional liquid holdup (-)
k_i^L	binary mass transfer coefficient for the liquid (m/s)
L, V	molar flow rate of liquid and vapor (kmol/s)
Re_L	Reynolds number for the liquid (-)
S	slant height of a corrugation (m)
u_s^L, u_s^V	superficial velocity for the liquid and vapor (m/s)
u_{Le}	effective liquid velocity through the channel (m/s)
We_L	Weber number for the liquid (-)
$\Delta P/\Delta Z$	pressure drop per unit height of the packing (Pa/m)
$\Delta P_d/\Delta Z$	dry pressure drop per unit height of the packing (Pa/m)
ε	void fraction of packing (-)
θ	angle with horizontal of falling film or corrugation channel (deg)
μ^L	viscosity of liquid (Pas)
ρ_t^L	density of liquid (kg/m^3)
$\bar{\rho}^L$	molar density of liquid (kmol/m^3)
σ	Liquid surface tension (N/m)

A2: Correlations for sieve tray columns

The liquid holdup and pressure drop correlations for sieve tray columns are from Bennett et al. [2]. The mass transfer correlation for sieve tray columns is from Chan and Fair [3].

Liquid holdup:

$$h_L = h_{cl} A_b \qquad (1)$$

Total head loss per tray:

$$h_t = h_d + h_{cl} + h_\sigma \qquad (2)$$

Binary mass transfer coefficient for the liquid:

$$k_i^L = 19700\left(D_i^L\right)^{0.5} \frac{0.4F_s + 0.17}{\overline{a}} \qquad (3)$$

Liquid clear height on tray:

$$h_{cl} = \alpha\left(h_w + \left(0.5 + 0.438e^{-137.8h_W}\right)\left(\frac{Q_L}{l_w \alpha}\right)^{2/3}\right) \qquad (4)$$

Relative froth density:

$$\alpha = \exp\left(-12.55\left(u_s^V \left(\frac{\rho_t^V}{\rho_t^L - \rho_t^V}\right)^{0.5}\right)^{0.91}\right) \qquad (5)$$

Froth height:

$$h_f = \left(h_w + \left(0.5 + 0.438e^{-137.8h_W}\right)\left(\frac{Q_L}{l_w \alpha}\right)^{2/3}\right) \qquad (6)$$

Dry tray head loss:

$$h_d = 0.0051\left(\frac{v_o}{C_o}\right)^2 \rho_t^V \left(\frac{\rho_w}{\rho_t^L}\right)\left(1 - \left(A_h / A_a\right)^2\right) \qquad (7)$$

Head loss due to surface tension:

$$h_\sigma = \frac{6\sigma}{g\rho_t^L d_o} \qquad (8)$$

Interfacial area per unit volume of liquid:

$$\overline{a} = a^I / \alpha A_b h_f \qquad (9)$$

Superficial F-factor:

$$F_S = u_s^V \left(\rho_t^V\right)^{0.5} \qquad (10)$$

List of symbols

A_a	tray active area (m^2)
A_b	total active bubble area on tray (m^2)
A_h	tray hole area (m^2)
a^I	Total interfacial area for mass transfer (m^2)
$\overline{a}$	Interfacial area per unit volume of the liquid (m^2/m^3)

C_o	orifice coefficient (-)
d_o	diameter of a tray hole (m)
D_i^L	diffusivity of the liquid (m^2/s)
F_S	superficial F-factor
g	gravitational constant (m/s^2)
h_{cL}	clear liquid height (m)
h_d	dry head loss (m)
h_f	froth height (m)
h_L	volumetric liquid holdup (m^3)
h_w	weir height (m)
h_σ	head loss due to surface tension (m)
k_i^L	binary mass transfer coefficient for the liquid (m/s)
l_w	weir length (m)
$\overline{Q}_L$	average volumetric flow rate per pass for liquid (m^3/s)
u_s^L, u_s^V	superficial velocity for the liquid and vapor (m/s)
α	relative froth density (-)
ρ_w	density of water (kg/m^3)
ρ_t^L	density of liquid (kg/m^3)
ρ_t^V	density of vapor (kg/m^3)

References

[1] J.L. Bravo, J.A. Rocha, J.R. Fair, A comprehensive model for the performance of columns containing structured packings, in: I. ChemE. Symp. Ser., 1992, pp. A439.
[2] D.L. Bennett, R. Agrawal, P.J. Cook, New pressure drop correlation for sieve tray distillation columns, AIChE Journal, 29 (1983) 434.
[3] H. Chan, J.R. Fair, Prediction of point efficiencies on sieve trays. 1. Binary systems, Industrial & Engineering Chemistry Process Design and Development, 23 (1984) 814.

List of Publications

Journal Publications:

1. M. Shah, E. Zondervan, M.L. Oudshoorn, A.B. de Haan, A novel process for the synthesis of unsaturated polyester, *Chemical Engineering and Processing: Process Intensification*, **2011**, 50, 747-756
2. M. Shah, E. Zondervan, M.L. Oudshoorn, A.B. de Haan, Reactive distillation: an attractive alternative for the synthesis of unsaturated polyester, *Macromolecular symposium Journal*, **2011**, 302, 46-55
3. M. Shah, E. Zondervan, A.A. Kiss, A.B. de Haan, Modeling the liquid back mixing characteristics for a kinetically controlled reactive distillation process, *Computer Aided Chemical Engineering,* **2011**, 29, 11-15
4. E. Zondervan, M. Shah, A.B. de Haan, Optimal solution for a reactive distillation column, *Chemical Engineering Transactions*, **2011**, 24, 295-300
5. M. Shah, E. Zondervan, A.B. de Haan, Modelling and simulation of an unsaturated polyester process, *Journal of Applied Science,* **2010**, 10 (21), 2551-2557
6. M. Shah, E. Zondervan, A.B. de Haan, Process modelling for the synthesis of unsaturated polyester process, accepted in *Journal of Polymer Engineering and Science,* DOI: 10.1002/pen.22038
7. M. Shah, A.A. Kiss, E. Zondervan, A.B. de Haan, Influence of liquid back mixing on kinetically controlled reactive distillation process, accepted in *Chemical Engineering Science Journal*
8. M. Shah, A.A. Kiss, E. Zondervan, A.B. de Haan, A systematic framework for the economical and technical evaluation of reactive distillation processes, submitted to *Chemical Engineering Science Journal*
9. M. Shah, E. Zondervan, A.B. de Haan, Internals characterization of the bubble column: Study of gas holdup, liquid-phase back mixing and mass transfer in viscous system*, in preparation*

10 M. Shah, E. Zondervan, A.B. de Haan, Experimental investigation and model validation of a reactive distillation process for the synthesis of unsaturated polyester*, in preparation*

11 M. Shah, E. Zondervan, A.B. de Haan, Intensified process for the synthesis of unsaturated polyester*, in preparation*

Peer reviewed conference proceedings:

1. M. Shah, E. Zondervan, M.L. Oudshoorn, A.B. de Haan, Development of a model for the synthesis of unsaturated polyester by reactive distillation, *Proceeding of Distillation Absorption 2010 conference,* Eindhoven The Netherlands, **2010**, 247-252
2. M. Shah, E. Zondervan, A.B. de Haan, Improved dynamic model for an unsaturated polyester process by non-ideal thermodynamics, *Proceedings of 21st International Symposium on Chemical Reaction Engineering - ISCRE21*, Philadelphia, U.S.A, **2010**, 76-77

Presentations

Oral presentations:

1. E. Zondervan, M. Shah, A.B. de Haan, Optimal solution for a reactive distillation column, *The 10th International conference on Chemical and Process Engineering – IcheaP-10*, **2011**, Florence, Italy
2. M. Shah, E. Zondervan, M.L. Oudshoorn, A.B. de Haan, Reactive distillation: an attractive alternative for the synthesis of unsaturated polyester, *10th Polymer Reaction Engineering Workshop*, **2010**, Hamburg, Germany
3. M. Shah, E. Zondervan, M.L. Oudshoorn, A.B. de Haan, Development of a model for the synthesis of unsaturated polyester by reactive distillation, *Distillation and Absorption Conference*, **2010**, Eindhoven The Netherlands
4. M. Shah, E. Zondervan, A.B. de Haan, Reactive distillation for multi-product continuous plant, *Dutch Separation Technology Institute –DSTI Congress*, **2010**, Amersfoort, The Netherlands
5. M. Shah, E. Zondervan, A.B. de Haan, Modelling and simulation of an unsaturated polyester process, *3rd International Conference on Chemical and Bioprocess Engineering - ICCBPE*, **2009**, Kota Kinabalu, Malaysia

Poster presentations:

1. M. Shah, E. Zondervan, A.B. de Haan, Modeling the liquid back mixing characteristics for a kinetically controlled reactive distillation process, *21st European Symposium on Computer Aided Process Engineering – ESCAPE-21,* **2011**, Chalkidiki, Greece
2. M. Shah, E. Zondervan, A.B. de Haan, Improved dynamic model for an unsaturated polyester process by non-ideal thermodynamics, *21st International Symposium on Chemical Reaction Engineering – ISCRE21*, **2010**, Philadelphia, U.S.A
3. M. Shah, E. Zondervan, A.B. de Haan, Development of a model for the synthesis of unsaturated polyester by reactive distillation, *Netherlands Process Technology Symposium - NPS*, **2010**, Veldhoven, The Netherlands
4. M. Shah, E. Zondervan, A.B. de Haan, A novel process for the synthesis of unsaturated polyester, *Computer Aided Process Engineering – CAPE Forum*, **2010**, Aachen, Germany
5. M. Shah, E. Zondervan, A.B. de Haan, Reactive distillation for multi-product continuous plant, *Netherlands Process Technology Symposium - NPS*, **2009**, Veldhoven, The Netherlands

Curriculum Vitae

Mayank Shah was born on the 10th May 1984 in Vadodara, India. In April 2005 he obtained a bachelor degree in chemical engineering at Maharaja Sayaji Rao University (M.S.U) Vadodara. Between May 2005 and March 2006 he worked as a process engineer at Gharda chemicals in Ankleshwar, India. In April 2006 he came to Germany for his master study. In October 2007 he completed his master studies in chemical engineering at Otto-von-Guericke University Magdeburg. During the master studies he worked as a research assistant at the Max Planck institute, Magdeburg for six months. He did the master thesis on "Drying of polymeric material in combination of flash and cyclone dryer" for the duration of six months at Vinnolit GmbH. Between December 2007 and November 2011 he accomplished his Ph.D. thesis "Intensification of polyester synthesis by continuous reactive distillation" at the process systems engineering group of Prof. André de Haan at Eindhoven University of technology. From November 2011 onwards he is working as a project leader in the Research Development & Innovation department of Akzo Nobel Chemicals B.V., Deventer, The Netherlands.